Advances in Colloid and Interface Science 310 (2022) 102773

Contents lists available at ScienceDirect

Advances in Colloid and Interface Science

journal homepage: www.elsevier.com/locate/cis

Historical Perspective

Stimuli-responsive polyelectrolyte multilayer films and microcapsules

Tomasz Kruk [a,1], Karolina Chojnacka-Górka [b,1], Marta Kolasińska-Sojka [a,*], Szczepan Zapotoczny [b,*]

[a] Jerzy Haber Institute of Catalysis and Surface Chemistry, Polish Academy of Sciences, Niezapominajek 8, 30-239 Krakow, Poland
[b] Jagiellonian University, Faculty of Chemistry, Gronostajowa 2, 30-387 Krakow, Poland

ARTICLE INFO

Keywords:
Polyelectrolyte multilayer films
Polymer microcapsules
Stimuli-responsive polymers
Layer-by-layer deposition

ABSTRACT

Polyelectrolyte multilayer (PEM) films and particularly hollow capsules composed of PEM shells have gained significant interest since their introduction. Their compositional versatility and easiness of preparation via so-called layer-by-layer assembly led to the development of numerous systems containing also stimuli-responsive components. This paper reviews the achievements related to the formation, determination of structure, and properties of PEM films and capsules responding to major physical, chemical, and biological stimuli. Their applications as e.g., microcarriers for controlled delivery release of active components, substrates for controlled cells' growth, coatings for enhanced surface adhesion, or self-healing anticorrosive systems are shown and discussed. The influence of various stimuli on integrity, permeability of the films or capsules shell are presented together with related applications in biomedicine for controlled drug release as well as in biotechnology and industrial protective coatings.

1. Introduction

Electrostatically driven self-assembly of charged polymers, often referred to as the layer-by-layer (LbL) approach, represents a facile and powerful path for fabrication of ultrathin polymer films of desired structure [1]. Since the pioneering report of G. Decher [2], the LbL technique has attracted increasing attention due to its versatility and simplicity. It is based on alternating adsorption of polyanions and polycations on charged surfaces and leads to the formation of ultrathin polyelectrolyte multilayers (PEM) (Fig.1).

The physicochemical parameters of the films, like thickness, stiffness, chemistry, stability, permeability, composition, biofunctionality, and dynamics might be modified to a certain extent by changing the assembly conditions. The thickness of the LbL coating might be well-controlled by varying the degree of protonation of the applied components changing ionic strength and/or pH of their solutions [3]. When PEM assemblies at a pH value near the pK_a value of any of the polyelectrolyte (PE), the polymer chains are not fully expanded leading to the formation of relatively thick films. As strong polyelectrolytes are charged over a wide pH range, it is not easy to control the properties of PEM based on such polymers unless one takes specific measures to disturb the polymer-polymer interactions by manipulating other stimuli like ionic strength, temperature, solvent polarity. Weak polyelectrolytes are charged in a smaller pH window, therefore, polymeric conformations could be easily modulated upon changing the pH of their solutions [4].

The LbL method was later extended to different types of interactions, e.g. ion-dipole interaction, hydrogen bonding, hydrophobic interaction, and biospecific recognition [6] as well as to many other charged nano-objects (nanoparticles, dendrimers) and virtually to any flat or curved surfaces [7,8]. The films may be deposited on a colloidal template and after its removal the hollow capsules in the nano or micrometer range may be formed [9,10] (Fig. 2). Other hollow micro/nanoobjects like vesicles, silicone spheres, polymersomes may be covered by LbL films to obtain functional capsules. Thus, using the LbL technique, very sophisticated systems may be obtained easily and inexpensively. Generally, multilayer formation by LbL technique is developed towards the formation of functional coatings, capsules [11,12,13] as well as free-standing planar membranes [14] for filtration and separation applications and as vehicles for delivering substances especially in biomedical applications [15,16]. They can be used in tissue engineering [17], as wound dressings [18], self-healing materials [19], biomimetic and/or bio-responsive surfaces [20], drug delivery systems [21], (bio)sensors, photovoltaics, microreactors, optoelectronic devices, or energy storage

* Corresponding authors.
E-mail addresses: marta.kolasinska-sojka@ikifp.edu.pl (M. Kolasińska-Sojka), s.zapotoczny@uj.edu.pl (S. Zapotoczny).
[1] Those authors equally contributed to this work.

https://doi.org/10.1016/j.cis.2022.102773
Received 6 January 2022; Received in revised form 20 August 2022; Accepted 5 September 2022
Available online 10 September 2022

[22,23,24,25].

A variety of materials can be used as cores and walls in the formation of the capsules via the LbL method, leading to fabrication of multifunctional carriers responding to various stimuli thus giving rise to diverse approaches for encapsulation and release of substances.

2. Fabrication of LbL capsules

The group led by Helmuth Möhwald demonstrated in 1998 the fabrication of hollow polymeric capsules by alternate deposition of oppositely charged polyelectrolytes on solid colloidal particles that were decomposed after formation of the polymeric multilayer shell. [26]. The deposition can be performed either by adding the exact amount of a polyelectrolyte necessary to form a monolayer at each step on the template particles (saturation method), or applying solutions with the excess of polyelectrolytes followed by washing steps. The former approach seems to be less time-consuming due to omitting the washing cycles and adventegeous thanks to lower consumption of polyelectrolytes, but the major problem such as formation of free polyelectrolyte complexes in solution and aggregation of colloidal particles remain challanging [27,28]. Therefore, rather the former method has been used more oftenly. In this approach, the nonadsorbed polyelectrolyte molecules must be removed before adding the next polyelectrolyte solution to the particles to avoid formation of polyelectrolyte complexes in the solution. This is usually done by performing at least three washing cycles with pure water. Each cycle consists of centrifugation and subsequent re-dispersion of core particles in water. An alternative to centrifugation is filtration of the particles' dispersion through size-matched filters [29]. Ones the deposition of desired number of polyelectrolyte layers is accomplished, the dissolution of the sacrificial template is required in order to obtain hollow capsules. This is done by a chemical treatment of core/shell particles in conditions that decompose core templates. Commonly used $CaCO_3$ particles are typically dissolved in ethylenediaminetetraacetic acid disodium salt (EDTA), SiO_2 particles in fluoric acid, melamine formaldehyde resins are

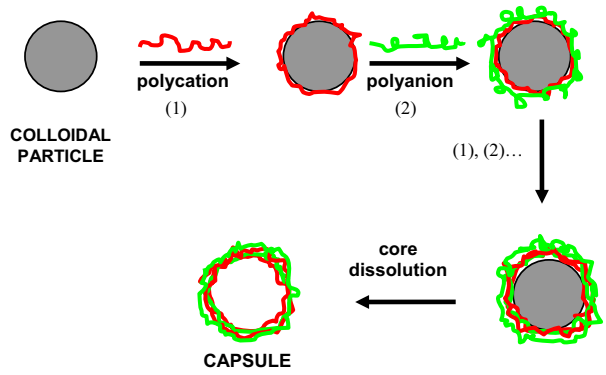

Fig. 2. The multistep process of the formation of hollow multilayered capsules via the LbL technique.

decomposed in diluted hydrochloride acid, and polystyrene latex particles in tetrahydrofuran [30]. For soft colloidal templates like vesicles, liposomes, micelles, and emulsion droplets the decomposition step is not considered to be necessary, however the washing process requires more sophisticated approach, as a typical centrifugation/re-dispersion may not work [31].When droplets of oil in water are used as templates, the excess polylectrolyte molecules can be remove by creaming/skimming cycles [32,33]. Application of liposomes or other vesicles as a core material involves a more complex procedure. After deposition of the first layer of polyelectrolyte, counter-polyelectrolyte is added without purification step in-between. This results in formation of soft templates with one bilayer of polyelectrolytes deposited and inter-polyelectrolyte complexes disspersed in the solution. At that stage polyelectrolyte complexes can be remove by centrifugation as the soft templates with polylelectrolyte shell are much more stable.

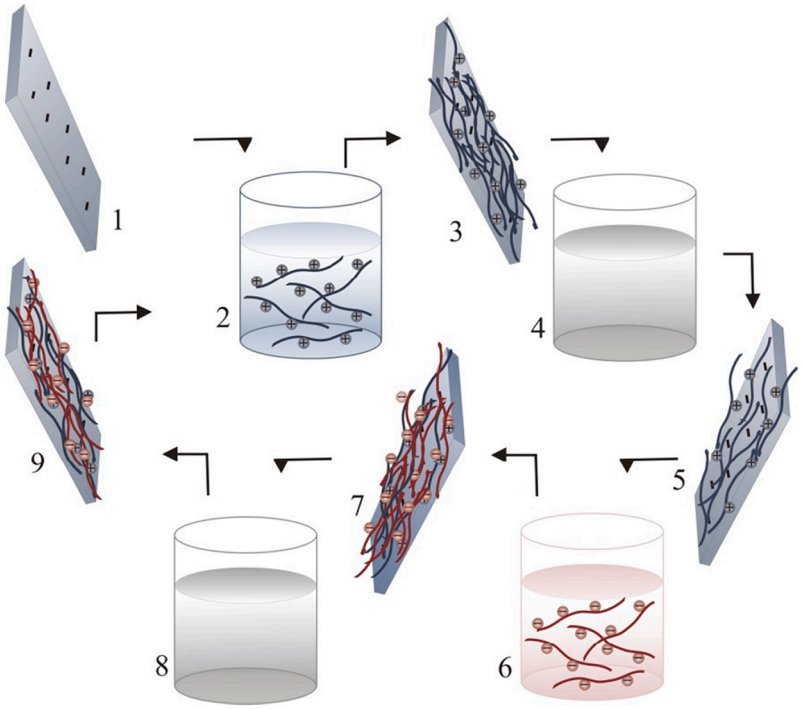

Fig. 1. Schematic illustration of alternating adsorption cycle. (1) initial negatively charged substrate, (2) polycation solution, (3) first adsorbed layer with weakly bounded chains, (4), (8) rinsing solutions, (5) first irreversibly adsorbed layer, (6) polyanion solution, (7) two-layers film with weakly bounded chains, (9) two-layers film after rinsing (reproduced from [5] with permission, copyright 2009 American Chemical Society).

3. Capsules loading and releasing strategies

In general, encapsulation could be performed in three ways.

(I) In the simplest method, the substance to be encapsulated is used as a core. This method can be applied for substances that can form colloidal crystals with a desired size and shape that are resistant to the conditions of adsorption of polyelectrolytes. For cores with low inherent surface charge, excipients such as surfactants can be applied to increase their surface charge. For example, paclitaxel nanoparticles were prepared in the presence of sodium docusate -negatively charged amphiphilic surfactant that remained adsorbed on the drug surface providing negative surface charge [34].

This method was used for encapsulation of ibuprofen [35,36], insulin [37], curcumin [38], vitamin K3 [39] dexamethasone [40], camptothecin [34,41], biotin and naproxin crystals [42,43], docetaxel [44], furosemide, isoxyl, nifedipine [45], paclitaxel [46], indomethacin [47], meloxicam [48], prednisolone [49], resveratrol [50]. Poorly water-soluble drugs can be also encapsulated in oil-core capsules [51,52]. While highly water-soluble compounds like e.g. proteins and vitamin C could be encapsulated in the organic phase with an assembly of non-ionized polyelectrolytes [53]. Very interesting group of core materials that can be used for encapsulation are soft colloidal nanosurfaces. This includes vesicles, liposomes, micceles and emulsion droplets that can be loaded with therapeutic compaunds and latter cover with shell material that can provide control over cargo release [16].

(II) The second approach involves adsorption of active substances on the surface of the sacrificial templates (the substance to be encapsulated can be the wall consistuent at the same time) [54] and loading [55] or co-precipitation of them within solid cores [56], followed by the shell formation. Hereby, encapsulated substances are entrapped within such created core/shell particles that the dissolution of the templating cores results in the formation of capsules [57]. In this context, colloidal mesoporous silica particles [58] and $CaCO_3$ particles [59] are the most representative and well-established inorganic materials that are under extensive research as drug carriers' systems. Both materials can be easily chemically modified giving them great potential for achieving multifunctionality and they are naturally applicable for LbL electrostatic assembly due to their negative surface charge, which can also be converted into a positive one after chemical modifications.

Both types of particles were demonstrated to be loaded with various hydrophobic and hydrophilic compounds. Mesoporous silica particles are characterized by a very high surface area (up to 1500 m^2/g) and controllable pore size (2–50 nm) [60,61,62]. Most substances, including a wide range of proteins [63] such as therapeutic lysozyme [64,65], lipase [66] and insulin [67] as well as chemotherapeutic drugs like doxorubicin (DOX) [68] and camptothecin [62] can be loaded inside the pores through a simple diffusion mechanism. Other methods of loading are less common. For example, gemcitabine (chemotherapeutic) was encapsulated during the evaporation of solvent from the casting ethanol/gemcitabine solution [69]. Another interesting, fast and easily scalable method was reported for loading ibuprofen by co-spray drying [70]. While direct medical applications of silica particles are hindered due to their toxicity [58,71], the problem can be overcome in LbL-modified systems by the application of biocompatible polyelectrolytes and the formation of core/shell particles [67,72,73,74] or capsules [60,75,76] after the dissolution of silica.

$CaCO_3$ particles have been widely investigated as a carrier medium [77,78] but also as sacrificial cores for the fabrication of capsules [79,80]. After core dissolution, polymeric microcapsules with loaded cargo molecules are obtained. Nowadays, $CaCO_3$ particles have become one of the mostly used decomposable matrices due to their biocompatibility, easiness of preparation, and dissolution in mild conditions. In addition, polymeric microcapsules as carriers provide a wide range of possibilities to apply various stimuli for the release of encapsulated substances in a controlled manner.

Encapsulation in the porous $CaCO_3$ particles is done mostly by the co-precipitation during particles synthesis by the addition of cargo molecules to the salt solutions. This approach can be performed either by encapsulation into the crystals fabricated by the solution precipitation or reverse emulsion method [78]. Cargo molecules added to the reaction mixture can affect the crystallization process influencing the structure, morphology, stability, size, and shape of resulting crystals, which can play either a positive or negative role [81,82]. A wide variety of bioactive compounds were demonstrated to be encapsulated in such a way, e.g., proteins [83], chemotherapeutic drugs such as 5-fluorouracil [84], DOX [85,86,87], antibiotics like tetracycline [88] and silver nanoparticles for antibacterial applications [89,90]. Another frequently used method to encapsulate molecules within $CaCO_3$ particles is based on infiltration. Cargo molecules are mixed with the $CaCO_3$ crystals followed by decreasing solubility of the molecules to be encapsulated via changing the pH or solvent evaporation [78,91]. 5-fluorouracil and Na-L-thyroxine were demonstrated to be loaded within $CaCO_3$ pores by a simple diffusion mechanism [84]. Cargo molecules can be also adsorbed on the $CaCO_3$ surface by mixing $CaCO_3$ crystals with a solution of cargo molecules. The investigation of the adsorption process for different therapeutic proteins (aprotinin, catalase, insulin, protamine) indicated that the main driving force in this process is inter-protein interactions [92,93].

A recently developed method of loading of $CaCO_3$ particles is based on the mixing of pre-synthesized particles with the material to be encapsulated while freezing at −20 °C. Freezing-induced loading method allowed for 3 times higher loading of magnetite nanoparticles and 4 times higher loading of protein molecules in comparison to the adsorption and coprecipitation methods [94].

(III) The third method of encapsulation is based on the reduction of capsules' walls permeability for molecules that initially easily permeate the walls of hollow capsules. It can be done by chemical cross-linking and rising of the temperature that leads to densification of microcapsules walls and irreversible decreasing of their permeability or by changes of pH [95], ionic strength, and UV irradiation that could lead to reversible changes in the walls of the microcapsules [96].

Once encapsulation and delivery are finalized the cargo molecules should be released in response to certain stimuli. Due to the deposition method and components used, most LbL multilayers have a structure that is kinetically trapped, meaning that they are prone to post-treatment under certain triggering factors, resulting in different types of reconfigurations [22]. Thus, they are perfect candidates to be utilized in the fields of stimuli-responsive materials. However, for this to happen, certain conditions must be met. First of all, external stimuli must generate a visible/measurable effect, typically caused by a change in the structure of the coating leading to e.g.: release of cargo molecules, enhancing/inhibition of surface adhesion. Secondly, the user should be able to control this process by changing the applied stimuli [97]. Possible external triggers may be classified into two groups: physical or chemical stimuli. Changes in temperature, application of light, ultrasounds, or magnetic field are examples of physical stimuli [98]. The chemical ones are: variations of pH, ionic strength, or proceeding chemical reactions. Effective action of the triggers requires the usage of specific components/additives in PEM that show desired behavior upon exposure to the selected stimuli. They can be metal nanoparticles, light/thermosensitive polymers, dyes, etc. [1] In the case of capsules the release could be induced by changes in parameters of the capsules medium like pH [99] ionic strength, and temperature or the presence of appropriate enzymes that can cause damaging of the capsules [100]. Reduction of the electrostatic interactions between oppositely charged polymeric units by pH and ionic strength can be used to stimulate reversible changes in microcapsules permeability and allow for cyclic loading and unloading of them. Another possibility is the remote release of the encapsulated molecules by external stimuli like electromagnetic waves (UV-VIS, NIR, microwaves), magnetic forces, and ultrasounds [101,102]. Remote triggers often lead to damaging of the capsules and burst release of the encapsulated substances.

4. Physical stimuli

4.1. Temperature

Variations of temperature is one of the environmental parameters applied to cause changes in the structure of some PEM that imply changes in their properties [103]. The mechanism of the temperature-driven structural rearrangements in polyelectrolyte films known as the coil-globule transition is a reversible switch of polymer chains conformation from an expanded coiled conformation into a globular one [104,105].

Poly(*N*-isopropylacrylamide) (PNIPAM) is one of the most explored in the field of temperature-sensitive polymers. Films containing PNIPAM were found to exhibit thermo-sensitive behavior [106,107,108]. The phase transition of an aqueous solution of PNIPAM observed by raising the temperature above ca. 32 °C (so-called lower critical solution temperature, LCST) originates from the breaking of the hydrogen bonds between the functional groups of PNIPAM and water molecules. Destruction of these hydrogen bonds leads to the exclusion of water from the chains and the formation of insoluble globules [109]. This process is reversible and can be inverted by lowering the temperature below LCST [103]. Jaber and Schlenoff discovered that the permeability of membranes built-up from cationic and anionic polymers containing PNIMAM segments was controlled by temperature [110]. The selected polyelectrolytes were: poly(allylamine hydrochloride) (PAH) serving as a polycation and poly(sodium 4-styrenesulfonate) (PSS) as polyanion, leading to the formation of PAH-*co*-PNIPAM/PSS-co-PNIPAM copolymers PEM. Its permeability upon heating was reduced by about 50% for potassium ferricyanide as an electroactive probe and the process was found reversible. It was a promising result for potential controlled drug release systems. On the other hand, PNIPAM-grafted interfaces proved to be useful in cells controlling the attachment/detachment of cells by switching the temperature above and below the phase transition one [111]. These studies were followed by others, confirming that the removal of cells from PNIPAM surface allows preserving the cells structure and surrounding [112,113,114,115], and thus, to maintain their size and secretion ability [103]. Ferreira et al. showed that poly[1-[4-(3-carboxy-4 hydroxyphenylazo)benzene sulfonamido]-1,2-ethanediyl, sodium salt] (PAZO) alternated with PAH interact with biomolecules in a controlled manner [116]. Those films were applied for the one-pot cell seeding approach which leads to an alignment of human dermal fibroblasts. Temperature decrease caused the formation of monolayers of such aligned cells. Those so-called "cell sheets" exhibited advantageous mechanical properties, showing differential shrinkage, which was direction-dependent, while maintaining the cells and polypeptides orientation [117].

Another impact of varying temperature on already formed PEMs was demonstrated by Diamanti et al. [118]. They showed the temperature annealing of poly-L-lysine (PLL) and alginate (ALG) multilayers. Reorganization of both PLL and ALG within the film into complexes resulting in maximal charge compensation was shown using AFM analysis - the PEM surface became smoother with increasing temperature. Simultaneously, the wetting properties of its surface changed from hydrophilic to hydrophobic. Kolasinska et al. [119] described the PAH/PSS films under exposure to elevated temperature. PAH/PSS subjected to hot (70 °C) water underwent glass-to-melt transition [117,120,121]. The structural changes of PAH/PSS after exposure to elevated temperature were also analyzed using neutron reflectometry [119]. The authors found that upon heating, water was excluded from the multilayer interior which resulted in the film densification and the multilayers became less rough. Koehler et al. observed a similar, but stronger effect for capsules, which will be described more in detail below [122]. Additionally, they observed the shrinkage of capsules' walls. In the case of films bounded to the surface, the change in PEM thickness was minor probably due to the fact that oppositely to free-standing capsules, PEM being assembled on the macroscopic surface reduced the freedom of chain conformations [123]. Kolasinska et al. observed also an increase in hydrophobicity of PEM upon heating. Moreover, they found a significant difference in the subsequent deposition of nanoparticles on PAH/PSS films depending on previous heating of PEM. In the case of nontreated films nanoparticles diffused inside the film resulting in a "mixture" of polyelectrolytes and nanoparticles. However, when multilayers were previously exposed to 70 °C water, a 2D "ordered" monolayer of nanoparticles formed on the surface of PAH/PSS [119].

Effect of densification of PEM upon heating, indicated by the decrease in scattering length density was also observed by Steitz et al. for poly(diallyldimethylammonium chloride) (PDADMAC)/PSS [115] and Zerball et al. [124]. Although different aspects of controlled loading/releasing of PEM are described mostly for polyelectrolyte capsules, some studies are dealing with PEM deposited on macroscopic supports. Saikaew et al. showed temperature-dependent loading/releasing of PDADMAC/PSS films by curcumin solution. Loading (additionally driven by solvent partitioning) reached the maximum at 5 °C, while releasing of curcumin occurred spontaneously by exposing the PEM to water at body temperature (37 °C) [125].

Golonka et al. studied the temperature-response of multilayers built up using thermosensitive polypeptides – ionic elastin-like recombinamers (ELR) [126]. ELR are artificial biopolymers, consisting of repeating sequences present in the tropoelastin domains, obtained by DNA recombination technique, which provides almost unlimited ability to tune their properties by a selection of components. Ionic mers built-in for this study were lysine (cationic) and glutamic acid (anionic). The authors observed reversible, thermally-induced shrinking-swelling behavior with a meaningful ratio of the thickness measured for the range of temperature from 25 °C to 40 °C. They showed that structural changes upon rising temperature stabilized the multilayers making them good candidates for biomedical applications as tissue scaffolds or coatings for implants. Sausa et al. studied LbL multilayers based on sequential cycloaoctyne- and azide-modified ELRs. They showed that the structure of the film depends on the incubation temperature, i.e., multilayers kept above the transition temperature were more rough and hydrophobic oppositely to films kept below this temperature (changes in the range 25 °C - 37 °C) [127]. They studied also cellular response for these two types of ELR, showing that cell adhesion, activity, and differentiation were related mainly to the chemistry of the ELR, which means that any designed ELR must be tested to prove its ability to some biomedical applications.

Other interesting studies on thermoresponsive multilayer systems were described by Xu et al. [128]. They presented films of hyaluronic acid (HA) with block copolymer micelles (BCM) containing PNIPAM. The use of BCM was to enhance the loading capacity of the films for active agents. They demonstrated reversible swelling/shrinking behavior upon the temperature change induced by alternating protonation/deprotonation of PNIPAM in BCM, indicating possible applications of such systems as hydrophobic drug nanocontainers.

As it is mentioned above, the behavior of capsules shells upon changing temperature was studied by Köhler et al. [122]. PEM at room temperature are typically in a kinetically stable glassy phase. When the temperature of a solution increases above the temperature of a glass transition, multilayers turn into a viscoelastic state. More mobile polyelectrolyte chains rearrange towards more thermodynamically stable systems that could lead to swelling or shrinking of capsules. The direction of polyelectrolyte rearrangement depends on the charge balance within shells and is forced by the interplay between competing electrostatic and hydrophobic forces. When the number of opposite charges within the shells is balanced so they compensate each other to a large extent, hydrophobic interactions dominate and the capsules shrink to reduce the interface area between the polymer layer and water. Otherwise, when in the polyelectrolyte shells there is an excess of the uncompensated charged groups, the electrostatic interactions dominate and capsules swell due to repulsion between the like charges. For better clarity discussed examples of temperature controlled polyelectrolyte

multilayer films are collected in the Table 1.

Capsules consisting of PDADMAC and PSS can swell or shrink upon exposure to temperature depending on which polyelectrolyte is the outermost layer. When the outermost layer is formed by more hydrophobic PSS the charge balance is more or less equilibrated. PSS adsorbs on the capsule's surface without diffusion within the shell and slightly overcompensates the outer positive charge. Due to the domination of hydrophobic interaction such capsules shrink. When the PDADMAC is the outermost layer electrostatic interactions dominate [129,130]. This is because of the penetration of PDADMAC chains within multilayers that causes irregular growth of the polymeric film and provides an excess of the positively charged groups. Repulsion between not compensated like charges leads to the capsules swelling. Thermally-induced swelling of capsules with PDADMAC as the outermost layer was employed to release dexamethasone (glucocorticoid drug) (Fig. 3) [40]. It was reported that the capsules formed in the absence of salt exhibit greater changes in permeability with increasing temperature than those synthesized in 0.5 M NaCl solution.

In the case of capsules consisting of PAH and PSS, shrinking was observed when capsules were terminated with PAH, while no significant shrinkage was observed for the capsules with PSS as the outermost layer [131]. Nevertheless, in both configurations permeability of the capsules was reduced after heating [132]. This is because both PSS, as well as PAH during the preparation of the capsules, adsorb on the surface without deep penetration within the shell providing an equilibrated charges ratio.

Temperature-sensitive capsules capable of reversible shrinking upon changing the temperature were fabricated by application of polymers that undergo coil-globular phase transitions. A fluorescence probe, fluorescein isothiocyanate (FITC) was entrapped within capsules made of PSS and thermo-responsive star polyelectrolyte, poly(*N*,*N*-dimethylaminoethyl methacrylate) (PDMAEMA) upon heating to 45 °C and subsequently it could be gradually released by cooling down to the room temperature [95]. Additionally, those capsules were able to change their size in response to the changes in pH and salt concentration. Another example of temperature-sensitive capsules that undergo reversible changes in their size are the capsules consisting of azido- and acetylene-functionalized PNIPAM copolymers. The capsules were synthesized by covalent bonding using click chemistry. After shrinking, the capsules become impermeable for higher molecular weight molecules [133]. Single component capsules made of 7 layers of poly(N-vinylcaprolactam) showed reversible thermoresponsive behavior as well. The capsules demonstrated a size decrease of 21% and 23% in the case of cubic and spherical capsules respectively, after heating from 25 °C to 50 °C. The capsules' size and shell thickness were completely recovered when cooling down to 25 °C [134].

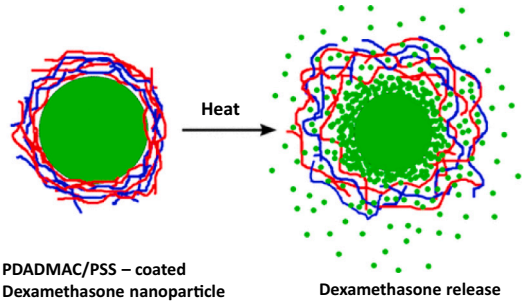

Fig. 3. Release of dexamethasone from the nanoparticles coated with PDADMAC/PSS multilayer upon increasing of temperature (reproduced from [40] with permission, copyright 2014 American Chemical Society).

For better clarity the discussed examples of temperature controlled polyelectrolyte multilayer capsules are collected in the Table 2.

Table 2
Examples of temperature controlled polyelectrolyte capsules.

Capsule's structure	Temperature	Mechanism of temperature triggering	Literature
PDADMAC/PSS/ dexamethasone NPs	37 °C	above Tg, PDADMAC penetrates within multilayers providing an excess of the positively charged groups repulsion between not compensated like charges leads to the capsules swelling	[40]
(PSS/PDMAEMA)	45 °C (pH = 7)	Due to a coil-globular phase transition of	[95]
Acetylene modified PNIPAM/Azido modified PNIPAM	30 °C	multilayer component, capsules shrink above glass transition temperature and	[133]
poly(N-vinyl-caprolactam)	50 °C	swell after temperature decreasing	[134]

Table 1
Examples of temperature controlled polyelectrolyte multilayer films.

Multilayer structure	Temperature responsive compound	Temperature	Mechanism of temperature triggering	Literature
poly(allylamine hydrochloride)-*co*-poly(*N*-isopropylacrylamide), PAH-*co*-PNIPAM; and poly (styrene sulfonate)- *co*-poly(*N*-isopropyl acrylamide), PSS-*co*-PNIPAM	poly(*N*-isopropylacrylamide) (PNIPAM)	33 °C and 45 °C	volume phase transition, enhancing hydrophobic interaction leading to change of its conformation from a well hydrated coil to an insoluble globule	[110]
poly(styrene sulfonate)- *co*-poly(*N*-isopropyl acrylamide), PSS-*co*-PNIPAM		32 °C	volume phase transition, enhancing hydrophobic interaction leading to change of	[111]
poly(*N*-isopropylacrylamide) (PNIPAM)			its conformation and increase in hydrophobicity of film's surface	[112] [114]
poly-L-lysine (PLL) / alginic acid sodium salt (Alg)	poly-L-lysine (PLL) / alginic acid sodium salt (Alg)	37 °C, 50 °C and 80 °C	reorganization of the PEMs from a layered structure into complexes with enhanced	[118]
poly(allylamine hydrochloride) (PAH) /poly(sodium 4-styrenesulfonate) (PSS)	poly(allylamine hydrochloride) (PAH)	70 °C	interactions of polycations and polyanions (glass-melt transitions)	[119]
poly(diallyldimethylammonium chloride) (PDADMAC) /poly(sodium 4-styrenesulfonate)(PSS)	poly(diallyldimethylammonium chloride) (PDADMAC)	40 °C 37 °C		[123] [125]
elastin-like recombinamers (ELR) with lysine or glutamic acid	elastin-like recombinamers (ELR)	40 °C	volume phase transition	[126]
cycloaoctyne- and azide-modified ELR	cycloaoctyne- and azide-modified ELR	37 °C	volume phase transition resulted in increase of roughness and more hydrophobic behavior	[127]
hyaluronic acid (HA) with block copolymer micelles (BCM) containing 2- hydroxyethyl methacrylate (PHEMA) and poly(*N*-isopropylacrylamide) PNIPAM	PNIPAM-b-PHEMA Block Copolymers	55 °C	volume phase transition resulted in more hydrophobic behavior, deswelling and thus, shrinkage	[128]

4.2. Ultrasounds

The ultrasound is a cyclic sound pressure with more than 20 kHz frequency. Ultrasound waves propagating through a certain medium can induce localized pressure variations and temperature increase, which can be employed for ultrasound-triggered release. Waves passing through the probe create microbubbles of air that oscillate in the surrounding fluid until they collapse causing cavitation that generates enormous energy in the fluid. This induces shear forces in the capsule shells and leads to their disintegration. Additionally to the capsule damaging it can contribute to local hyperthermia, bulk streaming of the fluid, or micro streaming of currents generated locally in the area of cavitating bodies [135]. Therefore, in most cases, capsules are completely destroyed within seconds and burst release of encapsulated molecules takes place. The behavior of the ultrasound-sensitive capsules depends on ultrasounds power and frequency as well as the exposure time [101].

The ultrasound-mediated release is strongly related to the mechanical robustness and rigidity of the capsules. Mechanically rigid PSS/PAH capsules are quite resistant to ultrasounds and require a very high power of ultrasonication for their disintegration [136]. Such capsules became more sensitive to ultrasounds after incorporation of ZnO [137], TiO_2 [138], SiO_2 [139], gold nanoparticles [140] and superparamagnetic Fe_3O_4 nanoparticles [102] into their shells. This could be related to the reduction of the capsules' elasticity due to the presence of a high amount of nanoparticles in the shell that made capsules prone to break upon exposure to ultrasounds [136,140]. Another explanation is that higher sensitivity for ultrasounds is the result of improved acoustic energy absorption due to the increase in density gradient across the water/shell with nanoparticles interface [140].

Lisunowa et al. demonstrated a broad study on ultrasound-sensitive capsules consisting of hydrogen-bonded tannic acid (TA) and poly(N-vinylpyrrolidone) (PVPON) that show high imaging contrast and release of DOX upon low power irradiation (100 mW/cm^2) used for diagnostic, as well as high power irradiation (above 10 W/cm^2) used for cancer therapy (Fig. 4) [141]. It was demonstrated that imaging contrast of these capsules was related to the capsules' mechanical properties and can be controlled by the type of polyelectrolyte, number of polyelectrolyte layers, and polyelectrolyte molecular weight. Capsules made of relatively rigid TA give lower contrast imaging than capsules with flexible poly(methacrylic acid) (PMA) as wall ingredients. Consequently, imaging contrast of capsules increased with decreasing number of polyelectrolyte layers as well as decreasing molecular weight of PVPON. It was demonstrated elsewhere that with decreasing molecular weight of PVPON from 1300 kDa to 360 kDa and 55 kDa, the elastic modulus of TA/PVPON capsules also decreased from 4.3 MPa to 1.6 MPa and 0.89 MPa respectively [142].

Other examples are capsules consisting of bovine serum albumin (BSA)/TA multilayer's loaded with magnetite nanoparticles. $CaCO_3$ microparticles were used as sacrificial core loaded by freezing-induced method with magnetite nanoparticles and fluorescently labeled BSA. Such prepared ultrasound responsive capsules were disintegrated within

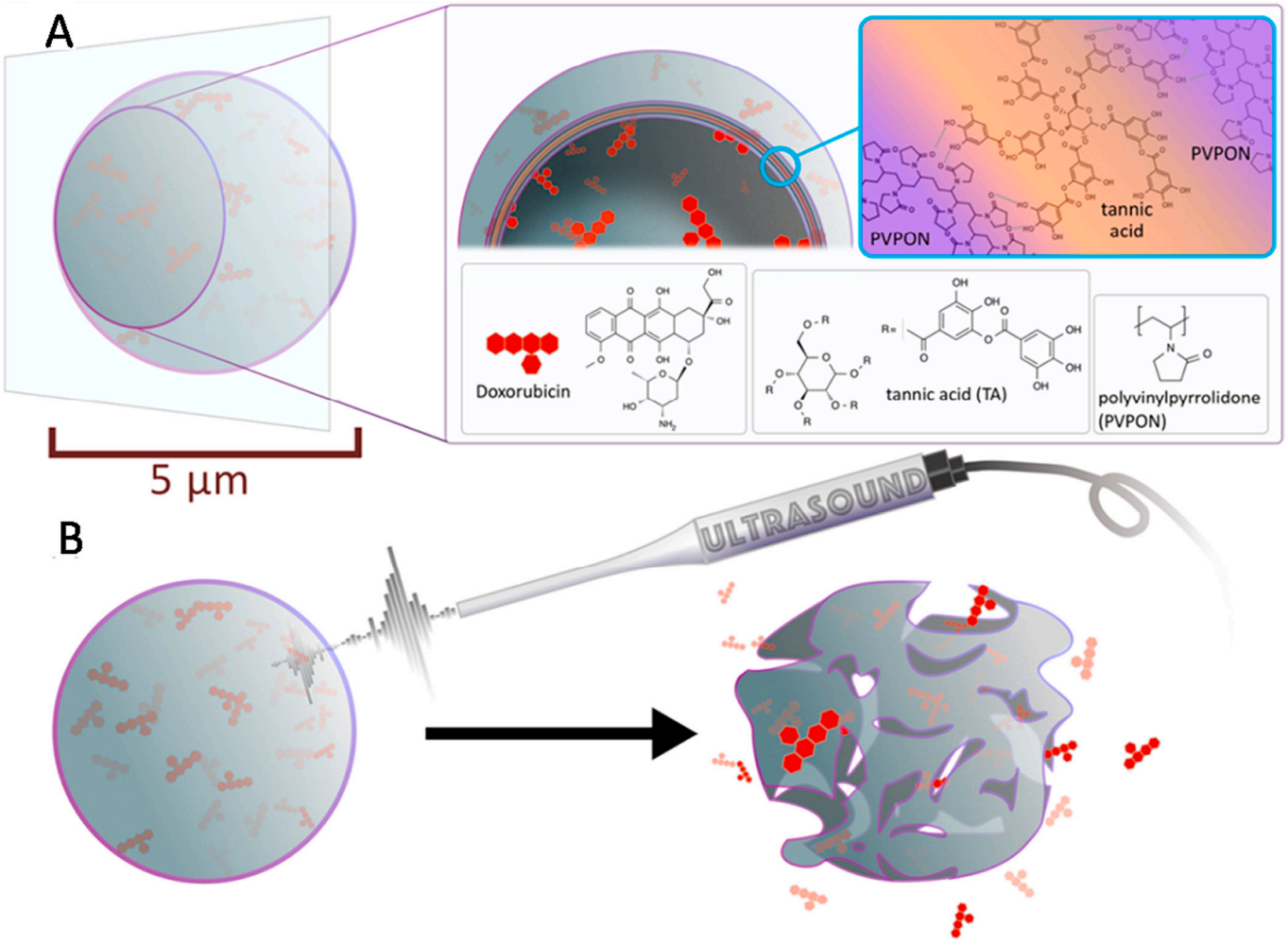

Fig. 4. Schematic representation of: (A) hydrogen-bonded TA/PVPON capsules with encapsulated DOX; (B) ultrasounds-triggered destruction of capsules (reproduced from [141] with permission, copyright 2017 American Chemical Society).

1 min under high-intensity focused ultrasound. The release behavior was tested by in vitro and in vivo studies [143]. Ultrasounds mediated systems are mostly developed towards theranostic applications, where both the tracking of drug carriers and triggering drug release in the desired place are crucial.

4.3. Light

Light irradiation has been used as an external trigger offering the ability to accomplish an easily adjusted and precise spatiotemporal control over the attachment/detachment of biomolecules, cells, or biosensors as well as the release of encapsulated cargo for controlled drug delivery. Since light is capable of penetrating deeply into tissues it has great potential in the biomedical field. Thus, the design of multilayer systems incorporating absorbing centers attracted the attention of researchers dealing with stimuli-responsive PEM. A number of various strategies based on the incorporation of light-responsive materials into polyelectrolyte films, such as metal nanoparticles, metal oxides, functional dyes, or polyoxometalate have been proposed to date [144] (Fig. 5).

Light interacting with PEM mainly causes their disassembly and (partial) removal from the support or release of cargo from the microcapsules. It was used in surface patterning as an external stimulus, which promotes the dissolution of some polymers [145]. Cao et al. used a polyaniline derivative with a photosensitive diazoresin polymer to achieve micropatterns of PEM after UV exposure through a photomask that led to photo-induced changes in solubility of the resin. Irradiated areas became insoluble while not irradiated ones were decomposed and removed with an alkaline solution. This system was applied for the fabrication of a pattern of fluorescent-labeled antibodies and described as a simple and fast immunoassay method of antigen-antibody recognition [146]. A similar mechanism was studied by Wang et al. who found that films containing poly(acrylic acid) (PAA) and an azobenzene-tailored surfactant were decomposed by exposure to UV light [147].

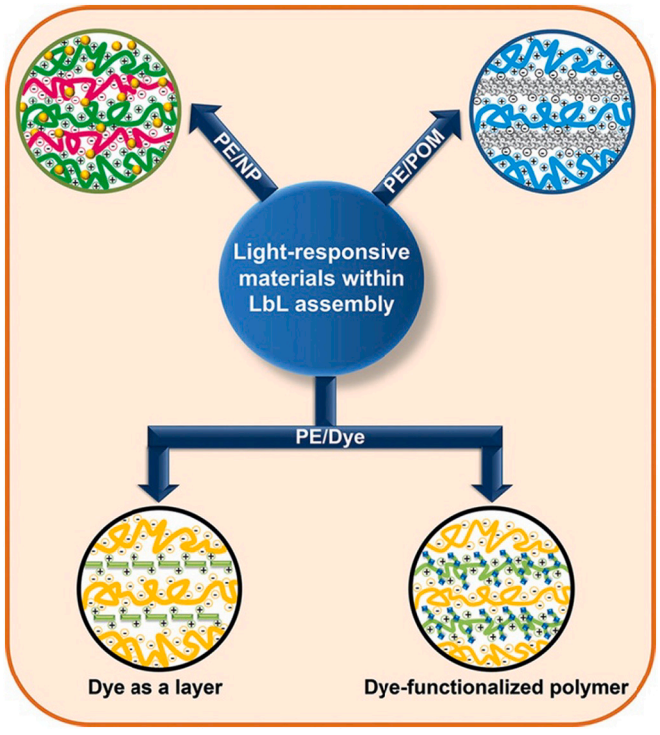

Fig. 5. Schematic illustration of various light-responsive components within multilayers: NP – nanoparticles, POM-polyoxymetalate, dyes, and dye-functionalized polymer (reproduced from [144] with permission, copyright 2014 WILEY-VCH Verlag GmbH & Co. KGaA).

By using a photomask they obtained a precisely controlled patterned surface. Tercjak et al. described a photoresponsive system of chitosan (CH) and water-soluble poly(vinylamine) with an azo dye as a side chain. By some manipulations they were able to achieve a high level of photo-orientation leading to the optically active system with potential applications in optics, electronics, and biotechnology due to biocompatibility and biodegradability of CH [148]. Tanchak et al. reported the photomechanical response of multilayer containing azobenzene-functionalized PAA related to conformational changes within the film occurring after irradiation [149]. Zhang and coworkers described photoresponsive and electrochromic properties of polyaniline and azobenzene-modified polyelectrolyte as promising in photonic devices [150]. Moreover, the studied structures showed high resistance to erosion by organic solvents. Pennakalathil and Hong reported PDADMAC/PSS PEM with a sacrificial multilayer composed of poly(acrylate) containing merocyanine pendant groups that rapidly disassemble when irradiated with visible light [151]. Due to photoisomerization of ionic merocyanine to neutral spiropyran the attractive electrostatic interactions within the film disappear and its hydrophobicity increases that leads to the release of PDADMAC/PSS free-standing film. The films with spiropyran groups can be applied for protein and cell adhesion control on surfaces [152,153]. When illuminated with UV light, spiropyran isomerizes from the hydrophobic spiro structure to the polar, zwitterionic merocyanine group. Desorption of fibrinogen, platelets, and mesenchymal stem cells from the surface covered with poly(spiropyran-*co*-methyl methacrylate) was observed by Higuchi et al. [152], while Edahiro et al. demonstrated reverse adhesion of living cells on films containing PNIPAM with spiropyran as side chains [153]. Moreover, they showed that different types of cells have unique sensitivity towards UV irradiation.

Another strategy for the use of light as a trigger is the incorporation of nanoparticles sensitive to irradiation into PEM. Yuan et al. introduced TiO_2 nanoparticles into the multilayers to enable their action of contact-killing of bacteria. TiO_2 was chosen for its potential to create biocidal radicals upon UV light irradiation to obtain long-term antimicrobial surfaces [154]. Corbitt et al. showed that poly(phenylene ethynylene)-type conjugated PEM microspheres entrapped and oxidatively killed bacteria in response to illumination with the visible light [155].

Möhwald et al. described functionalization of planar PLL/HA and PAH/PSS films with nanocapsules and gold nanoparticles used as triggers for the release of multilayer components, cargo as DNA for tissue engineering and biocoatings [156,157,158].

For better clarity the discussed examples of light controlled polyelectrolyte multilayer films are collected in the Table 3.

Nanoparticles and chromophore molecules that absorb light can be incorporated into PEM microcapsules walls for the triggered release of encapsulated substances under exposure to light irradiation. UV- and visible light-responsive capsules were designed to be applied in e.g. agriculture and cosmetics while NIR-sensitive systems are desired for biomedical applications. The light absorption by the skin, blood, and most tissues is relatively low for wavelengths in the range of 700–1700 nm (near-infrared therapeutic window) [159] allowing for deep and safe penetration of light into tissues by a few centimeters [160]. Thus, NIR-sensitive capsules have been intensively studied as carriers in intercellular delivery of drugs, time-specific release and as bioreactors [161,162,163,164]. Additionally, similar to magnetic hyperthermia, the NIR-induced local heating was investigated in the photodynamic treatment of cancer and could be combined with NIR-triggered release of encapsulated drugs in one system [165,166,167].

Pioneering research on NIR remote release of cargo from capsules concerned the incorporation of plasmonic gold and silver nanoparticles that exhibit strong absorption in the NIR region due to the surface plasmon resonance (SPR) oscillations [168,169,170]. An increase in vibration energy related to absorption of light in the SPR band induces temperature rising that can be used to affect capsules' permeability. SPR wavelength region is determined by structural features of the

Table 3
Examples of light controlled polyelectrolyte multilayer films.

Multilayer structure	Light responsive compound	Wavelength [nm]	Mechanism of light triggering	Literature
polyaniline derivative (PAAA)/ diazoresin (DR)	diazoresin (DR)	360	micropattern formation by DR disassembly regulated by DR solubility via irradiation by UV light through photo mask	[146]
poly(acrylic acid) (PAA)/ azobenzene-containing surfactant triethylamine (AzoTEA)	azobenzene-containing surfactant triethylamine (AzoTEA)	360	micropattern formation by DR disassembly regulated by DR solubility via irradiation by UV light through photo mask	[147]
chitosan (CH)/ azopolymer poly[1-[4-(3-carboxy-4-hydroxyphenylazo)benzenesulfonamido]-1,2-ethanediyl, sodium salt] (PCBS)	azopolymer poly[1-[4-(3-carboxy-4-hydroxyphenylazo)benzenesulfonamido]-1,2-ethanediyl, sodium salt] (PCBS)	365	photo-orientation upon azobenzene trans-cis isomerization cycles	[148]
azobenzene-functionalized polyacrylic acid	poly-disperse red 1 acrylate (PDR1A)	514	film expansion due to azobenzene trans-cis isomerization cycles	[149]
polyaniline (PANI) and azo-polyelectrolyte	azobenzene-containing polymers: PNACN, PPAPE, PNANT or PNATZ	488	photoinduced dichroism caused by the photoisomerization and subsequent reorientation of the azo chromophores	[150]
poly(acrylate, merocyanine) (PMC).poly (diallyldimethylammonium chloride) (PDADMAC)	PMC	360	photoinduced isomerisation of PMC to poly (acrylate), spiropyran PSP leading to film	[151]
copolymer of nitrobenzospiropyran and methyl methacrylate, poly(NSP-*co*-MMA)	poly(NSP- *co*-MMA)	365	disassembly for cell adhesion control	[152]
poly(*N*-isopropylacrylamide) having spiropyran (pNSp-NIPAAm)	pNSp-NIPAAm	365		[153]
heparyn/chitosan-TiO_2	TiO_2	365	photocatalytical, contact-active antibacterial agent	[154]
hyaluronic acid (HA) and poly-L-lysine (PLL) and poly (styrene sulfonate) (PSS) and poly(allylamine hydrochloride) (PAH) with au nanoparticles	au nanoparticles	830	localized heating of the au nanoparticles within the film by IR light leading to local destruction of the polymer network	[156]
hyaluronic acid (HA) and poly-L-lysine (PLL) with gold nanoparticles				[157] [158]

nanoparticles: their size, aspect ratio, and aggregation state [171]. Thus, control over capsules permeability can be done by optimization of particles shape, size, and particles concentration in the capsules shells on the one hand and NIR irradiation power and period on the other hand. Gold and silver nanoparticles absorb electromagnetic waves in the visible range but it is possible to shift their absorption spectrum into the NIR region or to create a second absorption region by changing their size and shape [172,173].

Skirtach et al. demonstrated that PAH/PSS shells with a high concentration of silver nanoparticles with a diameter of 8 nm were destroyed under exposure to NIR irradiation (803 nm, laser intensity 25 mW) [169]. Similarly, PAH/PSS capsules with incorporated gold nanoparticles with a diameter of 6 nm were destroyed under 1064 nm laser pulses (10 ns) [168]. In both systems, capsule rupturing was explained by heating of the shells above the spinodal point of water and thermal stresses. In later articles, Skirtach et al. demonstrated PAH/PSS capsules with incorporated gold sulfide core/gold shell nanoparticles [174], and PDADMAC/PSS capsules with gold nanorods [175] and gold nanoparticle aggregates [176] as NIR absorbing centers with higher absorption in the NIR region as an alternative of single, densely packed nanoparticles. In such systems local heating (around NIR absorbing agents), above the glass transition temperature of polymer complex, provides enough energy to surpass the barrier necessary for polymeric chains rearrangements. That in consequence allows for an increase in shell permeability and sustained cargo release without capsules damaging.

Another mechanism of non-destructive cargo release was involved in the system consisting of hydrogel shells cross-linked by glucosamine-boronate ester complexes and duplex nucleic acids with embedded Au nanoparticles with a diameter of 30 nm or Au nanorods [173]. Irradiation with the wavelengths of 532 nm in the case of capsules with nanoparticles and 910 nm for capsules with nanorods, resulted in reversible dissociation of the nucleic acid cross-linkers due to plasmonic heating and local temperature increase to 50 °C and 54 °C, respectively. Switching off the irradiation source resulted in shells regeneration and blockage of release.

The release of encapsulated material from capsules containing gold [170] and silver [177] nanoparticles was demonstrated also inside living cells. Capsules with embedded gold nanostars were used to study the intercellular spreading of 43 different fluorescent molecular cargos that were released from endocytosed capsules after short laser irradiation. It was demonstrated that intracellular spread is not because of free diffusion, but it is determined by the interaction of the released molecules with intracellular components [178]. Recently, it was shown that optically resonant dielectric iron oxide nanoparticles (α-Fe_2O_3) have a broader spectral range of efficient optical heating as noble metals. Such nanoparticles incorporated into the capsules shells were used to deliver and remote release of anticancer drug vincristine upon laser irradiation within a tumor and healthy cells [179].

Other materials that were incorporated into the capsules shells as NIR absorbing centers were graphene oxide [180], single-walled carbon nanotubes (SWCNTs) [181], and multi-walled carbon nanotubes (MWCNTs) (Fig. 6 A) [182]. Microcapsules consisting of alternate layers of graphene oxide and PAH were completely destroyed after 45 s of irradiation (laser power 30 mW, 1064 nm) [180]. Similarly, PDADMAC/PSS capsules with one layer of partially oxidized SWCNTs within 15 min of NIR irradiation were disintegrated into the small fragments (pulsed laser power 9 mW, 800 nm) [181]. It was shown that PDADMAC/PSS capsules with incorporated MWCNTs in the amount of 7% only can be loaded with high molecular weight molecules of both charges after irradiation with a NIR broadband lamp (780–1400 nm) [182]. The increase of the capsules' permeability most likely occurred only locally in the proximity of the MWCNTs as the whole capsules were not damaged even after 40 min of irradiation. On the other hand, it was demonstrated that small molecules, which may easily diffuse through capsules shells, can be entrapped within their interior by increasing the temperature of an aqueous medium and they can be subsequently released from the capsules by NIR irradiation. Thus, an increase of temperature can be applied to influence the capsules' permeability and used for encapsulation when applied to the bulk capsules dispersion, or for release of cargo when applied locally (e.g. optical or magnetic heating; see further).

UV-VIS responsive capsules are fabricated either by application of polyelectrolytes with photo-responsive groups or by incorporation of

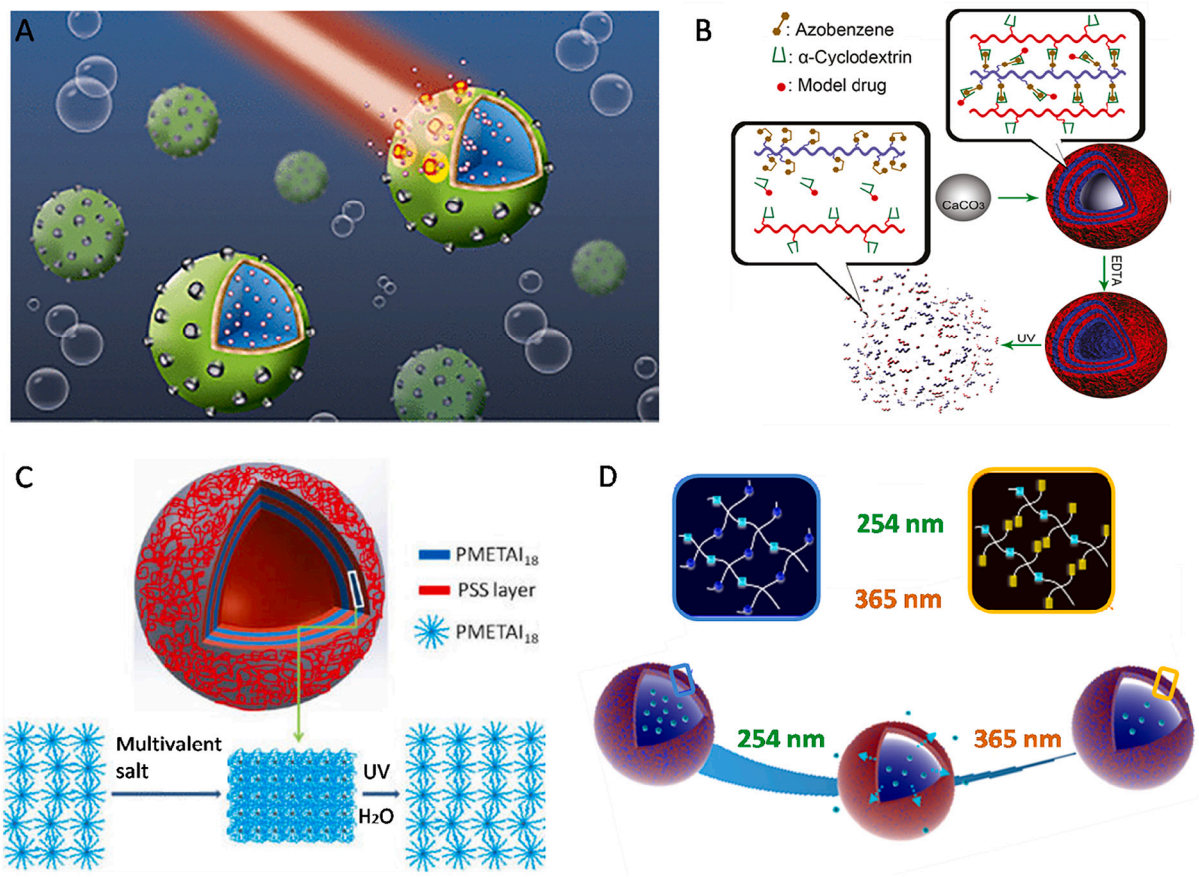

Fig. 6. PEM Capsules with light-sensitive ingredients: (A) Capsules with MWCNTs embedded across multilayer shells capable of nondestructive cargo release under NIR irradiation (reproduced from [182] with permission, copyright 2021 American Chemical Society). (B) Capsules containing α-cyclodextrin and azobenzene groups with photosensitive host-guest interaction (reproduced from [190] with permission, copyright 2011 American Chemical Society). (C) Capsules with star polyelectrolyte that reversible undergoes form collapse to expand state under UV-VIs irradiation (reproduced from [194] with permission, copyright 2012 American Chemical Society). (D) Capsules build of coumarin functionalized polymer capable of loading or unloading of cargo depending on the UV-VIs wavelength (reproduced from [195] with permission, copyright 2017 Elsevier).

inorganic nanoparticles that exhibit absorption in the UV-VIS region [183]. In capsules composed of photosensitive polymers, permeability changes can be the result of changes in a local polarity that is associated with (1) a shift in the hydrophobic/hydrophilic balance in the capsules shell or (2) degradation of the polymeric structure via selective cleavage of photolabile bonds or (3) crosslinking of polymeric components. These changes can be reversible or irreversible.

Poly[1-[4-(3-carboxy-4-hydroxyphenylazo)-benzenesulfonamido]-1,2-ethanediyl sodium salt (PAZO) with carbonated azobenzene side chains and maximum absorption band at 366 nm is one of the most used polyanion for the fabrication of UV-VIS responsive capsules. This is because azobenzene groups undergo a reversible cis-trans isomerization upon UV or visible light irradiation, and thus polymers with azobenzene moieties in their side chains or backbones can be used for fabrication of capsules with UV-VIS responsive encapsulation and/or release properties [184]. Capsules composed of PAZO as a polyanion and PAH as a polycation were shown to shrink irreversibly under UV irradiation that allowed for encapsulation of macromolecules in their interior [185,186]. An opposite behavior was observed for capsules composed of PAZO and PDADMAC that were damaged under exposure to UV-VIS. The different response of both types of capsules is related to the properties of the counterpart polycation that influence azobenzene groups orientation in multilayers and photoisomerization kinetics [187]. In the presence of PDADMAC, azobenzene moieties form end-to-end aggregates that under UV irradiation lead to phase separation and disintegration of the capsules [188]. The combination of PDADMAC/PAZO layers with diazo-resin/Nafion layers exhibited the opposite behavior under UV irradiation allowing to fabricate a system capable of encapsulation as well as the release of cargo. Diazo-resin/Nafion layers upon exposure to 380 nm irradiation underwent a rapid in situ crosslinking due to diazonium-related photolysis decreasing capsules permeability. On the other hand, PDADMAC/PAZO layers swell under irradiation at 360 nm and rupture after several hours of exposure [189].

Capsules disintegration was also achieved by the application of photosensitive host-guest interactions of azobenzene groups with α-cyclodextrin. Azobenzene groups in the trans form are well recognized by α-cyclodextrin, while the bulky cis form is excluded. Therefore UV-VIS switching from trans to cis form of azobenzene groups led to the disintegration of the shells and release of cargo molecules (Fig. 6B) [190]. Other walls ingredient that may cause capsules unsealing under UV-VIS irradiation are photodegradable o-nitrobenzyl derivatives [191,192] and photoacid generators (triphenylsulfoniumtriflate) that under UV light release protons leading to a decrease of pH of the medium that in turn causes capsules swelling [193].

There are also some examples of systems that can act reversibly under UV-VIS irradiation enabling encapsulation and subsequent release of substances. Capsules consisting of star polyelectrolyte, poly[2-(methacryloyloxy)ethyl] trimethyl ammonium iodide (PMATEI), and PSS in the presence of trivalent hexacyanocobaltate(III) ions shrink due to the collapse of PMATEI. While under UV irradiation trivalent ions turn into a mixture of mono- and divalent ions that lead to recovery of an expanded form of PMATEI (Fig. 6C) [194]. Reversible permeability

changes were also demonstrated for capsules made of coumarin functionalized polymer. Under the irradiation of 254 nm light the capsules were unsealed due to the photo-cleavage reaction, while under 365 nm light, the capsules' shells return to the sealed state due to photo-crosslinking (Fig. 6D) [195].

Another mechanism was involved for encapsulation in the capsules composed of weak polyelectrolytes: PMA modified with benzophenone and PAH. Cross-linking of the multilayers was done by hydrogen atom abstraction via excited benzophenone groups by UV irradiation. Importantly such photocrosslinking does not consume the functional groups of the polyelectrolytes thus the capsules preserved pH-responsive capability, while their stability in extreme pH conditions was improved [196].

Another approach involves the application of nanoparticles that absorb UV light. Gao et al. reported that polyelectrolyte microcapsules with needle-like TiO_2 nanoparticles with strong absorption in the UV range were destroyed upon exposure to UV light. The mechanism of disintegration of the capsules is not known yet but it is suspected that it is related to the generation of electron-hole pairs in TiO_2 nanoparticles that are transferred to the polyelectrolytes and decrease bonding forces [138].

For better clarity the discussed examples of light controlled polyelectrolyte capsules are collected in the Table 4.

4.4. Magnetic field

The use of the magnetic field in the area of polyelectrolyte multilayers is related to biomedical applications as targeted drug delivery systems based on microcapsules functionalized by magnetic nanoparticles and tissue visualization since biological tissues are transparent to magnetic fields. It opens a venue for designing drug delivery systems based on capsules with embedded magnetic nanoparticles that can be navigated by the permanent magnetic field and triggered to release the encapsulated substances by the alternating magnetic field in the place of destination. Biocompatible superparamagnetic nanoparticles have been already widely used in the medical field e.g. in intracellular drug delivery, magnetic hyperthermia therapy [197,198] magnetic resonance imaging [199] and biological sensing [200].

The behavior of the magnetic particles in an alternate magnetic field depends on the particle size, field frequency, and amplitude and can be affected by the environment [201]. At lower frequencies, the magnetic relaxation is done by the movement of a whole particle (Brown relaxation). At higher frequencies, where magnetic fields oscillate very fast and particles cannot follow it, relaxation takes place due to the movement of magnetic moment across an anisotropy barrier (Neel relaxation). The energy released during relaxation is dissipated and leads to the heating of the particles and their surroundings [202]. Both mechanisms of relaxation can be used to affect the permeability of capsules with embedded magnetic nanoparticles or/and to navigate them. Capsules responding to the magnetic field can be fabricated either by incorporation of magnetic particles into their walls [203] or by encapsulation of particles in their liquid interior [204,205].

Response of magnetic Fe_3O_4 nanoparticles incorporated into the PAH/PSS capsules to the applied alternating magnetic fields was utilized to release the encapsulated insulin. Immediate release of the cargo was the result of the structural reorganization of the shell caused by the movement of magnetic nanoparticles that led to an increase of the membrane permeability (Fig. 7A) [206]. Similarly, an alternating magnetic field was used to rotate the cobalt and gold nanoparticles embedded in PAH/PSS capsules. Deformed capsules became permeable for macromolecules with a molecular weight of 20 kDa after 30 min of exposure [207].

Much broadly investigated are capsules with magnetic nanoparticles used as a heat mediator for local heating caused by Nell relaxation or mechanical friction. Magnetically induced heating of nanoparticles is broadly investigated in hyperthermia treatment of cancer as well [208]. Combining both, anticancer drug release and hyperthermia in one system could give a more effective system for cancer treatment.

Hu et al. [209] monitored DOX release, capsules morphological changes, and temperature rise in the suspension of $(Fe_3O_4/PAH)_4$ microcapsules exposed to an alternating magnetic field. After 15 min of exposure, cracks appeared on the surface of the microcapsules, and after

Table 4
Examples of light controlled polyelectrolyte capsules.

Capsule's multilayer structure	Light responsive compound	Wavelength [nm]	Mechanism of cargo release	Literature
(PAH/PSS)/Au	ag NPs	803	local heating around NIR absorbing agents due to surface	[169]
(PAH/PSS)/Au	au NPs	532, 1064, 830	plasmon resonance (SPR) oscilations of NPs	[168,174]
(PDADMAC/Au/PSS)	au nanorods, Au NPs aggregates Au sulfide NPs	830		[170,175,176]
(PSS/PAH)/ α-Fe_2O_3	(α-Fe_2O_3) NPs	632.8	optical heating	[179]
graphene oxide/PAH	graphene oxide	1064	optical heating	[180]
PDADMAC/PSS/ SWCNTs	SWCNTs	800	local heating around SWCNTs	[181]
MWCNTs/PDADMAC/ PSS	MWCNTs	780–1400 nm broadband lamp	local heating around MWCNTs	[182]
$(PAH/PAZO)_3$/PAH/ PVS	PAZO	UV-VIS	reversible transition of azobenzene groups from cis to trans	[185]
PDADMAC/PAZO	PAZO	320–400 nm		[186]
PEI/4bromo-methyl-3nitro-benzoic acid	o-nitrobenzyl derivatives	362 nm	photodegradation	[191]
(PSS/PAH)/PAG	triphenylsulfoniumtriflate-photoacid generator (PAG)	254 nm	protons releasing and in turn decreasing of pH of the medium	[193]
PSS/PMETAI	PMETAI	365 nm + trivalent hexacyanocobaltate(III) ions trivalent hexacyanocobaltate (III) ions	trivalent ions turn into mono- and divalent ions that lead to an expanded form of PMATEI and capsules' swelling in the presence of trivalent ions capsules shrink due to the collapse of PMATEI	[194]
coumarin modified capsules	coumarin groups	254 nm 365 nm	capsules' unsealing due to the photo-cleavage reaction capsules' sealing due to photo-crosslinking	[195]
(PAH /PMA-BP)	benzophenone groups (BP)	275 nm	capsules' cross-linking by hydrogen atom abstraction via excited benzophenone groups	[196]
(PAH/PSS)/TiO_2	needle TiO_2 NPs	32–400 nm	electron-hole pairs in TiO_2 nanoparticles are transferred to the polyelectrolytes and decrease bonding forces	[138]

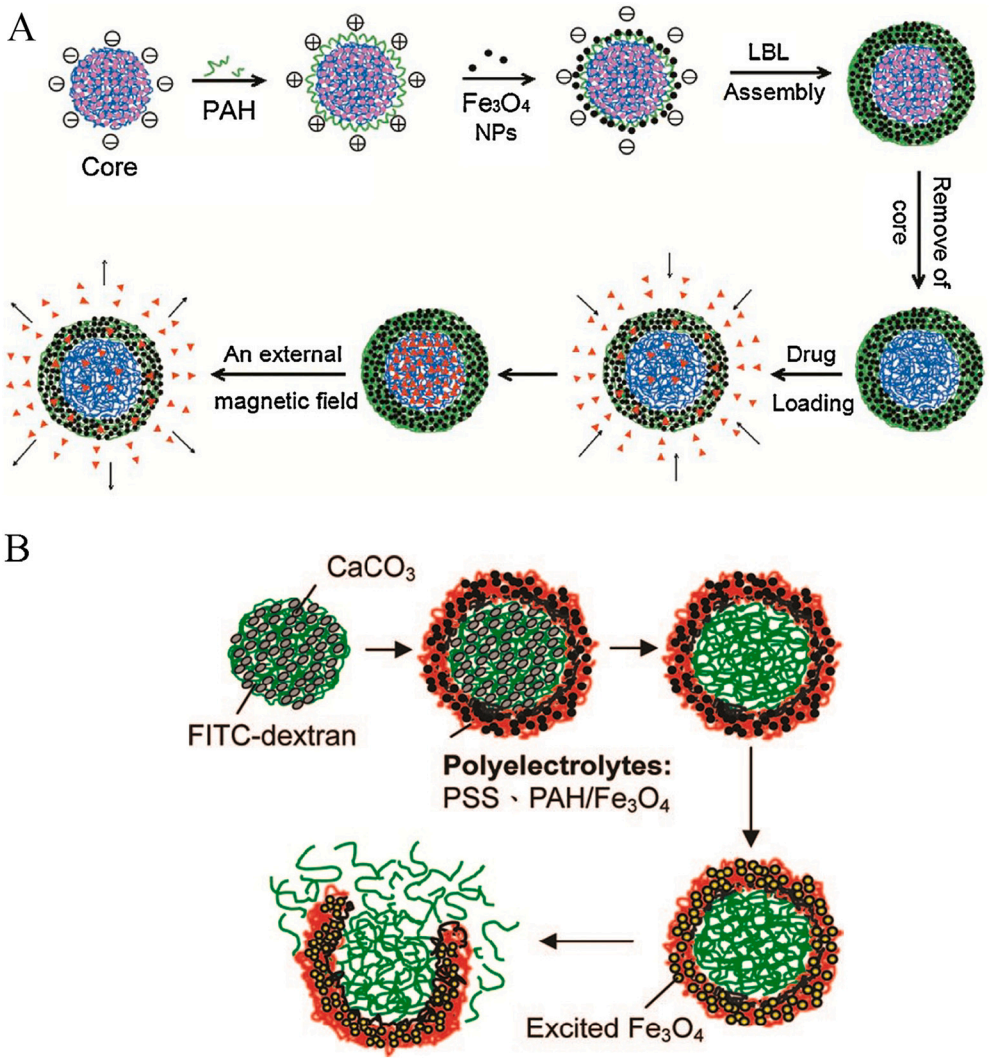

Fig. 7. (A) Schematic of highly magneto-sensitive multilayer microcapsules for controlled release of insulin. (reproduced from [206] with permission, copyright 2014 Elsevier). (B) Schematic presentation of the encapsulation and release of model macro-molecules (FITC-modified dextran) from the magneto-sensitive PEM capsules. After an alternating magnetic field treatment, the capsules rupture and release the encapsu-lated dextran (reproduced with permission from [209], copyright 2008 American Chemical Society).

30 min capsules were completely ruptured, causing a rapid increase in the DOX release. Fig. 7B presents the process schematically for a fluorescently-labeled dextran as a model cargo. Temperature rise from 23 °C to 46 °C was observed. Katagiri et al. [210,211] demonstrated that temperature rise in ((PSS/PAH)$_5$/Fe_3O_4/cationic lipid bilayer) micro-capsules suspension can be controlled by the concentration of Fe_3O_4 incorporated into the shells. The temperature rises from 19 °C to 58 °C in alternating magnetic field (within 15 min) was sufficient to induce the phase transition of a lipid bilayer that resulted in a non-destructive cargo release. Carregal-Romero et al. [212] confirmed that the final equilib-rium temperature of a medium that could be reached depends on Fe_3O_4 nanoparticles concentration and their shape. It was observed, that cubic magnetic nanoparticles have a higher adsorption rate of magnetic en-ergy compared to spherical ones and thus can be more efficient as heat mediators [213,214]. Cubic Fe_3O_4 nanoparticles incorporated into the PAH/PSS microcapsules in the concentration of 2.8 g/l allowed to rise suspension temperature up to 62 °C under exposure to alternating magnetic fields. Whereas, the concentration of 4.8 g/l enabled to reach suspension temperature as high as 90 °C (within 15 min) that resulted in the destruction of microcapsules walls and the release of loaded mole-cules [212].

5. Chemical and biological stimuli

5.1. pH and ionic strength

The physicochemical parameters of the films, such as thickness, stiffness, chemistry, stability, permeability, composition, might be modified to a certain extent by changing the assembly conditions. The thickness of the PEM coating might be well-controlled by varying the degree of protonation of the applied components changing ionic strength, pH of their solutions [215]. When PEM are assembled at a pH value near the pK_a value of any polyelectrolyte (PE), the polymer chains are not fully expanded leading to the formation of relatively thick films. As strong polyelectrolytes are charged over a wide pH range, it is not easy to control the properties of PEM based on such polymers unless one takes specific measures to disturb the polymer-polymer interactions by manipulating other stimuli like ionic strength, temperature, solvent polarity. Weak polyelectrolytes are charged in a smaller pH window, therefore, polymeric conformations could be easily modulated upon changing the pH of their solutions. The important feature of PEM formed from weak PEs is that they might be damaged at extreme pH conditions as the pH-induced charge imbalances in the coating overcompensate the attractive polymer-polymer interactions [216].

The pH-induced excess charge can be used to e.g.: binding and release low molecular weight compounds, such as drugs in PEM coatings composed of weak polyelectrolytes. Hiller and Rubner presented that

PAH and PSS could be embedded into a structured film with specifically designed molecular nanoarchitectures (by changing pH conditions during LbL adsorption) that made the film either virtually insensitive or highly responsive to small changes in post-assembly pH [217]. The elastic moduli of the coatings were dependent on the pH at which the polyelectrolyte multilayers were deposited. On the other hand, the stimulation conformational changes of polyelectrolytes chains in already prepared films/gels by varying pH or ionic strength of the environment commonly are relatively slow. In addition to limited conformational freedom of entangled or cross-linked polymer chains, these responses are slowed down by the necessary diffusion of ions into the coatings.

Park et al. showed that crosslinked weak PEMs present selective ion permeability for cationic and anionic probe molecules, which may be reversibly switched by changes of pH [218]. The most common results of the response of PEMs to environmental changes (ionic strength, pH variations) are (1) decomposition of the film or (2) selective release of the chains [219], which can diffuse through the PEM coating [220], or can take part in competition and replacement reactions within the multilayers.

The film thickness, composition, and layer interpenetration in PEMs made of weak polyelectrolytes may be precisely tailored at the molecular level by adjusting pH during the assembly. The pH effect on PEMs formation of synthetic weak polyelectrolytes e.g., PAH and poly(acrylic acid) (PAA) has been studied by Yoo et al. [221]. If pH increases from 2.5 to 4.5, the PAA layer thickness decreases because of the higher charge density and reduced loop and tail fragmental density. The PAH layer thickness is unchanged since the polyelectrolyte chain is nearly fully charged over this pH range. Furthermore, there is a preferred penetration of a polyelectrolyte from the thicker layer to the thinner one or a high level of interpenetration between thin neighboring layers pointing to the strong dependence of the interpenetration degree on pH. Similarly, for a natural polysaccharide such as CH and ALG, the layer thickness of CH increases with increasing the assembly pH, while that of ALG stays nearly the same because of the same assembly pH [75]. It was shown that pH-tunability of the natural biocompatible weak polyelectrolytes expands the biomedical applications of PEMs to immobilization of antibodies with high loading, and superior binding activity could be obtained via adjusting their surface chemical composition through pH control [222]. The swelling ability of PEM in aqueous solutions plays an important role in other applications related to e.g., membrane separation and drug delivery system [223]. The swelling behavior studies on PAH/PAA multilayers showed that the degree of swelling, swelling rate, and the time to obtain the maximum swelling could be tuned by assembly pH, possibly due to pH-tunable ionic cross-linking and varying loop density [224]. The highly pH-dependent swelling was also noticed for natural weak PEMs. PLL/HA films swell much more when formed at pH 9 than at pH 5 as weakly charged PLL molecules at the higher pH create loosely cross-linked films with HA [225]. The mechanical properties of PEM are associated with interchain ionic cross-linking and molecular conformation in the films that are tunable by changing the assembly pH [226]. The ionic conductivity of PEM made of weak PE could be tailored by assembly pH. For the PE pair linear polyethylenimine (LPEI)/PAA, the ionic conductivity of the films at pH 5 is one order of magnitude greater than that of multilayers assembled at pH 2. It is possible that at pH 5, there is a high content of a mobile and uncoordinated polyethylenimine (PEI) chains increasing ion mobility more effectively than carboxylic acid groups in PAA [227]. The pH-dependent changes of ionic conductivity were noticed also in hydrogen-bonded weak polyelectrolyte based multilayers, because of the pH-adjustable crosslinking degree of the polymer network, which can greatly affect the ion and water transport [228]. Weak polyelectrolyte films might be responsive to post-assembly pH. Novel structures were obtained through pH-induced ionic bond-breaking and reformation mechanisms. With a slight change in the post-treatment pH, various morphologies of PEI/PAA multilayers with pores from the nanometer scale to the micrometer scale were noticed (Fig. 8) [229,230].

The PEI/PAA films formation at pH 5 shows nanoporous morphology after rinsing with a solution at pH 1.75, but a heterogeneous structure with nanopore and micropore regions at pH 2. Properties such as wettability, swelling, and permeability could be also regulated by the post-assembly pH.

Burke et al. presented that the water contact angles of PLL/HA films change with the pH values. At high pH, the PLL has more $-NH_3^+$ groups deprotonated which decreases hydrophilicity, while HA has more -COOH groups ionized enhancing hydrophilicity. The thickness of PAH (pH 7.5)/PAA (pH 3.5) multilayers reversibly changes when subjected to pH above around 5.5 or 2 [231]. The multilayers swell at pH 2 because of the breakage of $NH_3^+ - COO^-$ ionic cross-links due to protonation of the carboxylate groups from PAA and is driven by osmotic forces and charge repulsion among the free, positively charged amine groups formed from the breakage of the ionic cross-links. However, the film deswells at pH 5.5 because the higher-pH solution deprotonates carboxylic acid groups from PAA to carboxylates and reforms carboxylate-based ionic linkages.

The stable weak PEMs formed via the LbL method of benzophenone-modified PAA and benzophenone-modified PAH followed by photo-cross-linking, show a pH-sensitive bipolar ion-permselective property, due to the change of electrostatic interaction between building blocks caused by changing the pH [218]. The properties of weak polyelectrolyte multilayers can be tuned by adapting the salt concentration. The nanoporous PAH/PAA films were formed by deposition of polymers in 0.2 M NaCl, followed by rinsing with pure water [232], making use of the distinction of electrostatic interactions with and without salt. The salt concentration might affect the formation and stability of weak PEMs. A critical “glass transition ionic strength” was reported, as a value at which the buildup of layers stops and the dissolution process starts. This effect was also found to be dependent on the salt type [233,234,235].

The pH-adjustable properties of weak polyelectrolytes might be maintained in weak polyelectrolyte/strong polyelectrolyte multilayer systems, e.g.; the systems of PAH/poly(vinylsulfonic acid) (PVS), PAH/sulfonated polystyrene (SPS), poly(diallyldimethylammonium chloride) (PDAC)/PAA, and poly(4- vinylbenzyltrimethylammonium chloride) (PVTAC)/PAA. The transition from thin layers to much thicker deposition layers appeared when the charge density of the weak polyelectrolyte decreased from its fully charged state to 70–90% charged units, comparable to the weak polyelectrolyte multilayers [236].

Elzbieciak et al. studied the formation of PEI/PSS PEMs by changing the PEI assembly pH [5]. The polyelectrolyte multilayer thickness increased regularly at the low pH of PEI while the nonmonotonic increase was observed at high PEI pH. The films formed from the high pH PEI solution present higher permeability than those from low pH solutions. Additionally, both synthetic and natural pairs of weak and strong polyelectrolytes PEMs were investigated. In [237] Elzbieciak et al. focused on PAH/PAA system, where both polyions were pH-sensitive, giving films of different thickness (including nonmonotonic growth) and morphology depending on pH value of the solutions used for the deposition. For the LbL assembly of CH and heparin, the charge density of CH decreases but the heparin charge density remains constant when the pH increases, leading to increased film thickness. Other properties of CH/heparin films e.g. surface roughness and wettability could be monitored by assembly pH as well [238,239].

The LbL deposition of weak polyelectrolytes and nanoparticles (NPs) can combine the advantages of both components of PEMs [240,241,242]. The formation of PEI/AuNPs multilayers at different pH conditions was studied [240]. Due to the pH-controlled charge density and conformation of weak polyelectrolytes, the interparticle distance of gold NPs might be extensively controlled by the assembly pH (Fig. 9A). In the end, the strength of Localized Surface Plasmon Coupling (LSPC) was successfully modulated in a broad range (Fig. 9B). The exponential

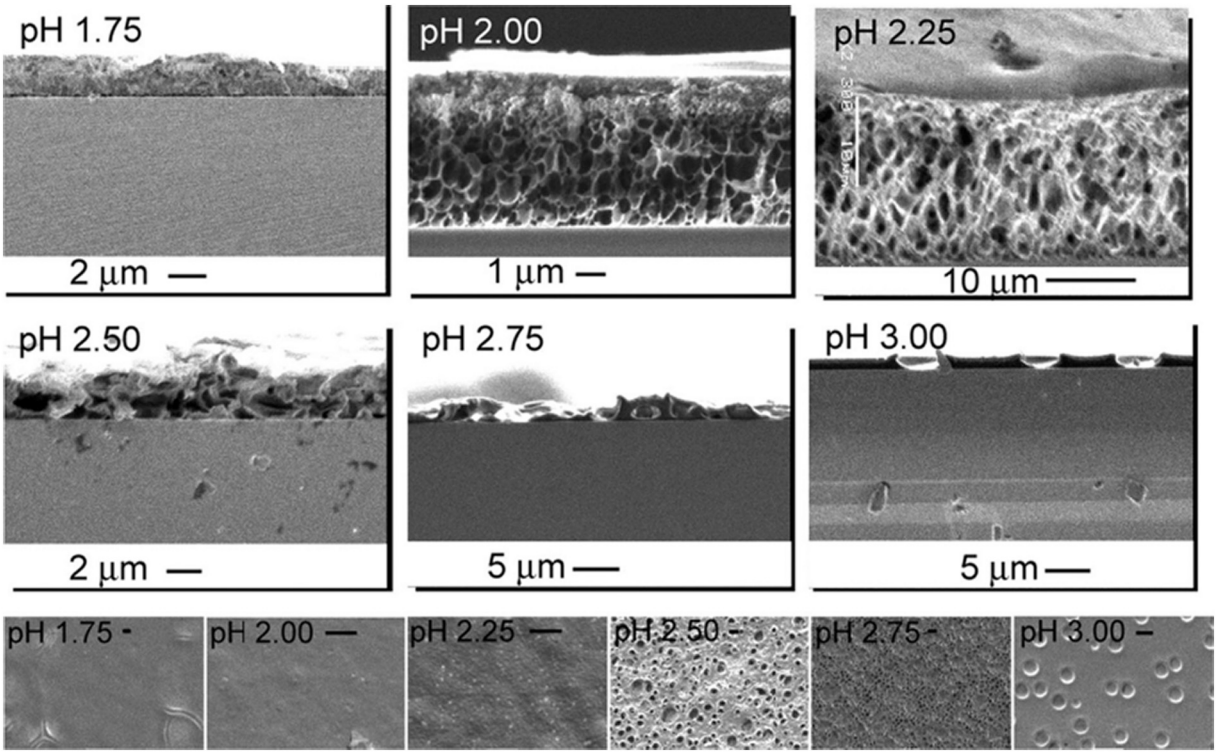

Fig. 8. SEM cross-section (upper two rows) and top-down images (bottom row) of LPEI/PAA films formed at pH 5 and treated at different pH (reproduced with permission from [229], copyright 2008 American Chemical Society).

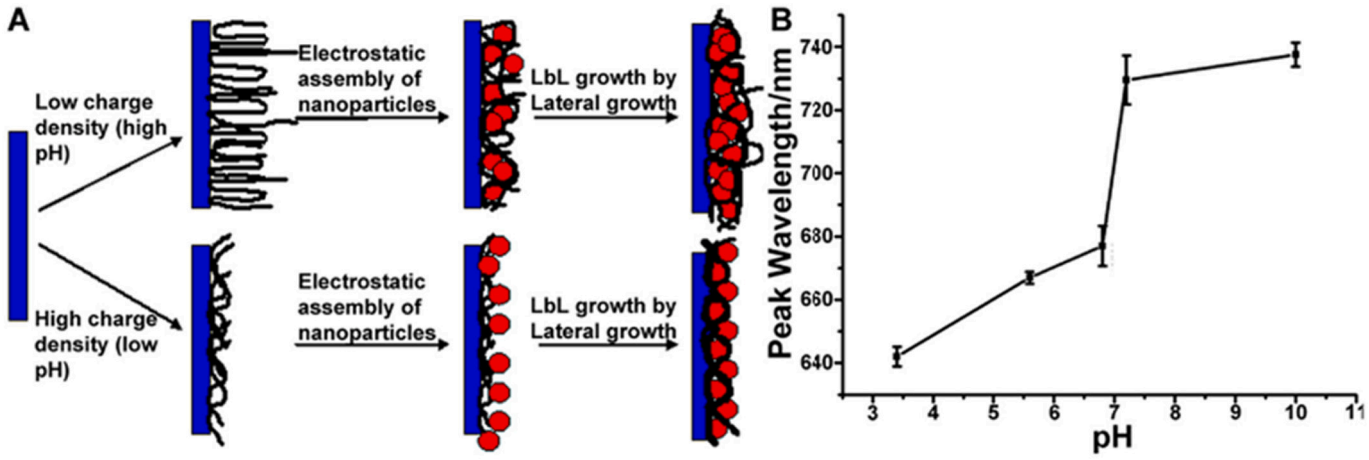

Fig. 9. Formation of PEM made of weak polyelectrolyte to tune the interparticle distance of gold NPs (A) and the modulation of LSPC via assembly pH (B) (reproduced with permission from [240]. Copyright 2009 American Chemical Society).

growth of multilayers is highly dependent on pH (in case of weak polyelectrolytes embedded). For the film consisting of PEI and PAA [243], where both PEI and PAA solutions have neutral pH, the growth is nearly linear. Decreasing the assembly pH of PAA or increasing the assembly pH of PEI highly accelerates the formation process. The thickness of several micrometers after less than 10 deposition cycles was obtained. The strong exponential growth could be due to the pH-enhanced PEI interdiffusion and pH-tunable charge densities of the film and the polyelectrolyte. The pH-dependent interdiffusion and charge density, exponentiality of the growth for the PLL/HA film is more or less pronounced in different pH regions [225]. Towards low or high pH values, PLL interdiffusion causing exponential growth is less relevant for the increase in mass coverage, but in the high ($pH > 9$) and the low ($pH < 5$) pH range, thicker PLL/HA multilayers are obtained. The coatings are less viscous and less elastic in comparison to the polyelectrolyte multilayers created at intermediate pH ($5 \leq pH \leq 9$) conditions [244].

Anandhakumar et al. presented a thin film for the encapsulation and release of proteins and drugs for a triggered drug delivery system [245]. PEM film consisting of weak polyelectrolytes, PAH and PMA was created by the LbL technique for a multi-drug delivery system. Environmental stimuli: pH and ionic strength demonstrated a significant influence of changing the film morphology from pore-free smooth structure to porous structure on the privileged triggered release of loaded molecules. The films containing BSA and ciprofloxacin hydrochloride were formed by controlling the porous polymeric structure. The release studies demonstrated that the amount of released substances might be controlled by changing the environmental conditions such as pH and ionic strength. Fig. 10 presents the scheme of PAH/PMA PEM film

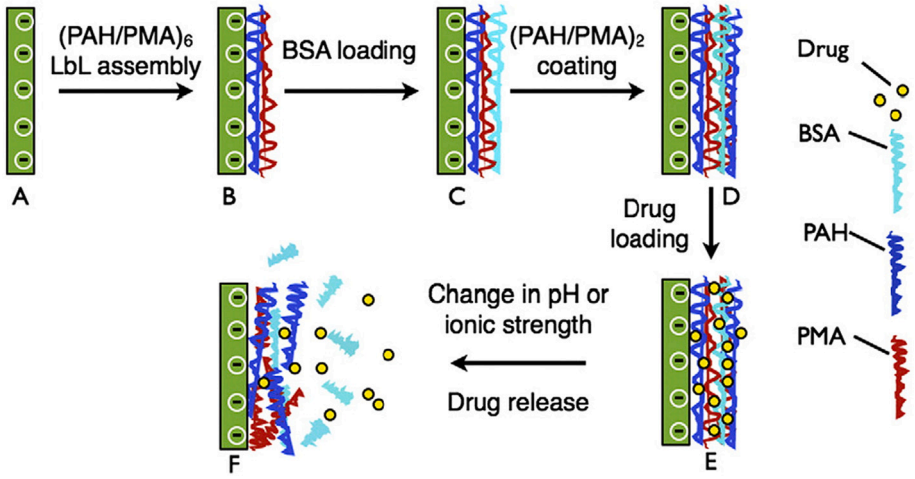

Fig. 10. The methodology of the formation of PEM films for stimuli-responsive drug and protein delivery. A, glass substrate; A–B, LbL deposition (PAH/PMA)6 layers; B—C, BSA loading; C—D, additional (PAH/PMA)2 layer adsorption; D–E, CH loading; E–F, stimuli-responsive release (reproduced from [245] with permission, copyright 2016 Elsevier).

formation and stimuli-responsive release of loaded protein and drug, while Fig. 11 presents AFM images of as-prepared multilayers dipped in solutions at different pH values to study their pH responsiveness. In the beginning, the new film was uniform and smooth without any pore and discontinuity (Fig. 11C). The average roughness and thickness of the film were about 5.17 ± 0.5 and 21.4 ± 1.5 nm. When the multilayer coating was rinsed with an aqueous solution of different pH, the film morphology changed from continuous pore-free to a porous one increasing the roughness as determined by AFM studies. It is worth noticing that the influence of pH on PEM film is meaningful at acidic and basic pH ranges in comparison with neutral pH. The transformation is ascribed to repulsion between the same functional groups when the degree of ionization of one of the polymer component decreases as a function of pH. The influence of ionic strength on film structure was investigated by varying the salt concentration from 0 to 0.4 M NaCl at pH 5. The presence of salt screens the interaction between charged components and the film loosens and creates nanopores [246]. The pore formation and growth were observed with increasing ionic strength and it did not increase the roughness value significantly up to 0.2 M NaCl. In the case when the concentration was grown to 0.4 M NaCl, the roughness increased from 4.9 ± 0.5 to 6.8 ± 0.5 nm. The presence of salt reduces the interaction between charged components leading to denser and folded PEs structures [247]. The reduction in thickness indicates that the polyelectrolytes are likely to detach from the surface.

These results confirm the previous studies [248] that higher salt concentration reduces polymer-polymer and polymer–surface

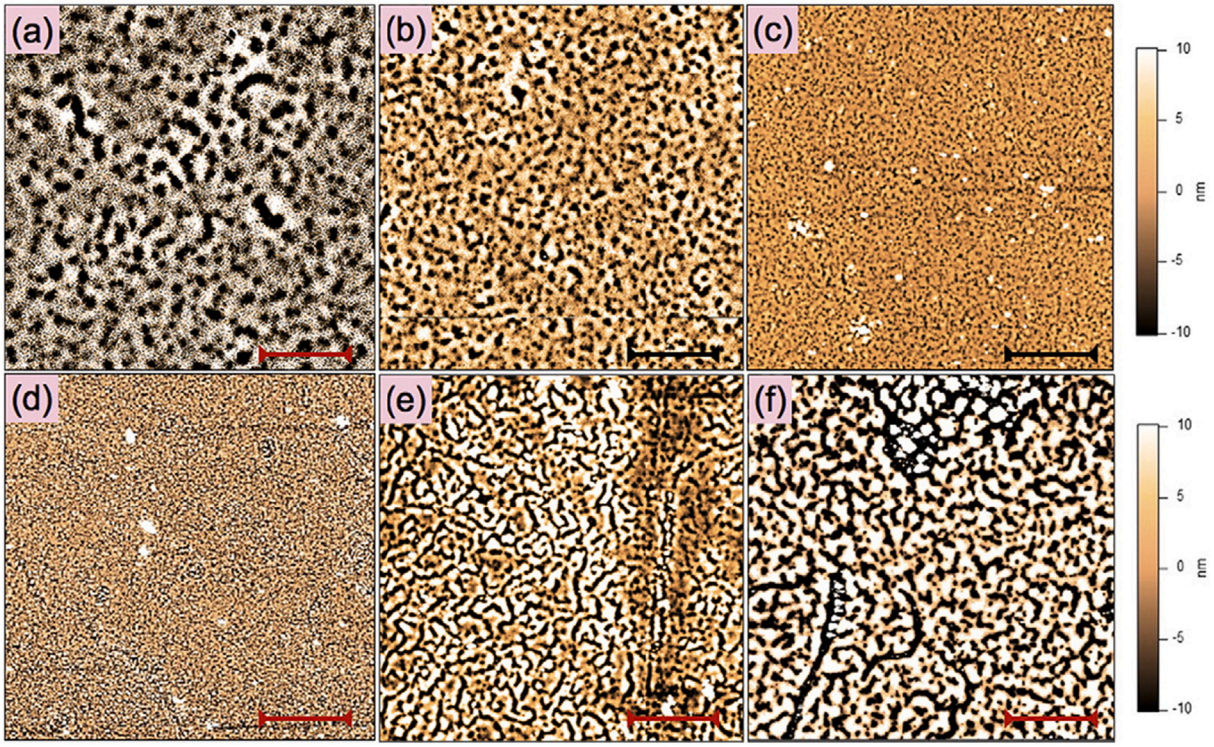

Fig. 11. AFM image of LbL assembled $(PAH/PMA)_8$ film to present the influence of pH on topography of the film. (a) pH 1.5, (b) pH 3, (c) pH 5, (d) pH 7, (e) pH 9 and (f) pH 11. Scale = 5 μm (reproduced from [245] with permission, copyright 2016 Elsevier).

interactions, making the films less interpenetrated and unstable, leading to detachment of macromolecules and creation of porous coatings.

The amount of drug released from the films depended on: (a) diffusion through pores in the polyelectrolyte structure and (b) release associated with the increased permeability when pH or ionic strength changes. The environmental stimuli, ionic strength, and pH affect the interaction between the drug and films and favor drug release by weakening the drug/protein–film interactions [245].

Sun presented LbL coatings sensitive to pH which were composed of PAH and PAA on electrode surfaces with pH reversible bioelectrocatalytic properties [249]. The type of biomaterials named 'smart' or biomimetic nanomaterials that react to the surrounding environment are developing into more complex materials which respond to multiple stimuli to maintain many diverse processes. The salt and pH-responsive PEM could be formed using a structure consisting of PNIPAM, montmorillonite clay nanosheet, and pH-responsive PMMA, leading to dual-network PNIPAM/clay/PNIPAM/ PMMA layers. The mixed PNIPAM/clay/PNIPAM/PMA coatings present significant deswelling at acidic pH values caused by hydrogen bonding between the PNIPAM and PMAA structure, and the diffusion of particles of 70 kDa dextran, in the polymeric network at acidic pH, is inhibited (Fig. 12).

The films permeability to dextran molecules was selective to solute molecular weights and might be further manipulated by pH and/or salt stimuli. Moreover, the incorporation of clay nanosheets within responsive films enhanced the mechanical robustness of the coating in comparison to their all-polymer counterparts. These robust "smart" materials are interesting candidates for a variety of applications, such as e.g. biosensing [250,251].

Huang et al. reported self-cross-linked multilayer coatings made of CH and ALG dialdehyde (ADA) [252]. Multilayer films of CH and ALG are of great interest due to their biocompatibility, biodegradability, and stimuli-responsiveness. The disruption of the electrostatic equilibrium when exposing the formed films to acidic and alkaline conditions causes their swelling independently of the outermost layer indicating the responsiveness of the film to ionic strength and pH variations (Fig. 13). It was investigated how changing the pH and ionic strength affect the film properties depending on its outermost layer. The internal part of the film particularly swells when pH is increased from 6 to 9, whereas slight swelling is noticed when pH is decreased from 6 to 3. Increasing the ionic strength, provides rise to swelling of the inner part specifically at pH 9, an effect exclusive to crowded weak polyelectrolyte systems. The multilayer film ended with ADA swells most under alkaline conditions, while if the outermost layer is CH it swells most under acidic conditions,

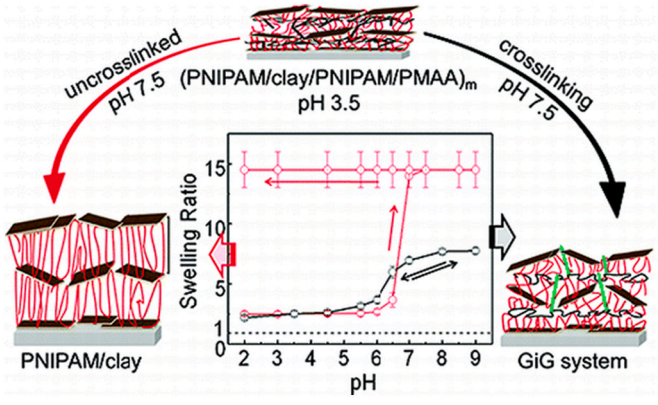

Fig. 12. In situ ellipsometry profiles for (PNIPAM/clay/PNIPAM/PMAA)3 uncross-linked coatings (red - open circles) and the same coatings, cross-linked in 3 mg/ml solutions of ethylenediamine and CDI for 2.3 h (black-filled circles). From acidic pHs, films were exhibited to 0.01 M phosphate buffers with increasing pH values for 15 min. After measurements at pH 9, buffer pH was gradually lowered. Dashed line indicates dry film (reproduced from [249] with permission, copyright 2011 WILEY-VCH Verlag GmbH & Co. KGaA).

a trend that is expected for "free" weak polyelectrolyte chains. Thus, self-cross-linked CH/ADA films are responsive to variations in the pH of the medium in terms of reversible swelling/collapse, without collapse of the coating that is also promising for their biomedical applications [253].

In other studies, two polysaccharides: dextran aldehyde (Dex-CHO) and carboxymethyl chitosan (CMCS), were synthesized and used to form a self-polishing antifouling and antimicrobial multilayer film via LbL adsorption using aldehyde-amine reactions [254]. The self-polishing capability of the multilayer films was obtained via cleavage of pH-responsive imine linkage under acidic environments. The stimuli-responsive linkages have been widely applied in drug delivery systems as the release of pro-drugs could be manipulated by regulating the pH value of a medium. The pH-sensitive linkages, e.g., imine, hydrazide, oxime, and β –thiopropionate bonds undergo cleavage at a specific pH range from 5.0 to 6.5, [255,256,257] while they are stable at conditions slightly above the neutral pH. The pH of seawater is typically basic (pH 7.5–8.4), [258] and at these conditions, the linkages undergo minimal or slow cleavage. It seeks to evolve pH-cleavable linkages in self-polishing films obtained by LbL adsorption [259], to minimization biofouling in the aggressive marine environment [254].

Burke and Barett [260] showed the pH-dependent loading and release behavior of small hydrophilic molecular probes in PAH and HA PEM films. The embedding of the cationic dye, Indoine Blue, and the anionic dye, Chromotrope 2R, into $(PAH/HA)_{10}$ PEM showed strong dependence on the pH. The maximum loading was reached at pH conditions which showed the best electrostatic attraction between the dye molecules and the multilayers, minimum repulsive interactions between the two, and the largest J-aggregation of the molecules in the layers. The release rate and the percentage of dye released from the coatings also showed a pH dependence. The swelling of the coating helps to the release of the dye molecules by transferring counterions into the multilayers to screen the electrostatic interactions and by forming voids and pores through which the molecules could pass. Thus, the studied PEM can trap small molecules in their structure at a given pH and release them by changing the pH value. Both embedding and release functions of the studied PEM depend on the degree of swelling, the capability of the dye molecules to aggregate in the film, and the attractive and repulsive interactions occurring between the probe molecules and the acid-base functional groups in the layers. Both the degree of dissociation of the acid-base functional groups and the level of film swelling are pH-sensitive.

Cationic CH with ionizable amino groups, having a pK_a value of about 6.2, and anionic HA having ionizable carboxyl groups were also used to form pH-responsive PEM showing reversible pH-dependent swelling and shrinkage [261]. The obtained films were loaded with a drug and placed in PBS solutions of varying pH for several days. The amount of drug released by the drug-loaded (aspirin derivative) film was shown to be dependent on the pH of the PBS solution.

Cao et al. developed a novel pH-responsive modulated drug-release formulation by using PEM as a gate-keeper to cover the *meso*/micropore openings of drug-loaded hierarchical hollow silica spheres. The mechanical stability, drug loading, and capacity of the system were higher in comparison with the conventional single-shelled hollow silica system. The obtained system a cap shell exhibited a stimuli-responsive release - the model drug release rate was shown to be well-controlled by the changes of the pH values of the releasing medium [262].

Han et al. studied some basic properties of the multilayer films built from polystyrene-*block*-polyacrylic acid (PS-b-PAA) amphiphilic BCM serving as nano-sized drug vehicles, functionalized graphene oxide (GO), and branched polyethylenimine (bPEI) having all a distinct pH-dependent ionization (Fig. 14) [263]. The films were formed by LbL taking advantage of mainly electrostatic interactions and hydrogen bondings between the carboxyl groups of BCM and amine groups of functionalized GO or bPEI under different pH conditions. A significant dependence of the properties of the films on pH during their formation

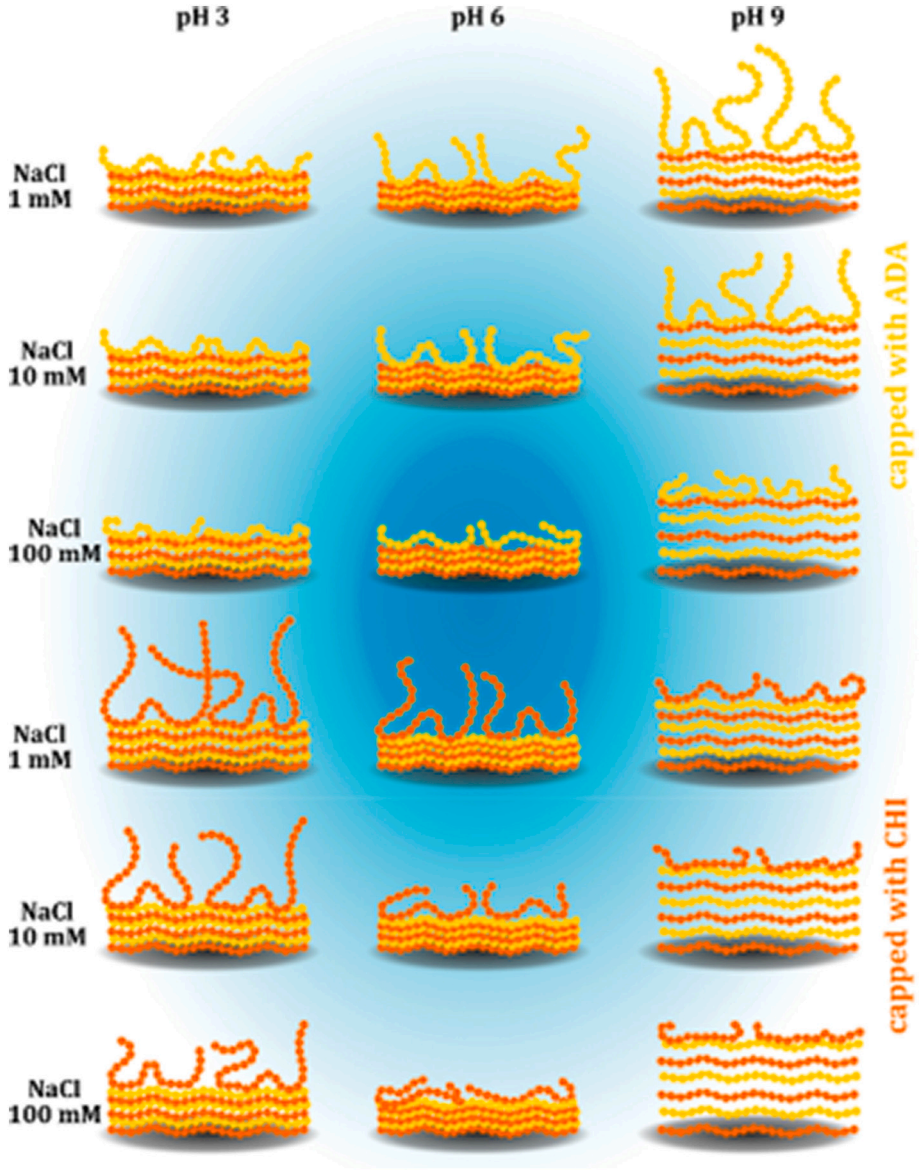

Fig. 13. The schematic presentation of structural conformation and swelling behavior of (CH/ADA)n films covered with ADA (left panel) or CH (right panel) at different pH and ionic strengths (reproduced from [252] with permission, copyright 2019 American Chemical Society).

was observed that was related to various pH dependences of each material used in PEM. A model fluorescence probe was encapsulated in BCM and its release rates from the GO/BCM film were found higher than those of the bPEI/BCM film in both pH 7.4 and pH 2 solutions.

Since the change of pH of the medium is an evident stimulus that affects the permeability of PEM films, composed of at least one weak polyelectrolyte, it has been applied also in PEM microcapsules. Such microcapsules exhibit structural alterations triggered by the pH changes as a consequence of protonation and/or deprotonation of their charged units.

The polyelectrolytes charge density directly influences the density of complexes of polyelectrolyte charge groups which in turn affects the mobility and permeability of PEM. Generally, the less charged polyelectrolytes, the more mobile the polyelectrolyte chains and the more permeable is the capsule shell. Similarly to PEM films on macroscopic supports, when the pH value of the microcapsules environment is close to the apparent pK_a of one of the polyelectrolyte component the capsules' walls, its charge density decreases, and the microcapsule swells as a result of repulsive forces between like-charged groups that become dominant in such conditions. Microcapsules in a swollen state are permeable for large molecules. This state can be reversed, and microcapsules shrinking can be triggered by tuning back the pH of a surrounding medium to the starting value. Such reversible swelling and shrinking of the microcapsules are very advantageous as it allows to switch them between permeable and impermeable states.

Changes in a polyelectrolyte multilayer structure with increasing pH can be observed for microcapsules consisting of strong polyanion, PSS, with fixed charge density and weak polycation, PAH, with charge density conditioned by pH [264]. The apparent pK_a of PAH in the PAH/PSS multilayers was determined to be ca. 10.8 [265]. When the pH of the surrounding medium is close to this value, the charge density of PAH decreases, and the PAH/PSS shells swell as a result of repulsive forces between an excess of not compensated negative groups of PSS and also because of the local increase of osmotic pressure induced by the attraction of counterions by PSS charge units. Swollen PAH/PSS capsules in basic conditions, shrunk when the pH is reduced [264]. This reversible swelling and shrinking that is accompanied by increasing and decreasing of the shell permeability can be applied for loading and/or releasing of substances.

Capsules consisting of two weak polyelectrolytes can react in both

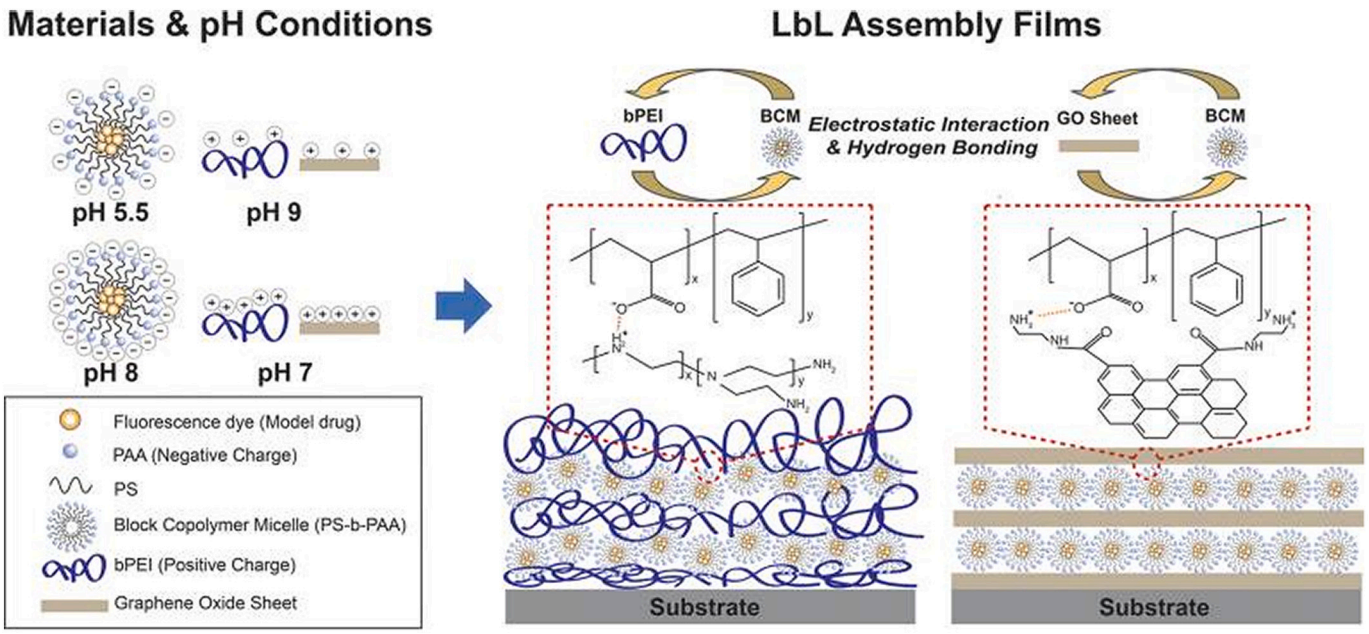

Fig. 14. Schematic illustration of the materials, the pH-dependent charge density of the LbL assembly building block (left), and bPEI/BCM and GO/BCM multilayers formed by the LbL technique with electrostatic interactions and hydrogen bonding (right) [263].

acidic and alkaline pH regions. An example is capsules made of weak polyanion, PMA, and weak polycation, PAH, that were able to change their diameters reversibly from 4 to 8 μm by varying the pH in the range of 2.5–11.5 [266]. Beyond these borders, capsules disintegrate due to the loss of most charges in PMA chains below pH 2.5 and in PAH above 11.5. It happens because repulsive forces between like-charged groups are no longer compensated by the attraction forces of the oppositely charged groups. When other than electrostatic interactions are additionally engaged within multilayer shells, the capsules become stable in a swollen state in a broader range of pH. For PMA/PAH shells it can be observed that in acidic conditions, capsules are stable in a swollen state in a very narrow pH range, whereas in alkaline conditions hydrophobic reactions within PMA chains prevent swollen capsules from disintegration in a wider extent of pH. The swollen state can be stabilized in acidic conditions when applying as a polycation weak poly(4-vinylpyridine) (PVP) that is insoluble in the water below pH 5. PVP/PMA capsules show swelling and shrinking in the pH range of 2–8 and they are stabilized in both borders of the swollen state: in acidic as well as alkaline conditions due to counteracting hydrophobic as well as hydrogen bonding interactions [267].

There are many other reported polyelectrolyte systems that respond to the pH changes, e.g.: poly(ethylene oxide)/PMA (with disintegration threshold of pH = 4.6), poly(N-vinylpyrrolidone)(PVPON)/PMA (with disintegration threshold of pH = 6.9), poly(ethylene oxide)/PAA (with disintegration threshold of pH = 3.6) [268,269], chondroitin sulfate/PLL [270], PLL/PLG [271], PAA/PVA [272], PLL/HA [273]. An interesting example is capsules consisting of poly(2-vinyl-4,4-dimethylazlactone) with an acetal-containing linker that are stable under physiologically relevant conditions (pH = 7.4), but degrade in the acidic environment due to the hydrolysis of the acetal group (Fig. 15A) [274].

Another group of pH-responsive capsules are capsules composed of negatively charged TA with a range of neutral polymers: PVPON, PNIPAM, and poly(N-vinylcaprolactam) [275] and with positively charged CH [276]. Capsules composed of TA/CH layers embedded with triclosan (TCS) encapsulated in cetyltrimethylammonium bromide (CTAB) micelles (TCS@CTAB/TA/CH) were shown to release antibacterial TCS in an acidic environment. In acidic conditions, the ionization of TA decreases, and the excess of uncompensated positively charged groups of CH leads to repulsion within the polymer system and capsules swelling (Fig. 15B).

pH-responsive capsules were also fabricated by application of two strong polyelectrolytes PDADMAC and PSS with aminoclays entrapped between polyelectrolyte layers. Such capsules swell increasing their diameter by 60% as a result of the protonation of the amino group of aminoclay when the pH decrease from 9 to 4. That allowed to release of encapsulated ibuprofen and eosin [277].

A very interesting multifunctional core/shell system for cancer therapy with pH-sensitive polyelectrolytes was demonstrated. The complex system consists of mesoporous silica particles with entrapped DOX molecules, glucose oxidase coupled to the particles surface, and pH-sensitive polyelectrolyte bilayer (PAH/PSS). The idea was to use glucose oxidase to deprive the cancer cells of glucose (starvation therapy), to increase the concentration of poisonous H_2O_2, and to affect the tumor microenvironment by locally reducing the pH. Increased acidity, in turn, increases the rate of the depolymerization of the outermost pH-sensitive polyelectrolyte layer, causing the DOX release within tumor cells (Fig. 15C) [278].

The main potential application of pH-responsive capsules is local drug delivery in target tissues or cells with specific pH conditions like e.g. intestine pH = 8.4, stomach pH = 1–1.5 tumor tissues pH = 6.8, normal tissues pH = 7.4 [279], endosome pH = 6.0–6.5, mitochondria pH = 8.0 [280], lysosome pH = 4.5 [281], intercellular environment pH = 7.0–7.4 [282]. Practical application of capsules with a pH-triggered release under physiological conditions is still challenging mainlue to the narrow pH range in which the release should take place.

Unlike the pH-based attempt, the permeability manipulation by changing the ionic strength of polyions solutions applied for PEM formation is not restricted only to weak polyelectrolytes but can be employed for strong polyelectrolyte systems as well. Charge groups along the polyelectrolyte chains in an aqueous solution are surrounded by small counterions. During the adsorption of oppositely charged polyelectrolyte, some of these small ions are released from the close surrounding of the polyelectrolyte chains which induces an increase in their degrees of freedom and hence in the entropy of a system. Due to the gain in counterions entropy, the complexation between polyelectrolyte charged units is favored against charge compensation by small counterions and assembly can be also performed at high ionic strength.

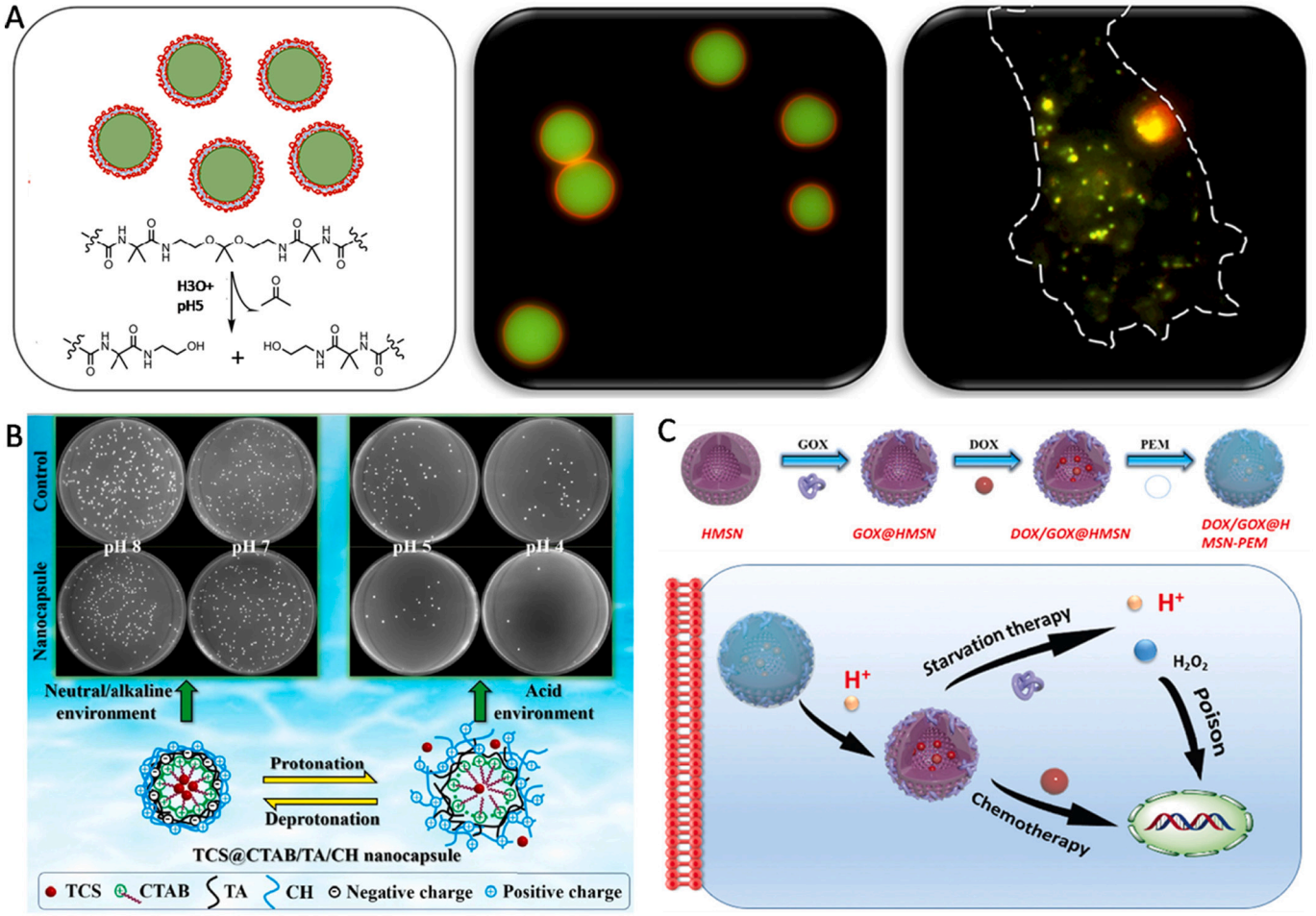

Fig. 15. (A) Capsules cross-linked by acetal-containing diamine linkages that decompose in acidic environments due to the hydrolysis of acetal groups (reproduced from [274] with permission, copyright 2019 American Chemical Society). (B) Schematic illustration of the pH-responsive release of triclosan (TCS) from TCS@CTAB/TA/CH capsules that causes the reduction of bacteria colony with decreasing pH value (reproduced from [276] with permission, copyright 2019 Elsevier). (C) Schematic illustration of the preparation of DOX/GOX@HMSN-PEM capsules and release of DOX in an acidic environment, combined with GOX-catalyzed starvation therapy (reproduced from [278] with permission; copyright 2019 Royal Society of Chemistry).

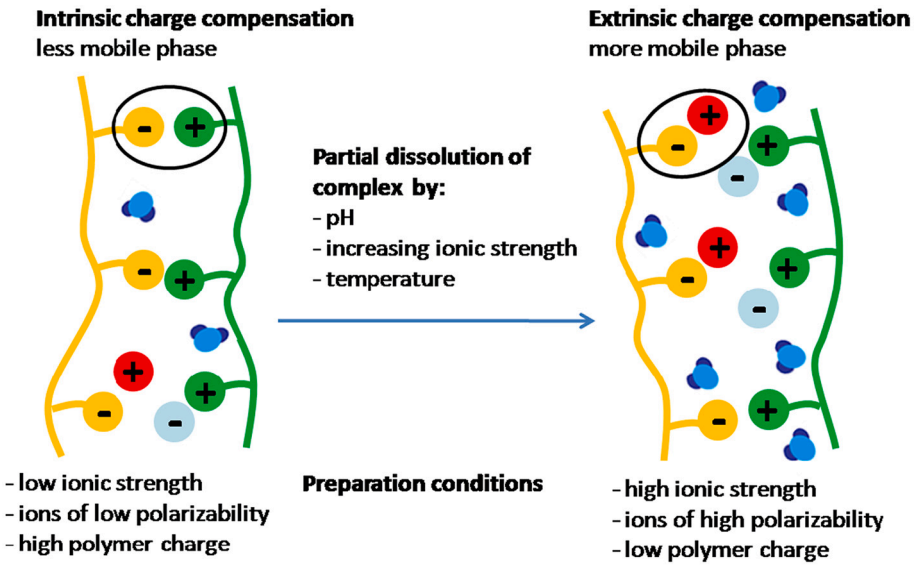

Fig. 16. Effect of salt, pH, and polymer charge density on the multilayer structure.

Whereas, in the case of polyelectrolytes with a low charge density or short chains, an increase in counterion entropy could be not enough for multilayer formation.

For a variety of systems, it is possible to tune the strength of the polyanion-polycation interactions and the mobility of the polyelectrolyte chains within the shell by adjusting the ionic strength during the LbL process as well as after completion of the adsorption process. Salt concentration directly controls the degree of association and interaction between polymer segments and thus can be used to influence microcapsules permeability [283]. Generally, higher external salt concentration leads to the weakening of the interactions between polyelectrolyte chains.

The multilayer structure depends on the type of polyelectrolyte and the type of salt. The addition of salt leads to the screening and thus weakening of the electrostatic interactions between the oppositely charged polyelectrolytes that become more mobile. This results in an increase in capsules permeability until the shell is completely dissolved [284,285].

The schematic illustration of this phenomenon is presented in Fig. 16.

The ionic strength has a significant influence on the film growing mechanism, which switches from a linear regime at low salt concentrations to an exponential trend at high ionic strengths. As a consequence, for a given number of polymer layers, the film thickness and its surface roughness are much larger for high concentrations of salt. The change of the growing regime is accompanied by a change in the mechanism of charge compensation. This mechanism is intrinsic at low, and essentially extrinsic at high ionic strengths [286].

This phenomenon was utilized for the release of DNA constituting a building block of the DNA/PLL capsules, and FITC-dextran encapsulated in the interior of those capsules by the dissolution of the DNA/PLL shell in the solution of NaCl [287]. Interestingly, an opposite effect was observed when one of the polyelectrolyte has hydrophobic groups like PSS. Upon increase of salt concentration in a certain range, the electrostatic interactions between the charged groups weaken, while hydrophobic interactions that strive to reduce the interface between PSS and water become dominant. That leads to the capsules shrinking and reduction of their permeability [288].

The changes in the polyelectrolyte shells induced by the increasing salt concentration were also employed for a fusion of PDADMAC/PSS capsules and mixing their content by solvent evaporation from 3 M NaCl solution [289].

5.2. Chemical and electrochemical reactions

Electrosensitive polyelectrolytes have been considered for applications in numerous nanosystems for e.g., tissue engineering, drug delivery, and biomedical imaging [290,291]. The electrical conductivity of conjugated polyelectrolytes might be reversibly tuned through oxidation and reduction processes introducing charge carriers to the polymeric backbone (doping) chemically or electrochemically. However, also nonconjugated polyelectrolytes can be used to form PEM sensitive to the application of electric field and the implied (electro)chemical processes.

Electric field was applied to manipulate the properties of LPEI/PAA films [292]. It locally lowers the pH inducing a morphological change in such a PEM film leading to the formation of a porous structure. Non-connected nanoscale pores at the electrode/multilayer interface were produced first, then an asymmetric porous structure, and finally microsized pores connected throughout the film. The capability to control the application of electric potential, therefore, enables the tailoring of the porous structures of PEM.

The controlled release of biomolecules from PEM could be achieved by the decomposition of the polyelectrolytes through hydrolysis, enzyme-triggered degradation, or other chemical reaction. The proper design of the coating composition may provide controlled release of e.g., plasmid DNA in physiological conditions. An effective approach was proposed by the formation of the coatings using DNA and hydrolytically degradable polymers, poly(amino ester)s [293]. The decomposition of the polymer resulted in small steps of dissolution of the film and slow release of DNA during several days. The controlled release of DNA up to 90 days was obtained by using a new"charge-shifting" cationic polyelectrolyte which inverses the charges upon hydrolysis leading to disassembly of the PEM.

The controlled DNA release might be also triggered by the presence of enzymes. The PEM formed from PLL and DNA were stable in PBS but decomposed when α-chymotrypsin, an enzyme enhancing degradation of PLL, was added to PBS [294]. Chemically triggered DNA release was realized using a layer of plasmid DNA and a high molecular weight cationic polypeptide with disulfide bonds [295]. This polypeptide is stable in non-reducing media, but degrade when the disulfide bonds in the backbone are cleaved upon exposure to a chemical reducing agent. Finally, the films with loaded DNA were generally stable in physiological media but disassembled and released plasmid DNA in the presence of a reducing agent, dithiothreitol.

Electrochemically responsive PEM have found numerous applications in the fabrication of sensors, electrochromic devices, light-emitting diodes, and controlled drug release. Electroactive PEM composite films composed of cationic LPEI and anionic Prussian Blue (PB) nanoparticles were shown to change stiffness under electrochemical reduction [296]. After immersing a dry film in a potassium hydrogen phthalate electrolyte solution, the film swells passively due to hydration. When the potential of 0.2 V (vs. Ag/AgCl) was applied to the film, PB was electrochemically reduced to Prussian White and the negative charge generated on PB particles upon the reduction caused an influx of water and ions from the solution to the film to maintain the charge neutrality. Finally, an influx caused swelling of the film by 2–10% and changes of the elastic modulus up to 50%. The reduced system can be oxidized back to the PB state by applying +0.6 V (vs. Ag/AgCl). The reversible, electrochemically controlled swelling offers important implications for responsive mechanically tunable surfaces (Fig. 17). The electrochemical reaction at electrodes can also change the structure of the film due to the generation of ions which break the electrostatic interaction between PE. For example, when an electric current was applied to PLL/heparin PEM films, the local decrease in pH near the anode (resulting from the generation of H^+ ions) caused a disruption of electrostatic bonds between the two oppositely charged PE, leading to a local electrodissolution of the multilayers and the release of heparin.

PEM with electrochromic materials change color with an applied potential through a redox process [297]. The redox switchable conjugated polymers could have an electrochromic (EC) response (e.g. concurrent color, transmittance change) to an applied electric field. The performance of an EC device depends on several factors including the availability of finely tuned color, EC contrast (% transmittance change at a certain wavelength), coloration efficiency (electrochemical charges required to obtain an absorbance change at a certain wavelength), switching rate (time needed to change colors), optical memory (the ability to keep the color upon removing the external bias) and stability. Using the LbL formation of poly(3,4-ethylenedioxythiophene) (PEDOT) colloids doped with PSS (PEDOT:PSS) and poly(aniline) (PANI), an EC device was formed by assembling a cathodically coloring film with an anodically coloring film [298]. The cathodically coloring film was a fabrication from the LPEI polycation and PEDOT:PSS as the polyanion while the anodically coloring film was assembled from the PANI polycation and poly(2-acrylamido-methane-2-propane-sulfonic acid) (PAMPS) as the polyanion. The resulting solid electrochromic device gave a maximum transmittance change of 30% within one second.

5.3. Biology-related stimuli

An important feature of PEM films is possible functionalization by introducing e.g., drugs, biomacromolecules (proteins, DNA, lipids,

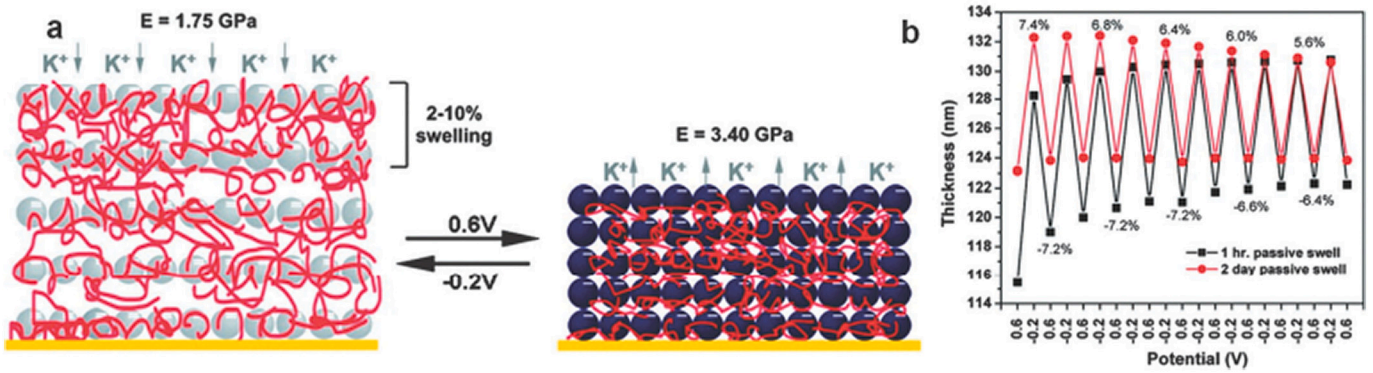

Fig. 17. (a) Schematic of an $(LPEI/PB)_{30}$ film swelling under the influence of an electric potential. Water molecules and positive charges on the polymer are omitted for clarity. (b) Active swelling of two $(LPEI/PB)_{30}$ films subjected to 10 redox cycles after 1 h and 2 days of passive swelling. Reprinted with permission from ref. [296]. Copyright (2009) American Chemical Society.

polypeptides, polysaccharides, etc.) and their subsequent release. The porous structure of some PEM films permits the incorporation of different therapeutic molecules and a stimuli-responsive release. However, the common problems are related to low encapsulation performance and too fast release, which limit their use in drug delivery systems and biomedicine.

PEM coatings could be used for the incorporation of free molecules directly (e.g., pharmaceutical drug, proteins, DNA, enzymes) or molecules in encapsulated form (e.g., in liposomes, polymeric capsules). Encapsulation of free molecules is realized by using them as layer components or directly embedding them into the film by a dipping process. Fig. 18 presents different encapsulation processes that are being used to encapsulate drugs, NPs, and other macromolecules in polyelectrolyte coatings [299].

Anandhakumar showed dual drug-loaded coatings [299]. The porous and supramolecular structures of PEM films were effectively used to embed both ciprofloxacin hydrochloride and BSA in the films making them very interesting candidates for externally activated drug delivery applications. Polymer/NP composite films were formed by in situ syntheses of metallic NPs through metal ion-polymer interactions and inbuilt of pre-synthesized NPs via electrostatic interactions [300,301]. These kinds of approaches give an almost uniform nanocomposite structure with good control over NP size and distribution.

Numerous works have been devoted to encapsulation of bioactive molecules: proteins, peptides, nucleic acids, enzymes into the structure of PEM films. Biomolecules can interact with the PEM components irrespective of the charge of biomolecules and film because it involves not only electrostatic but also hydrophobic interactions, and hydrogen bonding. The important question which needs to be answered is the configurational stability and activity of the films containing such biomolecules. The reports concerning loaded proteins, enzymes show that the PEM-bound molecules are able to keep their secondary structures and enzyme activity demonstrating also tolerance against harsh conditions [302]. The Lvov's group reported also that platelets coated with anti-IgG-containing multilayers can be targeted to IgG-coated surfaces [303]. However, often an encapsulation of bioactive molecules in nanocarriers before their embedding into PEM is required to shield them from the external environment and preserve their activity. Caruso et al.

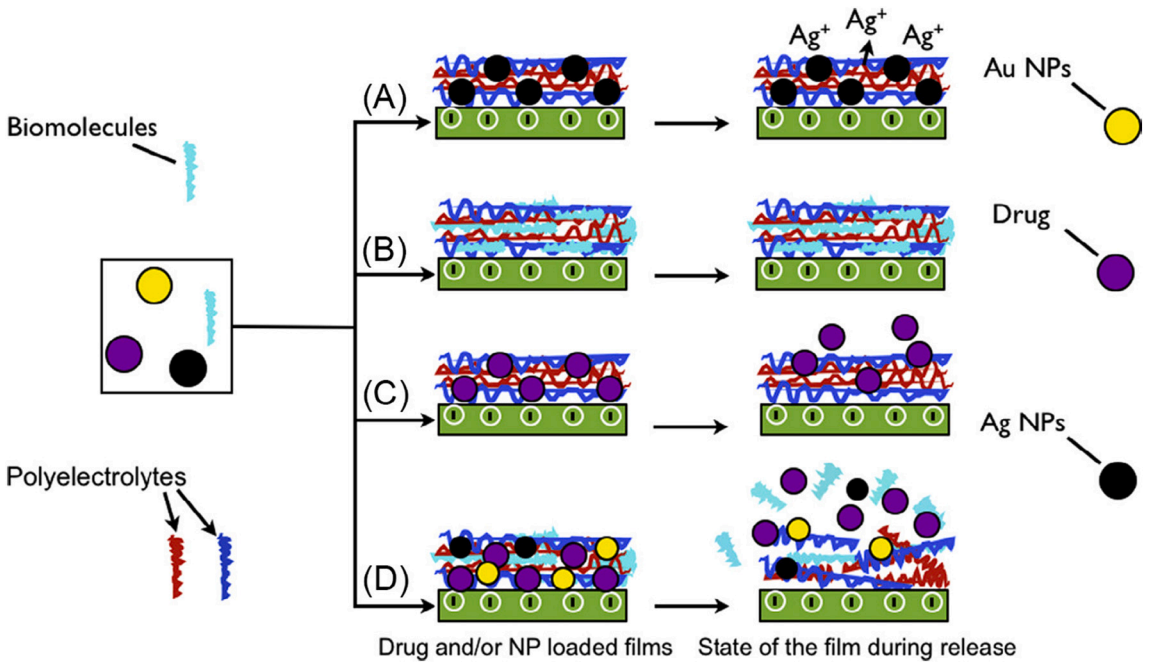

Fig. 18. The thin film-based creation for drug delivery system and antibacterial coatings. PEM films with (A) silver NPs for antibacterial coatings, (B) biomolecules for tissue engineering applications, (C) drugs for drug delivery, and (D) both Ag or Au NPs and drugs for dual drug delivery system (reproduced from [299] with permission, copyright 2013 Elsevier).

presented a successful development of dendrimer/PSS coatings and showed the release of loaded molecules through concentration-dependent diffusion in isotonic saline solutions [304]. Volodkin et al. developed HA and PLL film incorporated with a liposomal carrier containing carboxyfluorescein, and demonstrated its controlled release by varying the temperature [305]. The exponentially growing films, such as PGA/PAH [306] and PLL/HA [307] were found to be suitable for the incorporation of liposomes due to high water content, and a gel-like structure providing a suitable environment for liposomes. The amount of substances loaded into the film is largely dependent on carrier deposition steps, a charge of the carrier, and nature of the polymeric matrix. The release of loaded molecules from the film is of crucial importance in developing thin film-based drug delivery platforms for various biomedical applications. Films containing biomolecules/drugs within their layered architecture offer the ability to vary not only the number of active molecules under exposure to diffusion-based environmental triggers but also the ability to trigger the release using external stimuli in proper timing and order (e.g., simultaneous, sequential, pulsatile release).

Serizawa et al. demonstrated the selective degradation of self-assembled DNA by DNA-specific enzyme which was deposited on the surface layer [308]. The disintegration of the multilayer was induced by the presence of Mg^{2+} and Ca^{2+} ions in solution and might be tailored by varying their concentrations. Hydrolytic degradation of a self-assembled polycation was also used as a trigger for releasing DNA in its native form from PEM [309]. Biologically active films containing an enzyme, organo-phosphorus hydrolase, are promising as a component of enzymatic sensors for the detection of a wide range of highly toxic organophosphorus compounds in the environment [310]. Inoue et al. showed interesting results on the decomposition of PEMs triggered by a specific recognition event [311]. Specifically, avidin–biotin specific binding between avidin and polymer-conjugated biotin was taken to form LbL coatings which decomposed in response to the presence of free biotin molecules in solution.

The responsive polymer conjugates based on host-guest chemistry and PEGylated nanoparticles have been assembled to form pH, light, and ionic strength multiresponsive coatings for drug-delivery applications [312]. By manipulating their supramolecular structure it was possible to observe a synergistic effect between their components - an azobenzene-containing copolymer, cyclodextrins that could be loaded and release drugs by triggered by light, while the PEGylated nanoparticles can be triggered by physiological conditions.

Capsules capable of biologically induced release are developed as a biomimetic platform for the intercellular transfer of drugs and genetic materials e.g. for genetic therapy purposes. The biologically induced release is the result of the interactions of the shell material with biomolecules, such as enzymes, oligonucleotides, or saccharides that in most cases leads to capsule degradation. For example capsules with phenylboronic acid as a wall ingredient are glucose-sensitive and could be used as a carrier for the delivery of insulin [313]. Capsules composed of glucose-sensitive enzymes, glucose oxidase, catalase, and synthetic polyelectrolyte, PEI, with prioritized proton binding capability that act as a buffer for pH variation, were able to release insulin in response to exceeded glucose level, while at normal glucose level (5 mM) insulin release was hindered. It was demonstrated that the release threshold can be tuned in the desired glucose concentration range from 5 to 20 mM by adjusting the amount of PEI within capsules shells.

Enzymes or reagents of the reactions they catalyze can be used as walls materials providing numerous potential triggers with high selectivity. Many diseases are accompanied by an anomalous level of specific enzymes, which can be a starting point to create enzyme-responsive capsules as drugs carriers, especially with an intracellular target such as proteins and nucleic acids [98]. An example is a trypsin and other trypsin-like enzymes that cleave peptide chains at the carboxyl side of the amino acids lysine and arginine, which are on the abnormal level in some inflammation conditions [314] and cancer [315]. Following this lead, the capsules consisting of arginine-rich cationic protein and anionic polysaccharide, heparin, were constructed. Drug molecules embedded within such capsules walls were shown to be released in the presence of trypsin due to decomposition of the capsules [316].

Microcapsules with polypeptide as building blocks can be disintegrated by the pronase (a mixture of proteolytic enzymes) that hydrolyses proteins into individual amino acids (Fig. 19) [100]. It was demonstrated that the rate of pronase catalyzed degradation of capsules shells with the poly(L-arginine) (pArg) as a polycation and poly(L-glutamic acid) (pGlu) as polyanions increased with the increasing enzyme concentration. Whereas it can be slowed down by increasing the number of the polypeptide layers or by incorporation of additional layers of synthetic polyelectrolytes like PSS and PAH.

A similar observation was made for capsules consisting of polysaccharides: CH as a polycation and heparin as a polyanion. In the presence of heparanase, an enzyme degrading polymeric heparin sulfate into shorter chain lengths, the capsules were decomposed. Application of enzymatically degradable polyelectrolytes together with synthetic ones like PAH and PSS in one system led to higher resistivity of capsules to the enzymatic degradation, and prolonged release [317].

Capsules build of other polysaccharides pair: CH as a polycation and HA [318] as a polyanion as well as capsules consisting of HA and PLL [319] were degraded by hyaluronidases - a group of enzymes that catalyze the degradation of HA. Moreover, capsules containing CH as a shell ingredient can be non-specifically decomposed by a variety of colonic and pancreatic enzymes. The capsules based on liquid oil cores with shells composed of HA derivatives were also shown to be degraded by hyaluronidases both in dispersion and after cellular uptake [320]. Capsules with DNA as a shell component were degraded by nuclease that is an enzyme capable of cleaving the phosphodiester bonds between nucleotides of nucleic acids [321].

Further examples of capsules that decompose after internalization by cells contain enzymatically or hydrolytically degradable polycations such as pArg and poly (hydroxypropyl methacrylamidedimethylaminoethyl) [322]. Capsules consisting of dextran sulfate and pArg were able to transfer and release mRNA and siRNA within tumor cell lines. The capsules after cell internalization were degraded due to intercellular proteolytic activity and released most of their loads within 24–48 h [323].

Active compounds can be entrapped not only in the capsule's interior but can be assembled as multilayer constituents. Such a solution was used to deliver α1-antitrypsin (AT) (serine protease inhibitor) to covalently bind human neutrophile elastase (HNE) that contributes to tissue damage in chronic inflammation. The formed HNE-AT complex can be then phagocytosed and degraded. Additionally, cefoperazone was applied as another wall constituent to protect AT against inactivation. Both agents were positioned within separator multilayers composed of protamine sulfate and dextran sulfate [324]. To improve the clarity of this chapter, the described examples are summarized in the Table 5

6. Microparticle/microcapsule deposition and controlled release

For some applications, microcapsules have to be immobilized to offer soft coatings with tunable mechanical and interfacial properties. The potential of such systems results from the compartmentalized structure which can be utilized by catalysis or controlled release including drug delivery [15].

Gahan et al. [325] used the LbL technique to deposit multilayers of polymer-coated microparticles containing mutually reactive polymers, either poly(2-vinyl-4,4-dimethylazlactone) (PVDMA) or PEI as terminated layers. The authors claimed that the template-based approach provided opportunities to control the particle packing and to design cargo-loaded planar systems that kept the capsules' internal structure, geometry, and interconnections between them, which would not be possible by applying an approach based on the deposition of hollow

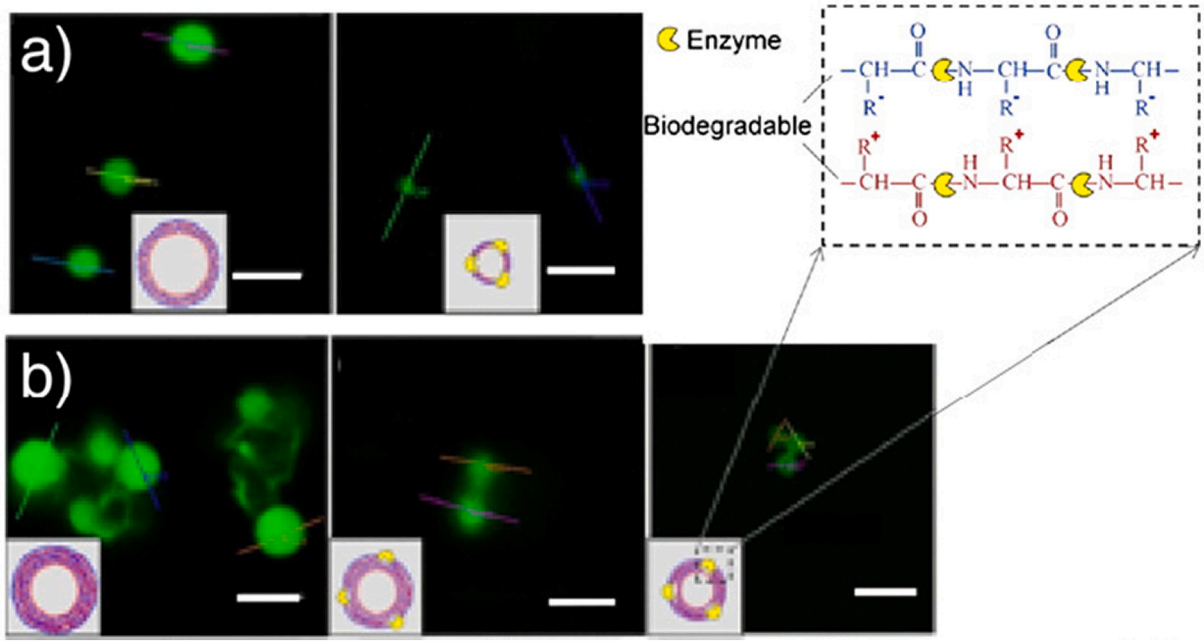

Fig. 19. Confocal laser scanning microscope images of enzyme-catalyzed degradation of: (a) four layer-pair $(pArg/pGlu)_4$ polyelectrolyte capsules with encapsulated FITC-dextran before and 60 min after incubation in a solution containing Pronase; (b) $(pArg/pGlu)_8$ capsules before (at 0 min), after 60 and 90 min of enzyme-catalyzed degradation (reproduced from [100] with permission, copyright 2012 Elsevier).

Table 5
Biology-related stimuli containing enzymes and degraded polymers.

Multilayer films/ capsules	Enzym	Degradable polymer	Reference
films - $(PDADMAC/DNA)_n$	endonuclease deoxyribonuclease I (DNase I)	PDADMAC	[308]
films - $(CH/PTAA(poly(thiophene-3-acetic acid))_n$	organophosphorus hydrolase (OPH)	PTAA	[310]
capsules - (protamine (PRM)/ heparin $(HEP))_n$	trypsin	PRM	[316]
capsules - $(pArg/pGlu)_n$ and $((PAH/PSS)(pARG/pGLU))_n$	pronase	pARG/pGLU (PAH/PSS) (pARG/ pGLU)	[100]
capsules - $(CH/HEP)_n$	heparinase (HPA)	CH/HEP	[317]
films - $(CH/HA)_n$	hyaluronidase (Hase)	HA	[318]
capsules - $(PLL/HA)_n$ and $(PAH/HA)_n$	hase	HA	[319]
capsules - (CCH (cationic chitosan) C12-OA (oleic acid)-ACH(anionic $chitosan))_n$ and $(HAC12\text{-}OA)_n$ and $(HAC12\text{-}CO (corn oil))_n$	hase	CCHC12-OA-ACH HAC12-OA HAC12-CO	[320]
capsules - $(PEI/DNA)_n$	nuclease	PEI/DNA	[321]
capsules - (pARG/ dextran sulfate $(DEXS))_n$	pronase (Proteases)	pARG/DEXS	[322]
films – $(PRM/DEXS)_n$	human Neutrophile Elastase (HNE) –AT (α1-Antitrypsin)	PRM/DEXS	[324]

capsules. Such coated microparticles were adsorbed alternately on PEI/PVDMA modified planar substrate followed by subsequent dissolution of the microparticle cores leading to the formation of the film of hollow microcapsules. It showed a disordered structure indicating that the assembly was driven by kinetic entrapment rather than close packing of microparticles (Fig. 20). The resulting film of hollow capsules was physically stable in an aqueous environment and could be reversibly dried and rehydrated without damage. It could also be loaded with macromolecular cargo for controlled release. The iterative nature of LbL deposition gave the possibility to design a system of different constituents providing various, additional functions/control over the properties of assembly as stimuli responsiveness, leading to a versatile technology platform.

Shchukin et al. developed an active corrosion protection system with self-healing ability based on nanocontainers that released entrapped corrosion inhibitors in response to pH changes caused by the corrosion process [326]. As nanocontainers assembled on the metallic support, silica nanoparticles were applied. They were coated with LbL polyelectrolyte films modified by benzotriazole molecules acting as a corrosion inhibitor. The authors showed that local corrosion activity triggered the release of benzotriazole from the polyelectrolyte shell due to local change of pH in the corrosive area. Polyelectrolyte shell opened upon this pH change and released the corrosion inhibitor to suppress the corrosion. Upon the inhibitor activity, the local pH increased closing the polyelectrolyte shell, which prevented the further release of benzotriazole. Such a nanocontainer approach allows substituting the harmful chromates with a new generation system of self-healing capacity. Similar concepts of an anticorrosion system utilizing capsules assembled on flat substrate were further elaborated [327]. Volodkin et al. developed laser-activated releasing system containing PEM microcapsules with gold nanoparticles embedded in exponentially growing thick HA/PLL film modified with gold nanoparticles as well. Such microcapsules loaded with dextran and assembled onto the film could release cargo under triggering with NIR light [158].

In addition to research on practical applications of such systems, there is a number of fundamental studies on the adsorption of microcapsules/microparticles onto planar substrates. Szyk-Warszynska et al. studied deposition of model microcapsules on a bare mica surface and mica modified with PEM [328]. They used oblique impinging jet (OIJ) [329,330,331] cell to determine the initial deposition rate of microcapsules in dependence on the various thickness of polyelectrolyte shells around the colloidal cores. They demonstrated that this rate was governed by the charge of the solid/liquid interface and the charge of the

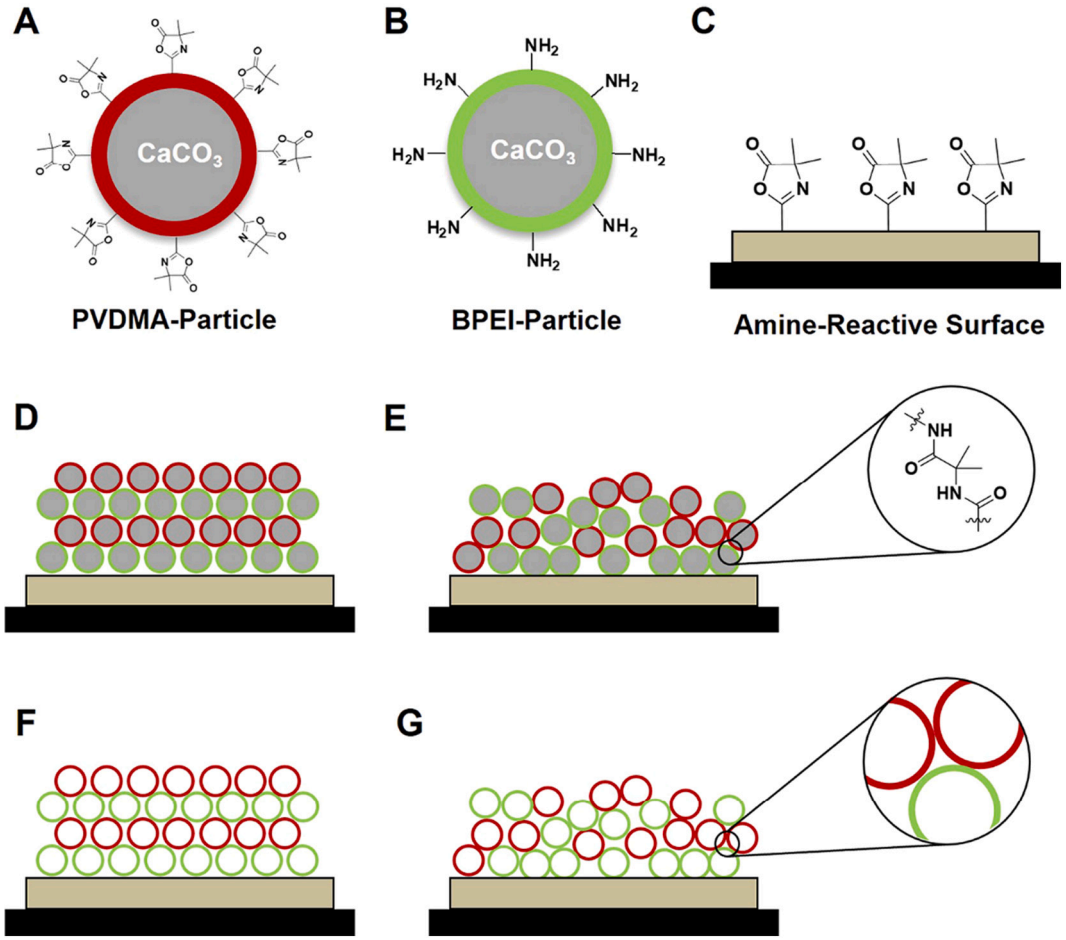

Fig. 20. (A – C) Schematic illustrations showing (A) a PVDMA-terminated, PEI/PVDMA multilayer film-coated $CaCO_3$ microparticle (an amine- reactive particle), (B) a BPEI-terminated, PEI/PVDMA multilayer film-coated $CaCO_3$ microparticle (an amine-containing particle), and (C) a PEI/PVDMA base layer-coated (yellow) planar substrate (black) presenting amine-reactive azlactone functionality. (D – G) Schematic illustrations showing two possible arrangements ((D, F) ordered; (E, G) disordered) in assemblies of amine-containing and amine-reactive particles on amine- reactive surfaces before (D, E) and after (F, G) removal of the sacrificial $CaCO_3$ templates (reproduced with permission from [325]. Copyright 2021 American Chemical Society).

capsules' terminating layer. On the other hand, the authors noticed that the initial deposition rate was negligibly dependent on the thickness of polyelectrolyte shell of the capsules and the thickness of PEM on the mica surface. They showed that the depositions rates were in good agreement with theoretical predictions based on the convective-diffusion theory of particle transport inclusive attractive interactions between oppositely charged microcapsules and PEM assembled on mica surface [332,333]. In another paper Szyk-Warszynska et al. studied the deposition of PEM-coated latex particles serving as model microcapsules on heterogeneous metal surfaces bare or covered by PEM [334]. Authors coupled already established OIJ cells with the fluorescent microscope to enable in situ observations of fluorescently labeled microcapsules' deposition on highly reflective, rough metallic surfaces. Authors found that modification of any studied metal surface with several nanometer thick PEM unified their surface charge, increasing attractive interactions between the surface and the oppositely charged microcapsules, affecting the deposition efficiency and resulting in good agreement of microcapsules' deposition rate on PEM modified metallic surface with convective-diffusion theory.

Declaration of Competing Interest

All authors declare no financial and personal relationships with other people or organizations that could inappropriately influence (bias) our work.

Acknowledgment

S.Z. would like to acknowledge the financial support provided by Polish National Science Center in a grant Beethoven Classic (2018/31/G/ST5/03955).

M.K.-S. would like to acknowledge the financial support provided by Polish National Science Center in a contract No. 2016/23/B/ST8/03128.

References

[1] Decher G, Schlenoff JB. Multilayer thin film. Wiley-VGH Verlag & Co. KGaA; 2012.
[2] Decher G. Fuzzy nanoassemblies: toward layered polymeric multicomposites. Science 1997;277:1232–7.
[3] Volodkin D, Von Klitzing R. Competing mechanisms in polyelectrolyte multilayer formation and swelling: polycation–polyanion pairing vs. polyelectrolyte–ion pairing. Curr Opin Colloid Interface Sci 2014;19:25–31.
[4] Elzbieciak M, Kolasinska M, Warszynski P. Characteristics of polyelectrolyte multilayers: the effect of polyion charge on thickness and wetting properties. Colloid Surf A Physicochem Eng Asp 2008;321:258–61.
[5] Elżbieciak M, Zapotoczny S, Nowak P, Krastev R, Nowakowska M, Warszyński P. Influence of pH on the structure of multilayer films composed of strong and weak polyelectrolytes. Langmuir 2009;25:3255–9.
[6] Zhang X, Xu Y, Zhang X, Wu H, Shen J, Chen R, et al. Progress on the layer-by-layer assembly of multilayered polymer composites: strategy, structural control and applications. Prog Polym Sci 2019;89:76–107.
[7] Schönhoff M. Self-assembled polyelectrolyte multilayers. Curr Opin Colloid Interface Sci 2003;8:86–95.

[8] Bertrand P, Jonas A, Laschewsky A, Legras R. Ultrathin polymer coatings by complexation of polyelectrolytes at interfaces: suitable materials, structure and properties. Macromol Rapid Commun 2000;21:319–48.
[9] Caruso F, Caruso RA, Möhwald H. Nanoengineering of inorganic and hybrid hollow spheres by colloidal templating. Science 1998;282:1111–4.
[10] Peyratout CS, Dähne L. Tailor-made polyelectrolyte microcapsules: from multilayers to smart containers. Angew Chem Int Ed 2004;43:3762–83.
[11] Lengert EV, Koltsov SI, Li J, Ermakov AV, Parakhonskiy BV, Skrob EV, et al. Nanoparticles in polyelectrolyte multilayer layer-by-layer (LbL) films and capsules-key enabling components of hybrid coatings. Coatings 2020;10:1131.
[12] Tsirigotis-Maniecka M, Szyk-Warszyńska L, Michna A, Warszyński P, Wilk KA. Colloidal characteristics and functionality of rationally designed esculin-loaded hydrogel microcapsules. J Colloid Interface Sci 2018;530:444–58.
[13] Guzmán E, Mateos-Maroto A, Ruano M, Ortega F, Rubio RG. Layer-by-layer polyelectrolyte assemblies for encapsulation and release of active compounds. Adv Colloid Interface Sci 2017;249:290–307.
[14] Li X, Liu C, Van der Bruggen B. Polyelectrolyte self-assembly: versatile membrane fabrication strategy. J Mater Chem A 2020;8:20870–96.
[15] Zhao S, Caruso F, Dähne L, Decher G, De Geest BG, Fan J, et al. The future of layer-bylayer assembly: a tribute to ACS Nano associate editor Helmuth Möhwald. ACS Nano 2019;13:6151–69.
[16] Mateos-Maroto A, Fernández-Peña L, Abelenda-Núñez I, Ortega F, Rubio RG, Guzman E. Polyelectrolyte multilayered capsules as biomedical tools. Polymers 2022;14:479.
[17] Tang Z, Wang Y, Podsiadlo P, Kotov NA. Biomedical applications of layer-by-layer assembly: from biomimetics to tissue engineering. Adv Mater 2006;18:3203–24.
[18] Séon L, Lavalle P, Schaaf P, Boulmedais F. Polyelectrolyte multilayers: a versatile tool for preparing antimicrobial coatings. Langmuir 2015;31:12856–72.
[19] Wang X, Liu F, Zheng X, Sun J. Water-enabled self-healing of polyelectrolyte multi- layer coatings. Angew Chem Int Ed 2011;50:11378–81.
[20] Sukhishvili SA. Responsive polymer films and capsules via layer-by-layer assembly. Curr Opin Colloid Interface Sci 2005;10:37–44.
[21] Daubiné F, Cortial D, Ladam G, Atmani H, Haïkel Y, Voegel JC, et al. Nanostructured polyelectrolyte multilayer drug delivery systems for bone metastasis prevention. Biomaterials 2009;30:6367–73.
[22] Gittleson FS, Hwang D, Ryu WH, Hashmi SM, Hwang J, Goh T, et al. Ultrathin nanotube/nanowire electrodes by spin−spray layer-by-layer assembly: a concept for transparent energy storage. ACS Nano 2015;9:10005–17.
[23] Guzmán E, Rubio RG, Ortega F. A closer physicochemical look to the layer-by-layer electrostatic self-assembly of polyelectrolyte multilayer's. Adv Colloid Interface Sci 2020;282:102197.
[24] Wolski K, Szuwarzyński M, Kopeć M, Zapotoczny S. Ordered photo- and electroactive thin polymer layers. Eur Polym J 2015;65:155–70.
[25] Szuwarzyński M, Wolski K, Kruk T, Zapotoczny S. Macromolecular strategies for transporting electrons and excitation energy in ordered polymer layers. Prog Polym Sci 2021;121:101433.
[26] Donath E, Sukhorukov GB, Caruso F, Davis SA, Möhwald H. Novel hollow polymer shells by colloid-templated assembly of polyelectrolytes. Angew Chem 1998;110:2324–7.
[27] Sukhorukov GB, Donath E, Lichtenfeld H, Knippel E, Knippel M, Budde A, et al. Layer-by-layer self assembly of polyelectrolytes on colloidal particles. Colloids Surf A 1998;137:253–66.
[28] Szczepanowicz K, Hoel HJ, Szyk-Warszynska L, Bielańska E, Bouzga AM, Gaudernack G, et al. Formation of biocompatible nanocapsules with emulsion core and pegylated Shell by polyelectrolyte multilayer adsorption. Langmuir 2010;26:12592–7.
[29] Voigt A, Lichtenfeld H, Sukhorukov GB, Zastrow H, Donath E, Baumler H, et al. Membrane filtration for microencapsulation and microcapsules fabrication by layer-by-layer polyelectrolyte adsorption. Ind Eng Chem Res 1999;38:4037–43.
[30] Parakhonskiy BV, Yashchenok AM, Konrad M, Skirtach AG. Colloidal micro- and nano-particles as templates for polyelectrolyte multialyer capsules. Adv Colloid Interface Sci 2014;207:253–64.
[31] Mateos-Maroto A, Abelenda-Núñez I, Ortega F, Rubio RG, Guzmán E. Polyelectrolyte multilayers on soft colloidal nanosurfaces: a new life for the layer-by-layer method. Polymers 2021;13:1221.
[32] Grigoriev DO, Bukreeva T, Möhwald H, Shchukin DG. New method for fabrication of loaded micro- and nanocontainers: emulsion encapsulation by polyelectrolyte layer-by-layer deposition on the liquid core. Langmuir 2008;24:999–1004.
[33] Thanasukarn P, Pongsawatmanit R, McClements D. Utilization of layer-by-layer interfacial deposition technique to improve freeze–thaw stability of oil-in-water emulsions. Food Res Int 2006;39:721–9.
[34] Shutava TG, Pattekari PP, Arapov KA, Torchilin VP, Lvov YM. Architectural layer-by-layer assembly of drug nanocapsules with PEGylated polyelectrolytes. Soft Matter 2012;8:9418–27.
[35] Qiu X, Leporatti S, Donath E, Möhwald H. Studies on the drug release properties of polysaccharide multilayers encapsulated ibuprofen microparticles. Langmuir 2001;17:5375–80.
[36] Santos AC, Pattekari P, Jesus S, Veiga F, Lvov Y, Ribeiro AJ. Sonication-assisted layer-by-layer assembly for low solubility drug nanoformulation. ACS Appl Mater Interfaces 2015;7:11972–83.
[37] Shiqu Y, Wang CW, Liu X, Tong Z, Ren B, Zeng F. New loading process and release properties of insulin from polysaccharide microcapsules fabricated through layer-by-layer assembly. J Control Release 2006;112:79–87.
[38] Zheng Z, Zhang X, Carbo D, Clark C, Nathan C, Lvov Y. Sonication assisted synthesis of polyelectrolyte coated curcumin nanoparticles. Langmuir 2010;26:7679–81.
[39] Dai Z, Heilig A, Zastrow H, Donath E, Möhwald H. Novel formulations of vitamins and insulin by nanoengineering of polyelectrolyte multilayers around microcrystals. Chem A Eur J 2004;10:6369–74.
[40] Zhou J, Pishko MV, Lutkenhaus JL. Thermoresponsive layer-by-layer assemblies for nanoparticle-based drug delivery. Langmuir 2014;30:5903–10.
[41] Parekh G, Pattekari P, Joshi C, Shutava T, DeCoster M, Levchenko T, et al. Layer-by-layer nanoencapsulation of camptothecin with improved activity. Int J Pharm 2014;465:218–27.
[42] Shenoy D, Sukhorukov GB. Engineered microcrystals for direct surface modification with layer-by-layer technique for optimized dissolution. Eur J Pharm Biopharm 2004;58:521–7.
[43] Ye S, Wang C, Liu X, Tong Z. Deposition temperature effect on release rate of indomethacin microcrystals from microcapsules of layer-by-layer assembled chitosan and alginate multilayer films. J Control Release 2005;106:319–28.
[44] Singh SK, Banala VT, Gupta GK, Verma A, Shukla R, Pawar VK, et al. Development of docetaxel nanocapsules for improving in vitro cytotoxicity and cellular uptake in MCF-7 cells. Drug Dev Ind Pharm 2015;41:1759–68.
[45] Strydom SJ, Otto DP, Stieger N, Aucamp ME, Liebenberg W, De Villiers MM. Self-assembled macromolecular nanocoatings to stabilize and control drug release from nanoparticles. Powder Technol 2014;256:470–6.
[46] Polomska A, Gauthier MA, Leroux JC. In vitro and evaluation of PEGylated layer-by-layer polyelectrolyte-coated paclitaxel nanocrystals. Small 2017;13:1602066.
[47] Milkova V, Kamburova K, Radeva T. Nanocolloids of indomethacin prepared using sonication and subsequent encapsulation with polysaccharide films. Colloids Surf B Biointerfaces 2013;108:279–84.
[48] Dev S, Toster J, Prasanna SV, Fitzgerald M, Iyer KS, Raston CL. Suppressing regrowth of microfluidic generated drug nanocrystals using polyelectrolyte coatings. RSC Adv 2013;3:695–8.
[49] Patil GB, Ramani KP, Pandey AP, More MP, Patil PO, Deshmukh PK. Fabrication of layer-by-layer self-assembled drug delivery platform for prednisolone. Polym-Plast Technol Eng 2013;52:1637–44.
[50] Santos AC, Sequeira JAD, Periera I, Cabral C, Gonzallez MC, Fontes-Ribeiro C, et al. Sonication- assisted layer-by-layer self-assembly naoparticles for resveratrol delivery. Mater Sci Eng C 2019;105:110022.
[51] Bazylińska U, Pietkiewicz J, Rossowska J, Chodaczek G, Gamian A, Wilk KA. Polyelectrolyte oil-core nanocarriers for localized and sustained delivery of daunorubicin to colon carcinoma MC38 cells: the case of polysaccharide multilayer film in relation to PEG-ylated shell. Macromol Biosci 2017;17:54–66.
[52] Szafraniec-Szczęsny J, Janik-Hazuka M, Odrobińska J, Zapotoczny S. Polymer capsules with hydrophobic liquid cores as functional nanocarriers. Polymers 2020;12:1999.
[53] Beyer S, Mak WC, Trau D. Reverse-phase LbL-encapsulation of highly water soluble materials by layer-by-layer polyelectrolyte self-assembly. Langmuir 2007;23:8827–32.
[54] Lupa D, Adamczyk Z, Oćwieja M, Duraczyńska D. Formation, properties and stability of silver nanoparticle monolayers at PDADMAC modified polystyrene microparticles. Colloids Surf A 2018;554:317–25.
[55] Richardson JJ, Maina JW, Ejima H, Hu M, Guo J, Choy MY, et al. Versatile loading of diverse cargo into functional polymer capsules. Adv Sci 2015;2:1400007.
[56] De Temmerman ML, Demeester J, De Vos F, De Smedt SC. Encapsulation performance of layer-by-layer microcapsules for proteins. Biomacromolecules. 2011;12:1283–9.
[57] Campbell J, Kastania G, Volodkin D. Encapsulation of low-molecular-weight drugs into polymer multilayer capsules templated on vaterite $CaCO_3$ crystals. Micromachines 2020;11:717.
[58] Chen Y, Che H, Shi J. In vivo bio-safety evaluations and diagnostic/therapeutic applications of chemically designed mesoporous silica nanoparticles. Adv Mater 2013;25:3144–76.
[59] Ferreira AM, Vikulina AS, Volodkin D. $CaCO_3$ crystals as versatile carriers for controlled delivery of antimicribials. J Control Release 2020;328:470–89.
[60] Wang Y, Cui J, Hosta-Rigau L, Heath JK, Nice EC, Caruso F. Encapsulation of water-insoluble drugs in polymer capsules prepared using mesoporous silica templates for intercellular drug delivery. Adv Mater 2012;22:4293–7.
[61] Zhang K, Xu LL, Jiang JG, Calin N, Lam KF, Zhang SJ, et al. Facile large-scale synthesis of monodisperse mesoporous silica nanospheres with tunable pore structure. J Am Chem Soc 2013;135:2427–30.
[62] Chen C, Gao Y, Chen HR, Zeng DP, Li YP, Zheng YY, et al. Engineering inorganic nanoemulsions/nanoliposomes by fluoride-silica chemistry for efficient delivery/co-delivey of hydrophobic agents. Adv Funct Mater 2021;22:1586–97.
[63] Xu C, Lei C, Yu C. Mesoporous silica nanoparticles for protein protection and delivery. Front Chem 2019;7:290.
[64] Kao KC, Lin TS, Mou CY. Enhanced activity and stability of lysozyme by immobilization in the matching nanochannels of mesoporous silica nanoparticles. J Phys Chem C 2014;118:6734–43.
[65] Tu J, Boyle AL, Friedrich H, Bomans PHH, Bussmann J, Sommerdijk NAJM, et al. Mesoporous silica nanoparticles with large pores for the encapsulation and release of proteins. ACS Appl Mater Interfaces 2016;8:32211–9.
[66] Kalantari M, Yu MH, Yang YN, Strounina E, Gu ZY, Huang XD, et al. Tailoring mesoporous-silica nanoparticles for robust immobilization of lipase and biocatalysis. Nano Res 2017;10:605–17.
[67] Zhao W, Zhang H, He Q, Li Y, Gu YJ, Li L, et al. A glucose-responsive controlled release of insulin system based on enzyme multilayers-coated mesoporous silica particles. Chem Commun 2011;47:9459–61.

[68] Chen Y, Chen HR, Guo LM, He QJ, Chen F, Zhou J, et al. Hollow/rattle-type mesoporous nanostructures by a structural difference-based selective etching strategy. ACS Nano 2010;4:529–39.
[69] Dai JT, Zhang Y, Li HC, Deng YH, Elzatahry AA, Alghamdi A, et al. Enhancement of gemcitabine against pancreatic cancer by loading in mesoporous silica vesicles. Chin Chem Lett 2017;28:531–6.
[70] Ruffel L, Soulie J, Coppel Y, Roblin P, Brouillet F, Frances C, et al. Ibuprofen loading into mesoporous silica nanoparticles using co-spray drying: a multi-scale study. Microporous Mesoporous Mater 2020;291:109689.
[71] Hudson SP, Padera RF, Langer R, Kohane DS. The biocompatibility of mesoporous silicates. Biomaterials 2008;29:4045–55.
[72] Xu C, Lei C, Huang L, Zhang J, Zhang H, Song H, et al. Glucose-responsive nanosysem mimicking the physiological insulin secretion via an enzyme-polymer layer-by-layer coating strategy. Chem Mater 2017;29:7725–32.
[73] Feng W, Zhou X, He C, Qiu K, Nie W, Chen L, et al. Polyelectrolyte multilayer functionalized mesoporous silica nanoparticles for pH-responsive drug delivery: layer thickness-dependent release profiles and biocompatibility. J Mater Chem B 2013;1:5886–98.
[74] Wan X, Zhang G, Liu S. pH-disintegrable polyelectrolyte multilayercoated mesoporous silica nanoparticles exhibiting triggered co release of cisplatin and model drug molecules. Macromol Rapid Commun 2011;32:1082–9.
[75] Shu S, Sun C, Zhang X, Wu Z, Wang Z, Li C. Hollow and degradable polyelectrolyte nanocapsules for protein drug delivery. Acta Biomater 2010;6:210–7.
[76] Rodriguez-Ramos A, Marin-Caba L, Iturrioz-Rofriguez N, Padin-Gonzalez E, Garcia-Hevia L, Mêna Oliviera T, et al. Design of polymeric and biocompatibile delivery systems by dissolving mesoporous silica template. Int J Mol Sci 2020;21:9573.
[77] Mydin RBSMN, Zahidi INM, Ishak NN, Ghazali NSSN, Moshawih S, Siddiquee S. Potential of calcium caronate nanoparticles for therapeutic applications. Mal J Med Health Sci 2018;14:201–6.
[78] Volodkin D. $CaCO_3$ templated micro-beads and-capsules for bioapplications. Adv Colloid Interface Sci 2014;207:306–24.
[79] Balabushevich NG, Lopez de Guerenu AV, Feoktistova NA, Skirtach AG, Volodkin D. Protein-containing multilayer capsules by templating on mesoporous $CaCO_3$ particles: POST-and PRE-loading approaches. Macromol Biosci 2016;16:95–105.
[80] Volodkin DV, Larionova NI, Sukhorukov GB. Protein encapsulation via porous $CaCO_3$ microparticles templating. Biomacromolecules. 2004;5:1962–72.
[81] Didymus JM, Oliver P, Mann S, DeVires AL, Hauschka PV, Westbroek P. Influence of low-molecular-weight and macromolecular organic additives on the morphology of calcium carbonate. J Chem Soc Faraday Trans 1993;89:2891–900.
[82] Kato T, Suzuki T, Amamiya T, Irie T, Komiyama M, Yui H. Effects of macromolecules on the crystallization of $CaCO_3$ the formation of organic/inorganic composites. Supramol Sci 1998;5:411–5.
[83] Petrov AI, Volodkin DV, Sukhorukov GB. Protein- calcium carbonate coprecipitation: a tool for protein encapsulation. Biotechnol Prog 2005;21:918–25.
[84] Lakkakula JR, Kurapati R, Tynga I, Abrahamse H, Raichur AM, Macedo Krause RW. Cyclodextrin grafted calcium carbonate particles: efficient system for tailored release of hydrophobic anticancer or hormone drugs. RSC Adv 2016;6:104537–48.
[85] Sudareva N, Suvorova O, Saprykina N, Vlasova H, Vilesov A. Doxorubicin delivery systems based on doped $CaCO_3$ cores and polyanion drug conjugates. J Microencapsul 2021;38:164–76.
[86] Li L, Yang Y, Lv Y, Yin P, Lei T. Porous calcite $CaCO_3$ microspheres: preparation, characterization and release behavior as doxorubicin carrier. Colloids Surf B Biointerfaces 2020;186:110720.
[87] Balabushevivh NG, Kovalenko EA, Le-Deygen IM, Filatova LY, Volodkin D, Vikulina AS. Hybrid $CaCO_3$- mucin crystals: effective approach for loading and controlled release of cationic drugs. Mater Des 2019;182:108020.
[88] Begum G, Reddy TN, Kumar KP, Dhevendar K, Singh S, Amarnath M, et al. In situ strategy to encapsulate antibiotics in a bioinspired $CaCO_3$ structure enabling pH-sensitive drug release apt for therapeutic and imaging applications. ACS Appl Mater Interfaces 2016;8:22056–63.
[89] Matei C, Berger D, Dumbrava A, Radu MD, Gheorghe E. Calcium carbonate as silver carrier in composite materials obtained in green seaweed extract with topical applications. J Sol-Gel Sci Technol 2019;93:315–23.
[90] Długosz M, Bulwan M, Kania G, Nowakowska M, Zapotoczny S. Hybrid calcium carbonate/polymer microparticles containing silver nanoparticles as antibacterial agents. J Nanopart Res 2012;14:1313.
[91] Schmidt S, Behra M, Uhlig K, Madaboosi N, Hartmann L, Duschl C, et al. Mesoporous protein particles through colloidal $CaCO_3$ templates. Adv Funct Mater 2013;23:116–23.
[92] Balabushevich NG, Lopez de Guerene AV, Feoktistova NA, Volodkin D. Protein loading into porous $CaCO_3$ microspheres: adsorption equilibrium and bioactivity retention. Phys Chem Chem Phys 2015;17:2523–30.
[93] Feoktistova NA, Balabushevich NG, Skirtach AG, Volodkin D, Vikulina AS. Inter-protein interactions govern protein loading into porous vaterite $CaCO_3$ crystals. Phys Chem Chem Phys 2020;22:9713–22.
[94] German SV, Novoselova MV, Bratashov DN, Demina PA, Atkin VS, Voronin DV, et al. High-efficiency freezing-induced loading of inorganic nanoparticles and proteins into micron- and submicron-sized porous particles. Sci Rep 2018;8:17763.
[95] Xu W, Ledin PA, Plamper FA, Synatschke CV, Müller AHE, Tsukruk VV. Multiresponsive microcapsules based on multilayer assembly of star polyelectrolytes. Macromolecules 2014;47:7858–68.
[96] Skirtach AG, Yashchenok AM, Möhwald H. Encapsulation, release and applications of LbL polyelectrolyte multilayer capsules. Chem Commun 2011;47:12736–46.
[97] Lavalle P, Voegel JC, Vautier D, Senger B, Schaaf P, Ball V. Dynamic aspects of films prepared by a sequential deposition of species: perspectives for smart and responsive materials. Adv Mater 2011;23:1191–221.
[98] Del Mercato LL, Ferraro MM, Baldassarre F, Mancarella S, Greco V, Rinaldi R, et al. Biological applications of LbL multilayer capsules: from drug delivery to sensing. Adv Colloid Interface Sci 2014;207:139–54.
[99] Liu X, Appelhans D, Wei Q, Voit B. Photo-cross linked dual-responsive hollow capsules mimicking cell membrane for controllable cargo post-encapsulation and release. Adv Sci 2016;4:1600308.
[100] Marchenko I, Yashchenko A, Borodina T, Bukreeva T, Konrad M, Möhwald H, et al. Controlled enzyme-catalyzed degradation of polymeric capsules templated on $CaCO_3$: influence of the number of LbL layers, conditions of degradation, and disassembly of multicompartments. J Control Release 2012;162:599–605.
[101] Korolovych VF, Grishina OA, Inozemtseva OA, Selifonov AV, Bratashov DN, Suchkov SG, et al. Impact of high-frequency ultrasound on nanocomposite microcapsules: in silico and in situ visualization. Phys Chem Chem Phys 2016;18:2389–97.
[102] Stavarac CE, Paniwnyk L. Controlled rupture of magnetic LbL polyelectrolyte capsules and subsequent release of contents employing high intensity focused ultrasound. J Drug Deliv Sci Technol 2018;45:60–9.
[103] Zapotoczny S. Stimuli responsive polymers for nanoengineering of biointerfaces. In: Navarro M, Planell J, editors. Nanotechnology in regenerative medicine. Methods in molecular biology (methods and protocols). vol. 811. Humana Press; 2012.
[104] Grosberg AY, Khokhlov AR, De Gennes PG. Giant molecules: here, there, and everywhere. Hackensack: World Scientific Publishing Co. Pte. Ltd; 2011.
[105] Khokhlov AR, Kremer F, Matyjaszewski K, Moller M. Basic concepts and polymer properties. Elsevier; 2012.
[106] Schild HG. Poly(N-isopropylacryl-amide): experiment, theory and application. Prog Polym Sci 1992;17:163–249.
[107] Cho EC, Lee J, Cho K. Role of bound water and hydrophobic interaction in phase transition of poly(N-isopropylacrylamide) aqueous solution. Macromolecules 2003;36:9929–34.
[108] Grinberg VY, Dubovik AS, Kuznetsov DV, Grinberg NV, Grosberg AY, Tanaka T. Studies of the thermal volume transition of poly(N-isopropylacrylamide) hydrogels by high-sensitivity differential scanning microcalorimetry. 2. Thermodynamic functions. Macromolecules 2000;33:8685–92.
[109] Shibayama M, Tanaka T. Volume phase transition and related phenomena of polymer gels. Adv Polym Sci 1992;109:1–62.
[110] Jaber JA, Schlenoff JB. Polyelectrolyte multilayers with reversible thermal responsivity. Macromolecules 2005;38:1300–6.
[111] Yamada N, Okano T, Sakai H, Karikusa F, Sawasaki Y, Sakurai Y. Thermo-responsive polymeric surfaces; control of attachment and detachment of cultured cells. Makromol Chem Rapid Commun 1990;11:571.
[112] Canavan HE, Cheng X, Graham DJ, Ratner BD, Castner DG. Cell sheet detachment affects the extracellular matrix: a surface science study comparing thermal liftoff, enzymatic, and mechanical methods. J Biomed Mater Res Part A 2005;75A:1–13.
[113] Yamato M, Okano T. Cell sheet engineering. Mater Today 2004;7:42–7.
[114] Ide T, Nishida K, Yamato M, Sumide T, Utsumi M, Nozaki T, et al. Structural characterization of bioengineered human corneal endothelial cell sheets fabricated on temperature-responsive culture dishes. Biomaterials 2006;27:607–14.
[115] Yang J, Yamato M, Konno C, Nishimoto A, Sekine H, Fukai F, et al. Cell sheetengineering: recreating tissues without biodegradable scaffolds. Biomaterials 2005;26:6415–22.
[116] Ferreira Q, Ribeiro PA, Oliveira ON, Raposo M. Long-term stability at high temperatures for birefringence in PAZO/PAH layer-by-layer films. ACS Appl Mater Interfaces 2012;4:1470–7.
[117] Mueller R, Koehler K, Weinkamer R, Sukhorukov GB, Fery A. Melting of PDADMAC/PSS capsules investigated with AFM force spectroscopy. Macromolecules 2005;38:9766–71.
[118] Diamanti E, Muzzio N, Gregurec D, Irigoyen J, Pasquale M, Azzaroni O, et al. Impact of thermal annealing on wettability and antifouling characteristics of alginate poly-l-lysine polyelectrolyte multilayer films. Colloids Surf B Biointerfaces 2016;145:328–37.
[119] Kolasinska M, Gutberlet T, Krastev R. Ordering of Fe_3O_4 nanoparticles in polyelectrolyte multilayer films. Langmuir 2009;25:10292–7.
[120] Koehler K, Shchukin D, Mohwald H, Sukhorukov GB. Thermal behavior of polyelectrolyte multilayer microcapsules. 1. The effect of odd and even layer number. J Phys Chem B 2005;109:18250–9.
[121] Leporatti S, Gao C, Voigt A, Donath E, Mohwald H. Shrinking of ultrathin polyelectrolyte multilayer capsules upon annealing: a confocal laser scanning microscopy and scanning force microscopy study. Eur Phys J E 2001;5:13–20.
[122] Koehler K, Shchukin D, Sukhorukov G, Möhwald H. Drastic morphological modification of polyelectrolyte microcapsules induced by high temperature. Macromolecules 2004;37:9546–50.
[123] Steitz R, Leiner V, Tauer K, Khrenov V, Von Klitzing R. Temperature-induced changes in polyelectrolyte films at the solid-liquid interface. Appl Phys A 2002;521:519–21.

[124] Zerball M, Laschewsky A, Köhler R, Von Klitzing R. The effect of temperature treatment on the structure of polyelectrolyte multilayers. Polymers 2016;8:120.
[125] Saikaew R, Marsal P, Grenier B, Dubas ST. Temperature controlled loading and release of curcumin in polyelectrolyte multilayers thin films. Mater Lett 2018; 215:38–41.
[126] Golonka M, Bulwan M, Nowakowska M, Testera AM, Rodrıguez-Cabello JC, Zapotoczny S. Thermoresponsive multilayer films based on ionic elastin-like recombinamers. Soft Matter 2011;7:9402–9.
[127] Sousa MP, De Torre IG, Oliveira MB, Rodríguez-Cabello JC, Mano JF. Biomimetic click assembled multilayer coatings exhibiting responsive properties. Mater Today Chem 2017;4:150–63.
[128] Xu L, Wang H, Chu Z, Cai L, Shi H, Zhu C, et al. Temperature-responsive multilayer films of micelle-based composites for controlled release of a third-generation EGFR inhibitor. ACS Appl Polym Mater 2020;2:741–50.
[129] Esser-Kahn AP, Sottos NR, White SR, Moore JS. Programmable microcapsules from self-immolative polymers. J Am Chem Soc 2010;132:10266–8.
[130] McCormick M, Smith RN, Graf R, Barrett CJ, Reven L, Spiess HW. NMR studies of the effect of adsorbed water on polyelectrolyte multilayer films in the solid state. Macromolecules 2003;36:3616–25.
[131] Mak WC, Cheung KY, Trau D. Influence of different polyelectrolytes on layer-by-layer microcapsules properties: encapsulation efficiency and colloidal temperature stability. Chem Mater 2008;20:5475–84.
[132] Ibarz G, Dähne L, Donath E, Möhwald H. Controlled permeability of polyelectrolyte capsules via defined annealing. Chem Mater 2002;14:4059–62.
[133] Huang C, Chang F. Using click chemistry to fabricate ultrathin thermoresponsive microcapsules through direct covalent layer-by-layer assembly. Macromolecules 2009;42:5155–66.
[134] Liang X, Kozlovskaya V, Chen Y, Zavgordonya O, Kharlampieva E. Thermosensitive multilayer hydrogels of poly(N-vinylcaprolactam) as nanothin films and shaped capsules. Chem Mater 2012;24:3707–19.
[135] Sirsi SR, Borden MA. State-of-the-art materials for ultrasound-triggered drug delivery. Adv Drug Deliv Rev 2014;72:3–14.
[136] Skirtach AG, De Geest BG, Mamedov A, Antipov AA, Kotov NA, Sukhorukov GB. Ultrasound stimulated release and catalysis using polyelectrolyte multilayer capsules. J Mater Chem 2007;17:1050–4.
[137] Kolesnikova TA, Gorin DA, Fernandes P, Kessel S, Khomutov GB, Fery A, et al. Nanocomposite microcontainers with high ultrasound sensitivity. Adv Funct Mater 2010;20:1189–95.
[138] Gao H, Wen D, Tarakina NV, Liang J, Bushby AJ, Sukhorukov GB. Bifunctional ultraviolet/ultrasound responsive composite TiO_2/polyelectrolyte microcapsules. Nanoscale 2016;8:5170–80.
[139] Gao H, Wen D, Sukhorukov GB. Composite silica nanoparticle/polyelectrolyte microcapsules with reduced permeability and enhanced ultrasound sensitivity. J Mater Chem B 2015;3:1888–97.
[140] Pavlov AM, Saez V, Cobley A, Graves J, Sukhorukov GB, Mason TJ. Controlled protein release from microcapsules with composite shells using high frequency ultrasound-potential for in vivo medical use. Soft Matter 2011;7:4341–7.
[141] Chen J, Ratnayaka V, Alford A, Kozlovskaya V, Liu F, Xue L, et al. Theranostic multilayer capsules for ultrasound imaging and guided drug delivery. ACS Nano 2017;11:3135–46.
[142] Lisunova MO, Drachuk I, Shchepelina OA, Anderson KD, Tsukruk VV. Direct probing of micromechanical properties of hydrogen-bonded layer-by-layer microcapsule shells with different chemical compositions. Langmuir 2011;27: 11157–65.
[143] Novoselova MV, Voronin DV, Abakumova TO, Demina PA, Petrov AV, Petrov VV, et al. Focused ultrasound-mediated fluorescence of composite microcapsules loaded with magnetite nanoparticles: in vitro and in vivo study. Colloids Surf B Biointerfaces 2019;181:680–7.
[144] Borges J, Rodrigues LC, Reis LC, Mano JF. Layer-by_layer assembly of light-responsive polymeric multilayers systems. Adv Funct Mater 2014;36:5624–48.
[145] Koylu D, Thapa M, Gumbley P, Thomas III SW. Photochemical disruption of polyelectrolyte multilayers. Adv Mater 2012;24:1451–4.
[146] Cao T, Wei F, Jiao X, Chen J, Liao W, Zhao X, et al. Micropatterns of protein and conducting polymer molecules fabricated by layer-by-layer self-assembly and photolithography techniques. Langmuir 2003;19:8127–9.
[147] Wang Y, Han P, Wu G, Xu H, Wang Z, Zhang X. Selectively erasable myltilayer thin film by photoinduced disassembly. Langmuir 2010;26:9736–41.
[148] Fernández R, Ocando C, Fernandes SCM, Eceiza A, Tercjak A. Optically active multilayer films based on chitosan and an azopolymer. Biomacromolecules 2014; 15:1399–407.
[149] Tanchak OM, Barrett CJ. Light-induced reversible volume changes in thin films of azo polymers: the pchotomechanical effect. Macromolecules 2005;38:10566–70.
[150] Zhang H, Yan X, Wang Y, Deng Y, Wang X. Sequentially adsorbed electrostatic multilayers of polyanilineand azo polyelectrolytes. Polymer 2008;49:5504–12.
[151] Pennakalathil J, Hong JD. Self-standing polyelectrolyte multilayer films based on light-triggered disassembly of a sacrificial layer. ACS Nano 2011;5:9232–7.
[152] Higuchi A, Hamamura A, Shindo Y, Kitamura H, Yoon BO, Mori T, et al. Photon-modulated changes of cell attachments on poly(spiropyran-co-methyl methacrylate) membranes. Biomacromolecules 2004;5:1770–4.
[153] Edahiro J, Sumaru K, Tada Y, Ohi K, Takagi T, Kameda M, et al. In situ control of cell adhesion using photoresponsive culture surface. Biomacromolecules 2005;6: 970–4.
[154] Yuan WY, Ji J, Fu J, Shen J. A facile method to construct hybrid multilayered films as a strong and multifunctional antibacterial coating. Biomed Mater Res Part B 2008;85B:556–63.
[155] Corbitt TS, Sommer JR, Chemburu S, Ogawa K, Ista LK, Lopez GP, et al. Conjugated polyelectrolyte capsules: light-activated antimicrobial micro "roach motels". ACS Appl Mater Interfaces 2009;1:48–52.
[156] Volodkin DV, Madaboosi N, Blacklock J, Skirtach AG, Möhwald H. Surface-suported multilayers decorated with bio-active material aimed at light-triggered drug delivery. Langmuir 2009;25:14037–43.
[157] Skirtach AG, Volodkin DV, Möhwald H. Bio-interfaces-interaction of PLL/HA thick films with nanoparticles and microcapsules. Chem Phys Chem 2010;11: 822–9.
[158] Volodkin DV, Delcea M, Möhwald H, Skirtach AG. Remote near-IR light activation of a hyaluronic acid/poly(l-lysine) multilayered film and film-entrapped microcapsules. ACS Appl Mater Interfaces 2009;1:1705–10.
[159] Jiang Y, Li J, Zhen X, Xie C, Pu K. Dual-peak absorbing semiconducting copolymer nanoparticles for first and second near-infrared window photothermal therapy: a comparative study. Adv Mater 2018;30:1705980.
[160] Fomina N, Sankaranarayanan J, Almutairi A. Photochemical mechanisms of light-triggered release from nanocarriers. Adv Drug Deliv Rev 2012;64:1005–20.
[161] Bedard MF, Sadasivan S, Sukhorukov GB, Skirtach A. Assembling polyelectrolytes and porphyrins into hollow capsules with laser-responsive oxidative properties. J Mater Chem 2009;19:2226–33.
[162] Palankar R, Skirtach AG, Kreft O, Bedard M, Garstka M, Gould K, et al. Controlled intracellular release of peptides from microcapsules enhances antigen presentation on MHC class I molecules. Small 2009;5:2168–76.
[163] Kreft O, Skirtach AG, Sukhorukov GB, Möhwald H. Remote control of bioreactions in multicompartment capsules. Adv Mater 2007;19:3142–5.
[164] Sharma V, Vijay J, Ganesh MR, Sundaramurthy A. Multilayer capsules encapsulating nimbin and doxorubicin for cancer chemo-photothermal therapy. Int J Pharm 2020;582:119350.
[165] Rai P, Mallidi S, Zheng X, Rahmanzadeh R, Mir Y, Elrington S, et al. Development and applications of photo-triggered theranostic agents. Adv Drug Deliv Rev 2010; 62:1094–124.
[166] Shen X, Li T, Xie X, Feng Y, Chen Z, Yang H, et al. PLGA-based drug delivery systems for remotely triggered cancer therapeutic and diagnostic applications. Front Bioeng Biotechnol 2020;8:381.
[167] Yang M, Yang T, Mao C. Enhancement of photodynamic cancer therapy by physical and chemical factors50; 2019. p. 14066–80.
[168] Radt B, Smith TA, Caruso F. Optically addressable nanostructured capsules. Adv Mater 2004;16:2184–9.
[169] Skirtach AG, Antipov AA, Shchukin DG, Sukhorukov GB. Remote activation of capsules containing ag nanoparticles and IR dye by laser light. Langmuir 2004;20: 6988–92.
[170] SkirtachAG Javier AM, Kreft O, Köhler K, Alberola AP, Möhwald H, Parak WJ, et al. Laser-induced release of encapsulated materials inside living cells. Angew Chem Int Ed 2006;45:4612–7.
[171] Treguer-Delapierre M, Majimel J, Mornet S, Duguet E, Ravaine S. Influence of single use and combination of reductants on the size, morphology and growth steps of gold nanoparticles in colloidal mixture. OJPC 2008;41:195–207.
[172] Skirtach AG, Karageorgiev P, De Geest BG, Pazos-Perez N, Braun D, Sukhorukov GB. Nanorods as wavelength-selective absorption centers in the visible and near-infrared regions of the electromagnetic spectrum. Adv Mater 2008;20:506–10.
[173] Wang C, Margarita M, Gonzales V, Fadeev M, Sohn YS, Nechushtai R, et al. Thermoplasmonic-triggered release of loads from DNA-modified hydrogel microcapsules functionalized with Au nanoparticles or Au nanorods. Small 2020; 16:2000880.
[174] Skirtach AG, Dejugnat C, Braun D, Susha AS, Rogach AL, Parak WJ, et al. The role of metal nanoparticles in remote release of encapsulated materials. Nano Lett 2005;5:1371–7.
[175] Skirtach AG, Karageorgiev P, Bedard MF, Sukhorukov GB, Möhwald H. Reversibly permeable nanomembranes of polymeric microcapsules. J Am Chem Soc 2008; 130:11572–3.
[176] Bedard MF, Braun D, Sukhorukov GB, Skirtach AG. Toward self-assembly of nanoparticles on polymeric microshells: near -IR release and permeability. ACS Nano 2008;2:1807–16.
[177] Lengert E, Parakhonskiy B, Khalenkow D, Zečić A, Vangheel M, Moreno JMM, et al. Laser-induced remote release in vivo in C. elegans from novel silver nanoparticles-alginate hydrogel shells. Nanoscale 2018;10:17249–56.
[178] Brkovic N, Zhang L, Peters JN, Kleine-Doepke S, Parak WJ, Zhu D. Quantitative assessment of endosomal escape of various endocytosed polymer-encapsulated molecular cargos upon photothermal heating. Small 2020;16:2003639.
[179] Zograf GP, Timin AS, Muslimov AR, Shishkin II, Nominé A, Ghanbaja J, et al. All-optical nanoscale heating and thermometry with resonant dielectric nanoparticles for controllable drug release in living cells. Laser Photon Rev 2020;14:1900082.
[180] Kurapati R, Raichur AM. Near-infrared light-responsive graphene oxide composite multilayer capsules: a novel route for remote controlled drug delivery. Chem Commun 2013;49:734–6.
[181] Saito H, Kato N. Polyelectrolyte/carbon nanotube composite microcapsules and drug release triggered by laser irradiation. Jpn J Appl Phys 2016;55. 03DF06.
[182] Chojnacka-Górka K, Wolski K, Zapotoczny S. Durable polyelectrolyte microcapsules with near-infrared-triggered loading and nondestructive release of cargo. ACS Appl Mater Interfaces 2021;13:1562–72.
[183] Bédard MF, De Geest BG, Skirtach AG, Möhwald H, Sukhorukov GB. Polymeric microcapsules with light responsive properties for encapsulation and release. Adv Colloid Interface Sci 2010;158:2–14.
[184] Akiba U, Minaki D, Anzai J. Photosensitive layer-by-layer assemblies containing azobenzene groups: synthesis and biomedical applications. Polymers 2017;9:553.

[185] Bédard M, Skirtach AG, Sukhorukov GB. Optically driven encapsulation using novel polymeric hollow shells containing an azobenzene polymer. Macromol Rapid Commun 2022;200(28):1517–21.
[186] Yi Q, Sukhorukov GB. UV-induced disruption of microcapsules with azobenzene groups. Soft Matter 2014;10:1384–91.
[187] El Halabieh R, Mermut O, Barrett CJ. Using light to control physical properties of polymers and surfaces with azobenzene dyes. Pure Appl Chem 2004;76:1445–66.
[188] Nithyanandhan J, Jayaraman N, Davis R, Das S. Synthesis, fluorescence and photoisomerization studies of azobenzene-functionalized poly(alkyl aryl ether) dendrimers. Chem A Eur J 2004;10:689–98.
[189] Yi Q, Sukhorukov GB. Externally triggered dual function of complex microcapsules. ACS Nano 2013;7:8693–705.
[190] Xiao W, Chen WH, Zhang J, Li C, Zhuo RX, Zhang XZ. Design of a photoswitchable hollow microcapsular drug delivery system by using a supramolecular drug-loading approach. J Phys Chem B 2011;115:13796–802.
[191] Li H, Tong W, Gao C. Photo-responsive polyethyleneimine microcapsules cross-linked by ortho-nitrobenzyl derivatives. J Colloid Interface Sci 2016;463:22–8.
[192] Bertrand O, Gohy JF. Photo-responsive polymers: synthesis and applications. Polym Chem 2017;8:52–73.
[193] Koo HY, Lee HY, Kim JK, Choi WS. UV-triggered encapsulation and release from polyelectrolyte microcapsules decorated with photoacid generators. J Mater Chem 2010;20:3932–7.
[194] Xu Choi I, Plamper FA, Synatschke CV, AHE Müller, Tsukruk VV. Nondestructive light-initiated tuning of layer-by-layer microcapsule permeability. ACS Nano 2012;7:598–613.
[195] Jiang N, Cheng Y, Wei J. Coumarin-modified fluorescent microcapsules and their photo-switchable release property. Colloids Surf A Physicochem Eng Asp 2017; 522:28–37.
[196] Yi Q, Wen D, Sukhorukov GB. UV-cross-linkable multilayer microcapsules made of weak polyelectrolytes. Langmuir 2012;28:10822–9.
[197] Aadinath W, Ghosh T, Anandharamakrishnan C. Multimodal magnetic nano-carriers for cancer treatments: chellenges and advancements. J Magn Magn Mater 2016;401:1159–72.
[198] Lachowicz D, Górka W, Kmita A, Bernasik A, Żukrowski J, Szczerba W, et al. Enhanced hyperthermic properties of biocompatibile zinc ferrite nanoparticles with a charged polysaccharide coating. J Mater Chem B 2019;7:2962–73.
[199] Kania G, Sternak M, Jasztal A, Chlopicki S, Błażejczyk A, Nasulewicz-Goldeman A, et al. Uptake and bioreactivity of charged chitosan-coated superparamagnetic nanoparticles as promising contrast agents for magnetic resonance imaging. Nanomedicine 2018;14:131–40.
[200] Chen YT, Kolhatkar AG, Zenasni O, Xu S, Lee TR. Biosensing using magnetic particle detection techniques. Sensors 2017;17:2300.
[201] Rudolf H, Silvio D, Robert M, Matthias Z. Magnetic particle hyperthermia: nanoparticle magnetism and materials development for cancer therapy. J Phys Condens Matter 2006;18:S2919.
[202] Fortin JP, Wilhelm C, Servais J, Menager C, Bacri JC, Gazeau F. Size-sorted iron oxide nanomagnets as colloidal mediators for magnetic hyperthermia. J Am Chem Soc 2007;129:2628–35.
[203] Szczepanowicz K, Warszynski P. Magnetically responsive liquid core polyelectrolyte nanocapsules. J Microencapsul 2015;32:123–8.
[204] Podgórna K, Szczepanowicz K. Synthesis of polyelectrolyte nanocapsules with iron oxide (Fe3O4) nanoparticles for magnetic targeting. Colloids Surf A Physicochem Eng Asp 2016;505:132–7.
[205] Gumieniczek-Chłopek E, Odrobińska J, Strączek T, Radziszewska A, Zapotoczny S, Kapusta C. Hydrophobically coated superparamagnetic iron oxides nanoparticles incorporated into polymer-based nanocapsules dispersed in water. Materials 2020;13:1219.
[206] Zheng C, Ding Y, Liu X, Wu Y, Ge L. Highly magneto-responsive multilayer microcapsules for controlled release of insulin. Int J Pharm 2014;475:17–24.
[207] Lu Z, Prouty MD, Guo Z, Golub VO, Kumar CSSR, Lvov YM. Magnetic switch of permeability for polyelectrolyte microcapsules embedded with co@au nanoparticles. Langmuir 2005;21:2042–50.
[208] Pankhurst QA, Thanh NTK, Jones SK, Dobson J. Progress in application of magnetic nanoparticles in biomedicine. J Phys D Appl Phys 2009;42:224001.
[209] Hu SH, Tsai CH, Liao CF, Liu DM, Chen SY. Controlled rupture of magnetic polyelectrolyte microcapsules for drug delivery. Langmuir 2008;24:11811–8.
[210] Katagiri K, Nakamura M, Koumoto K. Magnetoresponsive smart capsules formed with polyelectrolytes, lipid bilayers and magnetic nanoparticles. ACS Appl Mater Interfaces 2010;2:768–73.
[211] Katagiri K, Imai Y, Koumoto K. Variable o-demand release function of magnetoresponsive hybrid capsules. J Colloid Interface Sci 2011;361:109–14.
[212] Carregal-Romero S, Guardia P, Yu X, Hartmann R, Pellegrino T, Parak WJ. Magnetically triggered release of molecular cargo from iron oxide nanoparticle loaded microcapsules. Nanoscale 2015;7:570–6.
[213] Guardia P, Riedinger A, Nitti S, Pugliese G, Marras S, Genovese A, et al. One pot synthesis of monodisperse water solubleiron oxide nanocrystals with high values of the specific absorption rate. J Mater Chem B 2014;2:4426–34.
[214] Guardia P, Di Corato R, Lartigue L, Wilhelm C, Espinosa A, Garcia-Hernandez M, et al. Water-soluble iron oxide nanocubes with high values of specific absorption rate for cancer cell hyperthermia treatment. ACS Nano 2012;6:3080–91.
[215] Shiratori S, Rubner MF. pH-Dependent Thickness Behavior of Sequentially Adsorbed Layers of Weak. Macromolecules. 2000;33(11):4213–9.
[216] Makhlouf ASH, Abu-Thabit NY. Stimuli responsive polymeric nanocarriers for drug delivery applications, types and triggers. In: Woodhead publishing series in biomaterials. Elsevier; 2018. p. 1.
[217] Hiller J, Rubner MF. Reversible molecular memory and pH-switchable swelling transitions in polyelectrolyte multilayers. Macromolecules 2003;36:4078–83.
[218] Park MK, Deng S, Advincula RC. pH-sensitive bipolar ion-permselective ultrathin films. J Am Chem Soc 2004;126:13723–31.
[219] Kharlampieva E, Sukhishvili SA. Polyelectrolyte multilayers of weak polyacid and cationic copolymer: competition of hydrogen bonding and electrostatic interactions. Macromolecules 2003;36:9950–6.
[220] Lavalle Ph, Gergely C, Cuisinier FJG, Decher G, Schaaf P, Voegel JC, et al. Comparison of the structure of polyelectrolyte multi-layer films exhibiting a linear and an exponential growth regime: an insitu atomic microscopy study. Macromolecules 2002;35:4458–65.
[221] Yoo D, Shiratori SS, Rubner MF. Controlling bilayer composition and surface wettability of sequentially adsorbed multilayers of weak polyelectrolytes. Macromolecules 1998;31:4309–18.
[222] Yuan W, Dong H, Li CM, Cui X, Yu L, Lu Z, et al. pH-controlled construction of chitosan/alginate multilayer film: characterization and application for antibody immobilization. Langmuir 2007;23:13046–52.
[223] Miller MD, Bruening ML. Correlation of the swelling and permeability of polyelectrolyte multilayer films. Chem Mater 2005;17:5375–81.
[224] Tanchak OM, Barrett CJ. Swelling dynamics of multilayer films of weak polyelectrolytes. Chem Mater 2004;16:2734–9.
[225] Dörte B, Cornelia C, Monika S. pH-dependent growth laws and viscoelastic parameters of poly-l-lysine/hyaluronic acid multilayers. Adv Mater Interfaces 2017;4:1600592.
[226] Cho C, Xiang F, Wallace KL, Grunlan JC. Combined ionic and hydrogen bonding in polymer multilayer thin film for high gas barrier and stretchiness. Macromolecules 2015;48:5723–9.
[227] De Longchamp DM, Hammond PT. Fast ion conduction in layer-by-layer polymer films. Chem Mater 2003;15:1165–73.
[228] Argun AA, Ashcraft JN, Herring MK, Lee DKY, Allcock HR, Hammond PT. Ion conduction and water transport in polyphosphazene-based multilayers. Chem Mater 2009;22:226–32.
[229] Lutkenhaus JL, McEnnis K, Hammond PT. Nano- and microporous layer-by-layer assemblies containing linear poly(ethylenimine) and poly(acrylic acid). Macromolecules 2008;41:6047–54.
[230] Cho C, Zacharia NS. Film stability during postassembly morphological changes in polyelectrolyte multilayers due to acid and base exposure. Langmuir 2012;28: 841–8.
[231] Chia KK, Rubner MF, Cohen RE. pH-responsive reversibly swellable nanotube arrays. Langmuir 2009;25:14044–52.
[232] Fery A, Schöler B, Cassagneau T, Caruso F. Nanoporous thin films formed by salt-induced structural changes in multilayers of poly(acrylic acid) and poly (allylamine). Langmuir 2001;17:3779–83.
[233] Dressick WJ, Wahl KJ, Bassim ND, Stroud RM, Petrovykh DY. Divalent anion salt effects in polyelectrolyte multilayer depositions. Langmuir 2012;28:15831–43.
[234] Kharlampieva E, Kozlovskaya V, Chan J, Ankner JF, Tsukruk VV. Spin-assisted layer- by-layer assembly: variation of stratification as studied with neutron reflectivity. Langmuir 2009;25:14017–24.
[235] Yilmazturk S, Deligoz H, Yilmazoglu M, Damyan H, Oksuzomer F, Koç SN, et al. A novel approach for highly proton conductive electrolyte membranes with improved methanol barrier properties: layer-by-layer assembly of salt containing polyelectrolytes. J Membr Sci 2009;343:137–46.
[236] Choi J, Rubner MF. Influence of the degree of ionization on weak polyelectrolyte multilayer assembly. Macromolecules 2004;38:116–24.
[237] Elzbieciak M, Kolasinska M, Zapotoczny S, Krastev R, Nowakowska M, Warszynski P. Nonlinear growth of multilayer films formed from weak polyelectrolytes. Colloids Surf A Physicochem Eng Asp 2009;343:89–95.
[238] Boddohi S, Killingsworth CE, Kipper MJ. Polyelectrolyte multilayer assembly as a function of pH and ionic strength using the polysaccharides chitosan and heparin. Biomacromolecules 2008;9:2021–8.
[239] Fu J, Ji J, Yuan W, Shen J. Construction of anti-adhesive and antibacterial multilayer films via layer-by-layer assembly of heparin and chitosan. Biomaterials 2005;26:6684–92.
[240] Yuan W, Li CM. Direct modulation of localized surface plasmon coupling of au nanoparticles on solid substrates via weak polyelectrolyte-mediated layer-by-layer self assembly. Langmuir 2009;25:7578–85.
[241] Sham AYW, Notley SM. Layer-by-layer assembly of thin films containing exfoliated pristine graphene nanosheets and polyethyleneimine. Langmuir 2014; 30:2410–8.
[242] Metzman JS, Wang G, Morris JR, Heflin JR. Enhanced scratch resistance of self-assembled silica nanoparticle anti-reflection coatings. J Mater Chem C 2018;6: 823–35.
[243] Fu J, Ji J, Shen L, Küller A, Rosenhahn A, Shen J, et al. pH-amplified exponential growth multilayers: A facile method to develop hierarchical micro- and nanostructured surfaces. Langmuir 2008;25:672–5.
[244] Yuan W, Weng GM, Lipton J, Li CM, Van Tassel PR, Taylor AD. Weak polyelectrolyte-based multilayers via layer-by-layer assembly: approaches, properties, and applications. Adv Colloid Interface Sci 2020;282:102200–21.
[245] Anandhakumar S, Gokul P, Raichur AM. Stimuli-responsive weak polyelectrolyte multilayer films: A thin film platform for self triggered multi-drug delivery. Mater Sci Eng C 2016;58:622–8.
[246] Hoogeveen NG, Stuart CMA, Fleer GJ. Polyelectrolyte adsorption on oxides. 2. Reversibility and exchange. Colloid Interface Sci 1996;182:146–57.
[247] McAloney RA, Sinyor M, Dudnik V, Goh MC. Atomic force microscopy studies of salt effects on polyelectrolyte multilayer film morphology. Langmuir 2001;17: 6655–63.

[248] Dubas ST, Schlenoff JB. Swelling and smoothing of polyelectrolyte multilayers by salt. Langmuir 2001;17:7725–7.
[249] Sun P, Hu N, Liu H. pH switchable biocatalysis based on weak polyelectrolytes multilayers. Electroanalysis 2011;23:513–20.
[250] Bratek-Skicki A. Towards a new class of stimuli-responsive polymer-based materials - recent advances and challenges. Appl Surf Sci 2021;4:100068–89.
[251] Zhuk A, Mirza R, Sukhishvili S. Multiresponsive clay-containing layer-by-layer films. ACS Nano 2011;11:8790–9.
[252] Huang J, Moghaddam ZS, Thormann E. Structural investigation of a self-cross linked chitosan/alginate dialdehyde multilayered film with in situ QCM-D and spectroscopic ellipsometry. ACS Omega 2019;4:2019–29.
[253] Huang J, Moghaddam SZ, Maroni P, Thormann E. Swelling behavior, interaction, and electrostatic properties of chitosan/alginate dialdehyde multilayer films with different outermost layer. Langmuir 2020;36:3782–91.
[254] Xu G, Liu P, Pranantyo D, Neoh KG, Kang ET. Dextran- and chitosan-based antifouling, antimicrobial adhesion, and self-polishing multilayer coatings from pH-responsive linkages-enabled layer-by-layer assembly. ACS Sustain Chem Eng 2018;6:3916–26.
[255] Ge Z, Liu S. Functional block copolymer assemblies responsive to tumor and intracellular microenvironments for site-specific drug delivery and enhanced imaging performance. Chem Soc Rev 2013;42:7289–325.
[256] Fleige E, Quadir MA, Haag R. Stimuli-responsive polymeric nanocarriers for the controlled transport of active compounds: concepts and applications. Adv Drug Deliv Rev 2012;64:866–84.
[257] Tong R, Tang L, Ma L, Tu C, Baumgartner R, Cheng J. Smart chemistry in polymeric nanomedicine. Chem Soc Rev 2014;43:6982–7012.
[258] Schulz HD, Zabel M. Marine geochemistryvol. 2. Springer; 2006.
[259] Carre G, Garnier L, Moeller-Siegert J, Gies JP, Keller V, Andre P, et al. Antibacterial textiles functionalized by layer-by-layer assembly of polyelectrolytes and TiO2 photocatalyst. RSC Adv 2015;5:38859–67.
[260] Burke SE, Barrett CJ. pH-dependent loading and release behavior of small hydrophilic molecules in weak polyelectrolyte multilayer films. Macromolecules 2004;37:5375–84.
[261] Lu B, Luo D, Zhao A, Wang H, Zhao Y, Maitz MF, et al. pH responsive chitosan and hyaluronic acid layer by layer film for drug delivery applications. Prog Org Coat 2019;135:240–7.
[262] Cao S, Zhang Y, Zhou L, Chen J, Fang L, Fei D, et al. Stimuli-responsive controlled release and molecular transport from hierarchical hollow silica/polyelectrolyte multilayer formulations. J Mater Chem B 2014;2:7243–9.
[263] Han U, Seo Y, Hong J. Effect of pH on the structure and drug release profiles of layer-by-layer assembled films containing polyelectrolyte, micelles, and graphene oxide. Sci Rep 2016;6:24158.
[264] Déjugnat C, Sukhorukov GB. pH-responsive properties of hollow polyelectrolyte microcapsules templated on various cores. Langmuir 2004;20:7265–9.
[265] Petrov AI, Antipov AA, Sukhorukov GB. Base–acid equilibria in polyelectrolyte systems: from weak polyelectrolytes to interpolyelectrolyte complexes and multilayered polyelectrolyte shells. Macromolecules 2003;36:10079–86.
[266] Mauser T, Dejugnat C, Sukhorukov GB. Reversible pH-dependent properties of multilayer microcapsules made of weak polyelectrolytes. Macromol Rapid Commun 2004;25:1781–5.
[267] Mauser T, Déjugnat C, Sukhorukov GB. Balance of hydrophobic and electrostatic forces in the pH response of weak polyelectrolyte capsules. J Phys Chem B 2006; 11:20246–53.
[268] Sukhishvili SA, Granick SJ. Layered, erasable, ultrathin polymer films. J Am Chem Soc 2000;122:9550–1.
[269] Sukhishvili SA, Granick S. Layered erasable polymer multilayers formed by hydrogen-bonded sequential self-assembly. Macromolecules 2002;35:301–10.
[270] Zhao QH, Li BY. pH-controlled drug loading and release from biodegradable microcapsules. Nanomed Nanotechnol Biol Med 2008;4:302–10.
[271] Zhang S, Xing M, Li B. Capsules integrated polypeptide multilayer films for effective pH-responsive multiple drug co-delivery. ACS Appl Mater Interfaces 2018;10:44267–78.
[272] Yun J, Kim HI. Control of release characteristics in pH-sensitive poly(vinyl alcohol)/poly(acrylic acid) microcapsules containing chemically treated alumina core. J Appl Polym Sci 2010;115:1853–8.
[273] Burke SE, Barrett CJ. pH-responsive properties of multilayered poly(L-lysine)/ hyaluronic acid surfaces. Biomacromolecules 2003;4:1773–83.
[274] Guo X, Carter MCD, Appadoo V, Lynn DM. Tunable and selective degradation of amine-reactive multilayers in acidic media. Biomacromolecules 2019;20: 3464–74.
[275] Kozlovskaya V, Kharlampieva E, Drachuk I, Cheng D, Tsukruk VV. Responsive microcapsule reactors based on hydrogen-bonded tannic acid layer-by-layer assemblies. Soft Matter 2010;6:3596–608.
[276] Cai H, Wang P, Zhang D. pH-responsive linkages-enabled layer-by-layer assembled antibacterial and antiadhesive multilayer films with polyelectrolyte nanocapsuls as biocide delivery vehicles. J Drug Del Sci Technol 2019;54:101251.
[277] Chaturbedy P, Jagadeesan D, Eswaramoorthy M. pH-sensitive breathing of clay within the polyelectrolyte matrix. ACS Nano 2010;4:5921–9.
[278] Cheng K, Zhang Y, Li YJ, Gao Z, Chen F, Sun K, et al. A novel pH-responsive hollow mesoporous silica nanoparticle (HMSN) system encapsulating doxorubicin (DOX) and glucose oxidase (GOX) for potential cancer treatment. J Mater Chem B 2019;20:3291–302.
[279] Zhang X, Lin L, Gillies RJ. Tumor pH and its measurement. J Nucl Med 2010;51: 1167–70.
[280] Porcelli AM, Ghelli A, Zann C, Pinton P, Rizzuto R, Rugolo M. pH difference across the outer mitochondrial membrane measured with a green fluorescent protein mutant. Biochem Biophys Res Commun 2005;326:799–804.
[281] Asokan A, Cho MJ. Exploitation of intracellular pH gradients in the cellular delivery of macromolecules. J Pharm Sci 2002;91:903–13.
[282] Harguindey S, Stanciu D, Devesa J, Alfarouk K, Cardone RA, Orozco JDP, et al. Cellular acidification as a new approach to cancer treatment and to the understanding and therapeutics of neurodegenerative diseases. Semin Cancer Biol 2017;43:157–79.
[283] Tang K, Besseling NAM. Formation of polyelectrolyte multilayers: ionic strengths and growth regimes. Soft Matter 2016;12:1032–40.
[284] Nazaran P, Bosio V, Jaeger W, Anghel DF, Klitzing R. Lateral mobility of polyelectrolyte chains in multilayers. J Phys Chem B 2007;111:8572–81.
[285] Gong X, Gao C. Influence of salt on assembly and compression of PDADMAC/ PSSMA polyelectrolyte multilayers. Phys Chem Chem Phys 2009;11:11577–86.
[286] Guzman E, Ritacco H, Rubio JEF, Rubio RG, Ortega F. Salt-induced changes in the growth of polyelectrolyte layers of poly(diallyl-dimethylammonium chloride) and poly(4-styrene sulfonate of sodium). Soft Matter 2009;5:2130–42.
[287] Wang Z, Qian L, Wang X, Yang F, Yang X. Construction of hollow DNA/PLL microcpsules as a dual carrier for controlled delivery of DNA and drug. Colloids Surf A Physicochem Eng Asp 2008;326:29–36.
[288] Gao C, Möhwald H, Shen J. Enhanced biomacromolecule encapsulation by swelling and shrinking procedures. Chem Phys Chem 2004;5:116–20.
[289] Zhang R, Köhler K, Kreft O, Skirtach A, Möhwald H, Sukhorukov G. Salt-induced fusion of microcapsules of polyelectrolytes. Soft Matter 2010;6:4742–7.
[290] Gerard M, Chaubey A, Malhotra BD. Application of polyaniline as enzyme based biosensor. Biosens Bioelectron 2002;17:345.
[291] Puiggalí-Jou A, del Valle LJ, Alemán C. Drug delivery systems based on intrinsically conducting polymers. J Control Release 2019;309:244–64.
[292] Cho C, Jeon J-W, Lutkenhaus J, Zacharia NS. Electric field induced morphological transitions in polyelectrolyte multilayers. ACS Appl Mater Interfaces 2013;5: 4930–6.
[293] Zhang J, Lynn DM. Ultrathin multilayered films assembled from “charge-shifting” cationic polymers: extended, long-term release of plasmid DNA from surfaces. Adv Mater 2007;19:4218–23.
[294] Jessel N, Oulad-Abdelghani M, Meyer F, Lavalle P, Haïkel Y, Schaaf P, et al. Multiple and time-scheduled in situ DNA delivery mediated by beta-cyclodextrin embedded in a polyelectrolyte multilayer. Proc Natl Acad Sci 2006;103:8618–21.
[295] Blacklock J, Handa H, Manickam DS, Mao G, Mukhopadhyay A, Oupicky D. Disassembly of layer-by-layer films of plasmid DNA and reducible TAT polypeptide. Biomaterials 2007;28:117–24.
[296] Schmidt DJ, Cebeci FC, Kalcioglu ZI, Wyman SG, Ortiz C, Van Vliet KJ, et al. Electrochemically controlled swelling and mechanical properties of a polymer nanocomposite. ACS Nano 2009;3:2207–16.
[297] Zhai L. Stimuli-responsive polymer films. Chem Soc Rev 2013;42:7148–60.
[298] DeLongchamp D, Hammond PT. Layer-by-layer assembly of PEDOT/polyaniline electrochromic devices. Adv Mater 2001;13:1455–9.
[299] Anandhakumar S, Raichur Ashok M. Polyelectrolyte/silver nanocomposite multilayer films as multifunctional thin film platforms for remote activated protein and drug delivery. Acta Biomater 2013;9:8864–74.
[300] Rivero PJ, Goicoechea J, Matias IR, Arregui FJ. A comparative study of two different approaches for the incorporation of silver nanoparticles into layer-by-layer films. Nanoscale Res Lett 2014;9:301.
[301] Kruk T, Szczepanowicz K, Kręgiel D, Szyk-Warszyńska L, Warszyński P. Nanostructured multilayer polyelectrolyte films with silver nanoparticles as antibacterial coatings. Colloids Surf B Biointerfaces 2016;137:158–66.
[302] Boulmedais F, Schwinté P, Gergely C, Voegel JC, Schaaf P. Secondary structure of polypeptide multilayer films: an example of locally ordered polyelectrolyte multilayers. Langmuir 2002;18:4523–5.
[303] Ai H, Fang M, Jones SA, Lvov YM. Electrostatic layer-by-layer nanoassembly on biological microtemplates: platelets. Biomacromolecules 2002;3:560–4.
[304] Khopade AJ, Caruso F. Electrostatically assembled polyelectrolyte/dendrimer multilayer films as ultrathin nanoreservoirs. Nano Lett 2002;2:415–8.
[305] Volodkin D, Arntz Y, Schaaf P, Möhwald M, Voegel JC, Ball V. Composite multi-layered biocompatible polyelectrolyte films with intact liposomes: stability and temperature triggered dye release. Soft Matter 2008;4:122–30.
[306] Michel M, Izquierdo A, Decher G, Voegel JC, Schaaf P, Ball V. Layer by layer self-assembled polyelectrolyte multilayers with embedded phospholipid vesicles obtained by spraying: integrity of the vesicles. Langmuir 2005;21:7854–9.
[307] Volodkin DV, Schaaf P, Möhwald H, Voegel JC, Ball V. Effective embedding of liposomes into polyelectrolyte multilayered films: the relative importance of lipid- polyelectrolyte and interpolyelectrolyte interactions. Soft Matter 2009;5: 1394–405.
[308] Serizawa T, Yamaguchi M, Akashi M. Time-controlled desorption of ultrathin polymer films triggers by enzymatic degradation. Angew Chem Int Ed 2003;10: 1115–47.
[309] Vázquez E, Dewitt DM, Hammond PT, Lynn DM. Construction of hydrolytically-degradable thin films via layer-by-layer deposition of degradable polyelectrolytes. J Am Chem Soc 2002;124:13992–3.
[310] Constantine CA, Mello SV, Dupont A, Cao X, Santos D, Oliveira ON, et al. Layer-by-layer self-assembled chitosan/poly(thiophene-3-acetic acid) and organophosphorus hydrolase multilayers. J Am Chem Soc 2003;125:1805–9.
[311] Inoue H, Sato K, Anzai JI. Disintegration of layer-by-layer assemblies composed of 2-iminobiotin-labeled poly(ethyleneimine) and avidin. Biomacromolecules 2005; 6:27–9.

[312] Li J, Zhang X, Chen S, You Q, He R, Shi J, et al. Multi-responsive drug release from hydrogen-bonding multilayers containing PEGylated nanoparticles and azobenzenes. J Mater Chem B 2014;2:4422–5.
[313] De Geest BG, Jonas AM, Demeester J, De Smedt SC. Glucose-responsive polyelectrolyte capsules. Langmuir 2006;22:5070–4.
[314] Caughey GH. Mast cell tryptases and chymases in inflammation and host defense. Immunol Rev 2007;217:141–54.
[315] Yamamoto H, Iku S, Adachi Y, Imsumran A, Taniguchi A, Nosho K, et al. Association of trypsin expression with tumor progression and matrilysin in human colorectal cancer. J Pathol 2003;199:176–84.
[316] Radhakrishnan K, Raichur AM. Biologically triggered exploding protein based microcapsules for drug delivery. Chem Commun 2012;48:2307–9.
[317] Sun L, Xiong X, Zou Q, Ouyang P, Krastev R. Controlled heparinase-catalyzed degradation of polyelectrolyte multilayer capsules with heparin as responsive layer. J Appl Polym Sci 2017;134:44196.
[318] Cardoso MJ, Caridade SG, Costa RR, Mano JF. Enzymatic degradation of polysaccharide-based layer-by-layer structures. Biomacromolecules 2016;17:1347–57.
[319] Szarpak A, Cui D, Dubreuil F, De Geest BG, De Cock LJ, Picart C, et al. Designing hyaluronic acid-based layer-by-layer capsules as a carrier for intracellular drug delivery. Biomacromolecules 2010;11:713–20.
[320] Janik-Hazuka M, Szafraniec-Szczęsny J, Kamiński K, Odrobińska J, Zapotoczny S. Uptake and in vitro anticancer activity of oleic acid delivered in nanocapsules stabilized by amphiphilic derivatives of hyaluronic acid and chitosan. Int J Biol Macromol 2020;164:2000–9.
[321] Tian YZ, Li YL, Wang ZF, Jiang Y. Nuclease-responsive DNA-PEI hollow microcapsules for bio-stimuli controlled release. J Mater Chem B 2014;2:1667–72.
[322] De Geest BG, Vandenbroucke RE, Guenther AM, Sukhorukov GB, Hennink WE, Sanders NN, et al. Intracellularly degradable polyelectrolyte microcapsules. Adv Mater 2006;18:1005–9.
[323] Tarakanchikova Y, Alzubi J, Pennucci V, Follo M, Kochergin B, Muslimov A, et al. Biodegradable nanocarriers resembling extracellular vesicles deliver genetic material with the highest efficiency to various cell types. Small 2019;23:1904880.
[324] Brueckner M, Hollenbach-Latzko S, Reibetanz U. Dual transport of active substances with a layer-by-layer-based drug delivery system to terminate inflammatory processes. Macromol Biosci 2020;20:2000097.
[325] Gahan GC, Guo X, Manna U, Lynn DM. Polymer coatings comprised entirely of soft and semipermeable microcapsules. ACS Appl Polym Mater 2021;3:4044–54.
[326] Shchukin DG, Zheludkevich ML, Yasakau K, Lamaka S, Ferreira MGS, Möhwald H. Layer-by-layer assembled nanocontainers for self-healing corrosion protection. Adv Mater 2006;18:1672–8.
[327] Li GL, Zheng Z, Möhwald H, Shchukin DG. Silica/polymer double-walled hybrid nanotubes: synthesis and application as stimuli-responsive nanocontainers in self-healing coatings. ACS Nano 2013;7:2470–8.
[328] Szyk-Warszynska L, Trybala A. Deposition of core latex particles encapsulated in polyelectrolyte shells at modified mica surfaces. J Colloid Interface Sci 2007;314:398–402.
[329] Adamczyk Z, Musiał E, Siwek B. Kinetics of particle deposition in the oblique impinging jet cell. J Colloid Interface Sci 2004;269:53–60.
[330] Adamczyk Z, Szyk L, Warszynski P. Kinetics of colloid particle adsorption from slot impinging jets. Colloids Surf A 1993;75:185–93.
[331] Adamczyk Z, Siwek B, Szyk L, Zembala M. Fluctuations in the number of particles adsorbed under the influence of diffusion and flow. J Chem Phys 1996;105:5552–61.
[332] Adamczyk Z, Siwek B, Zembala M, Warszynski P. Enhanced deposition of particles under attractive double-layer forces. J Colloid Interface Sci 1989;130:578–87.
[333] Adamczyk Z, Siwek B, Warszynski P, Musial E. Kinetics of particle deposition in the radial impinging-jet cell. J Colloid Interface Sci 2001;242:14–24.
[334] Szyk-Warszynska L, Trybala A, Warszynski P. Deposition of latex particles encapsulated in polyelectrolyte shells at heterogeneous metal surfaces modified by multilayer films. Appl Surf Sci 2010;256:5388–94.